

Final response to the referees' comments for Olin et al.: "Traffic-originated nanocluster emission exceeds H₂SO₄-driven photochemical new particle formation in an urban area"

We thank the referees for their insightful comments and have corrected the manuscript according to them.

Referee reports are in *black italic* and authors' response in **blue roman** font. The marked-up manuscript and the Supplement highlighting the changes and the modified versions of them are included at the end of this file.

Referee #2 comments:

The paper deserves publication in the journal as I had noted in the review of the first version of the manuscript. I appreciate the work done by the authors to convincingly address all comments, including mine and the comments of the other reviewers. They have clarified points that were unclear in the first version. The revised version flows nicely and brings out both the new information and the questions they raise. I think it will be a useful contribution to the literature of particle formation mechanisms in urban areas.

We thank the referee for reading the revised manuscript.

Referee #3 comments:

General Comments: Olin et al. leverage previously collected nanocluster aerosol (NCA), trace gas (H₂SO₄, NO_x, CO₂), meteorological, and particle size distribution data from a month-long sampling campaign in Helsinki, Finland (Hietikko et al., 2018) to propose an updated model of NCA and H₂SO₄ formation in urban environments (Figure 4). This model is comprised of two pathways for generating NCA and H₂SO₄, respectively. Olin et al. argue that immediate implications from H₂SO₄-containing NCA on human health necessitates models including their H₂SO₄-NCA conceptual model. Generally, speaking none of the highlighted pathways are novel or new. Primary H₂SO₄ was identified by Arnold et al. (2012), and the direct emission of NCA from vehicles was identified by Rönkkö et al. (2017). To this end, the proposed model, and ensuing discussions, feel more well suited for a review-type article opposed to a research article. This particularly true as much of the analysis focused on supporting that NCA sourced from traffic and not regional NPF events. This argument seemed redundant to the earlier paper (Hietikko et al., 2018) which the NCA data was sourced from.

We agree and apologize that the current form of the manuscript does not highlight our new findings clearly enough. It is true that the direct NCA emissions from vehicles have already revealed by Rönkkö et al. (2017). We performed a new measurement campaign in Helsinki in 2017 and the NCA concentrations measured in this campaign were published by Hietikko et al. (2018). However, in the current manuscript we present, in addition to the NCA measurement data, also H₂SO₄ and solar irradiance data, providing new and unpublished data and analysis that presents a novel interpretation of the data.

According to our understanding of the referee's criticism, the referee has understood our proposed model in a way that we claim that NCA contains and is formed solely from primary H₂SO₄. However, this is not the purpose of our claim, and we agree that this was not expressed clearly enough. Our main message is that NCA in an urban environment is, mainly, not formed by secondary H₂SO₄, which does not imply that NCA is formed from primary H₂SO₄ solely. Instead, other routes, such as primary (possibly solid) emissions from vehicles, can explain the presence of NCA. This primary emission route was clearly missing from the referee's interpretation of our proposed model and is thus now clarified in the manuscript.

As far as H₂SO₄ emitted directly by vehicles, the route already identified by Arnold et al. (2012), our novel finding is the secondary route (includes solar radiation) of H₂SO₄ from vehicles. Additionally, instead of measuring H₂SO₄ directly from an engine (Arnold et al., 2012), our measurements are to our knowledge the first field measurements connecting urban H₂SO₄ concentrations to traffic sources quantitatively, and are therefore novel research. Our data measured at a curbside of a street provide reference data for primary H₂SO₄ emission data and the ability to determine emission factors of vehicles in a real-world driving situation, for the first time. With the fact that vehicles emit H₂SO₄ directly but our measurement at the curbside

displays no clear increase in H_2SO_4 concentrations with increasing traffic volumes, it can be concluded that other routes for primary H_2SO_4 emissions must exist. The most probable routes are related to gas-to-particle conversion, i.e. nucleation and condensation (routes 1A and 1B in Fig. 4). Thus, primary H_2SO_4 mainly terminates from the gas phase either by nucleating to new particles (1A) or by condensing onto existing particles (1B). However, we cannot identify the ratio of these two routes and thus do not claim that NCA contains or is formed from H_2SO_4 but do not rule that out either. Due to the fact that the primary H_2SO_4 and nucleation mode particle number concentrations in vehicle exhaust are correlated (Arnold et al., 2012; Rönkkö et al., 2013), it is likely that the nucleation route (1A) does exist. Additionally, because the sizes of the nucleation mode particles are also correlated with the primary H_2SO_4 concentrations (Rönkkö et al., 2013), it is likely that the condensation route (1B) exists as well. Because the ratio of the contribution of primary NCA emissions and the H_2SO_4 nucleation route (1A) is also not identified, the relative proportion of H_2SO_4 in the composition of the NCA particles is unknown. The text related to these is now clarified in the manuscript.

The manuscript is generally well written, and the arguments are comprehensible. The manuscript's shortfall is the lack of NCA composition data. The lack of composition data makes the influence of primary H_2SO_4 to both number and mass concentration of vehicle-emitted NCA unsubstantiated and, from my perspective undermines what would be the major contribution of this manuscript (in respect to the model). The authors adequately demonstrate that NCA is decoupled from NPF events via a series of regression and correlation analyses. However, the reliance on data published in Hietikko et al. (2018) undermines the impact of these observations, as this was the primary focus of the earlier study. In contrast to the earlier study, Olin et al. do provide an off-the-hand annual estimate of traffic-derived NCA in Helsinki using CO_2 emission factors. I find that the general applicability of this approach might be questionable. In particular, the authors suggest the pathways (Figure 4) need consideration in regional chemical transport models but provide no clear means to facilitate this implementation. I can imagine that the complexity of this challenge would likely be confounded by varying relationships between NCA and H_2SO_4 and vehicle emissions (engine types, fuel types, emission standards, etc.) but am not enough of an expert to make specific recommendations. The challenges in implementing the conceptual model in regional chemical transport models is not elaborated on in this manuscript.

We agree that the NCA composition data would have been very beneficial, but due to a lack of suitable technology on measuring that directly because of very small particle sizes, the exact composition remains unknown. Examining the formation mechanisms of particles provides an alternative way for getting clues on their compositions, which is done in this manuscript. This is now mentioned in the manuscript. So far, our results imply that the secondary routes (including solar radiation) from vehicle-originated NCA formation mechanisms are not dominant, but additional research is needed to get more clues.

The annual estimation of the contribution of traffic and regional NPF on the presence of NCA in urban air was a rough estimation only in order to obtain the significance of traffic on NCA loadings. The text related to this is now modified to highlight the roughness of the estimation.

The challenges in implementing our model in regional chemical transport models (CTMs) include the effects of vehicle, engine, fuel, and after-treatment system types on H_2SO_4 and NCA emission factors, which can vary markedly between the different types. Nevertheless, our emission factors represent the average fleet-level emission factors and are thus moderately applicable in regional CTMs at least for areas with the same average fleet composition as in our measurement site in Helsinki. More research is needed to obtain emission factors separated into the different types, but it is not an objective of this manuscript. Neither are the emission factors intended to act as quantitative emissions factors for regional CTMs, but are intended to distinguish the features of solar radiation and traffic levels. However, the results show that these processes need to be distinguished in modelling studies to obtain realistic results. These views are now added to the manuscript.

Lastly, I felt details pertaining to rationale and underlying assumptions were sometimes lacking in this manuscript. Specific points are made below. Although short manuscripts are ideal, I think this manuscript would greatly benefit from a more robust discussion on why certain decisions were made. For instance, the authors opt to utilize CO_2/NO_x as a proxy for traffic flow when the authors have direct measurements of traffic flow. Why not just use traffic flow? This was particularly odd as the authors state that background fluctuations in CO_2 make it an unreliable proxy for local traffic. I suspect these decisions might relate to the desire of making their observations relatable to chemical transport models and vehicle emission factors. There may be other reasons; however, they are not clearly stated in the manuscript.

The reason for using NO_x and CO_2 as traffic tracers is twofold. Firstly, traffic density was measured in only 15 min time resolution, but the NO_x and CO_2 data are available in 1 min resolution, which is the shortest resolution used in the analysis. Secondly, the flow field at the street canyon is turbulent with variable wind directions; thus, measured air parcels were diluted in a significantly different extent. Fortunately, the problem of different dilution ratios can be solved by using an exhaust-originated tracer because it has been diluted in the same extent as the emission of interest.

An ideal tracer is one that is universally emitted by all vehicles and is not altered in the atmosphere during the time scale of the exhaust plume dilution process. CO_2 is emitted by all combustion engines, with the emission rate proportional to the fuel consumption; additionally, it remains unchanged in the atmosphere. The drawback of CO_2 is its varying background concentration due to regional-level phenomena. The background concentration varied between 405 and 420 ppm during this measurement campaign; however, the effect of traffic on the CO_2 concentration levels at the curbside of the street canyon was only 50 ppm in maximum. Thus, the maximum deviation in the background concentration (15 ppm) compared to the traffic contribution is significant. On the other hand, as the main source of NO_x in urban areas is traffic (Clapp and Jenkin, 2001), the background concentration is low and causes thus no significant uncertainty to the traffic contribution. The ratio of the two components of NO_x (NO and NO_2) is altered in atmospheric oxidation, but the sum (NO_x) remains constant (Clapp and Jenkin, 2001). The drawback of NO_x as a tracer is its varying emission rates across the whole vehicle fleet (Yli-Tuomi et al., 2005). Concluding, we decided to use NO_x as the traffic tracer in our analysis, except in the emission factor analysis where we used CO_2 because it is directly connected to the fuel consumption. Fuel consumption-related emission factors are practicable because they can provide estimations on total regional emissions and because they are the most understandable by the general audience. As observed from Fig. 4, a linear behavior of the concentrations is seen when averaged to CO_2 concentration bins although the variance in the background concentration is an issue. As a comparison, Fig. FR1 presents examples of these graphs if the binning were done using traffic density or the NO_x concentration, and it can be seen that such a clear linear behavior is not obtained, especially in the case of traffic density. The clarification on the choice for traffic tracers is now added to the manuscript.

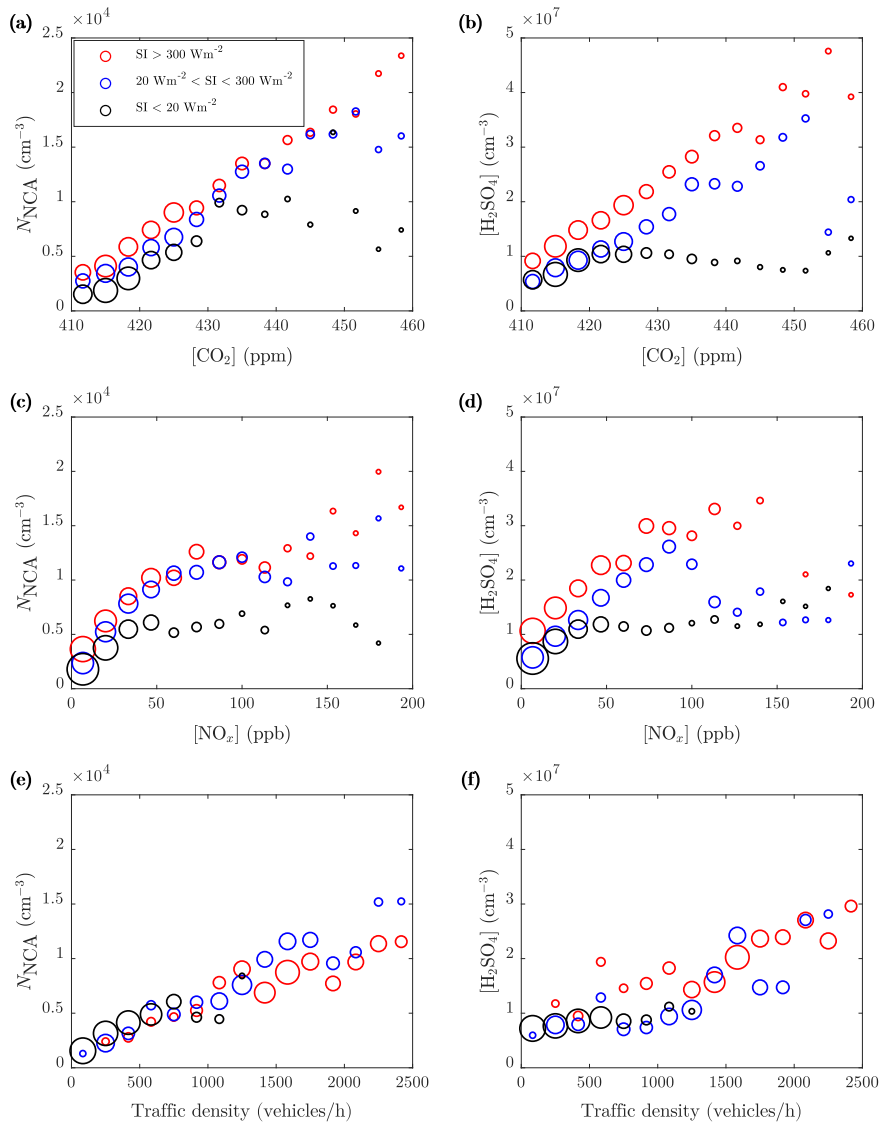


Figure FR1. Comparison of using (a,b) the CO_2 concentration, (c,d) the NO_x concentration, or (e,f) traffic density as a binned quantity.

Specific Comments: 1) As stated in the general comments, my most significant issue with the manuscript is that the composition of the NCA is not actually measured during the deployment in question. This is important as much of the manuscript relies on the argument that NCA composition is decoupled from secondary H₂SO₄, and thus, NCA should be compositionally influenced only by primary H₂SO₄ (Figure 4). To this point, the authors state on line 32, page 2: “the unknown chemical composition of traffic-originated NCA-sized particles. . .”. Although, I do not view the author’s conclusion as impossible, or even unlikely, as evidence exists that emissions from motor vehicles contain H₂SO₄ gas which may contribute NCA emissions (Arnold et al., 2012). Nonetheless, the authors fail to support their argument with results at hand. At present, the evidence suggests NCA formation can occur independent of NPF events in respect to the H₂SO₄ condensation sink (CS). I appreciate the challenge in measuring the composition of particles on a particle-by-particle basis or the small size range of NCA due to mass constraints; however, pathway 1A (figure 4) is not supported in their data.

Please refer to the first reply.

2) From my understanding organic vapors, NH₃, NO_x, and H₂SO₄, are all precursor gases to new particle formation events (Kerminen et al, 2018). I am not an expert in NPF events and do not have a great sense of the relative occurrence and frequency that these different gases contribute to NPF events. At present, CS is only calculated in respect to H₂SO₄. I encourage the authors calculate CS in respect to trace gases known to contribute to NPF events. The argument that these are truly primarily emitted particles will be supported by a more robust calculation of CS.

At least low volatile organic compounds, H₂SO₄, NH₃, and amines are possible precursor gases to NPF (Kerminen et al., 2018). CS is in most cases calculated only for H₂SO₄ (Lehtinen et al., 2007) and the NPF frequency quantified with respect to CS for H₂SO₄ only, even though H₂SO₄ would have not been measured. CS was calculated using the function (Kulmala et al., 2001):

$$CS = 2\pi\mathcal{D} \int_0^{\infty} \beta(D_p) \cdot D_p \cdot \frac{dN}{d\log D_p} d\log D_p \quad (\text{FR1})$$

where \mathcal{D} is the diffusion coefficient of the condensing vapor and $\beta(D_p)$ is the transition regime correction factor, which also depends on the condensing vapor. Choosing a different condensing vapor in calculating CS adds mainly a constant multiplier to the CS time series calculated for H₂SO₄, the multiplier depending on the molecular size of the vapor. Figure FR2 presents examples of the CS diurnal variations calculated for different vapors and it is now added to the Supplement.

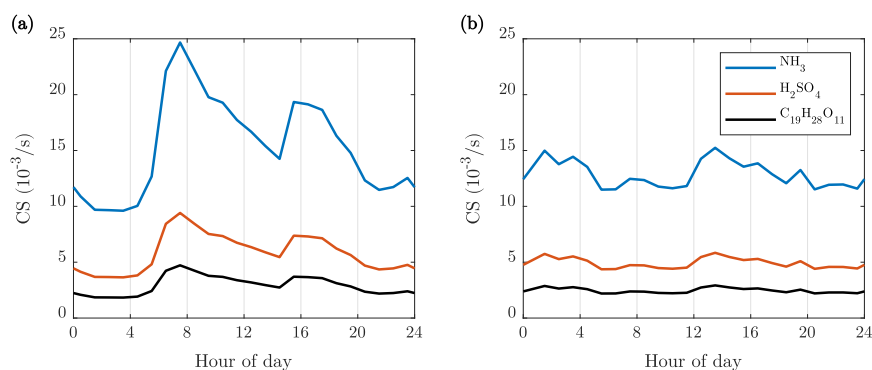


Figure FR2. Diurnal variations of condensation sinks for different condensing vapors (a) on weekdays and (b) on weekends. NH₃ and C₁₀H₂₈O₁₁ are selected to represent condensing vapors having small and large molecular sizes, respectively. C₁₀H₂₈O₁₁ represents a low volatile organic compound having a molar mass of 432 g mol⁻¹ (Ehn et al., 2014).

3) Presently, it is unclear about the frequency of NCA events in respect to the CS. Timeseries data for NCA and CS are included as supplementary figures. The authors' current presentation makes it difficult to distinguish events as there appears to be a lot of covariance between CS and NCA (and other diurnal properties). I encourage the authors to include these panels (as well as traffic flow and solar radiation) as a main figure. Furthermore, it would be nice if the authors provided a more quantitative feel for the frequency that NCA events occur during periods of high CS. There may be better ways to do it, but something along the lines of a running (windowed) Pearson's correlation (defining an R threshold as an event) between CS and NCA would prove helpful in distinguishing these periods.

Analyzing atmospheric NPF events from data measured at the curbside of a highly trafficked street is not very straightforward due to particle concentrations dominated by the traffic sources. Presenting the time series of the NCA concentration and CS in a same graph (Fig. FR3) indicates that they are well correlated. This occurs because traffic causes the both, NCA particles and larger particles contributing to CS. Regional NPF events are frequently suppressed by high CS values (Kerminen et al., 2018). Therefore, decreasing CS can lead to a NPF event. However, there are no clear NCA concentration increases observed with simultaneous CS decrease in our data. Figure FR4 represents one-hour averages of the NCA concentrations and CS as a scatter plot, Pearson's R being 0.56 confirms their positive correlations. Moving Pearson's R is presented in Fig. FR5, from where it can be observed that the correlation is mostly positive and never falls to the negative side in a high extent. These findings imply that no clear atmospheric NPF events can be distinguished from the data. Figure FR3 is now added to the Supplement and text related to these is now added to the manuscript.

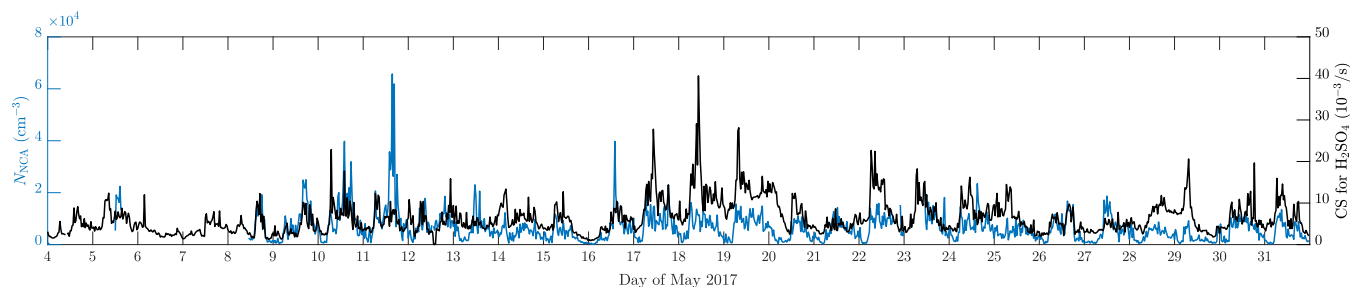


Figure FR3. Time series of the NCA concentration and CS for H_2SO_4 .

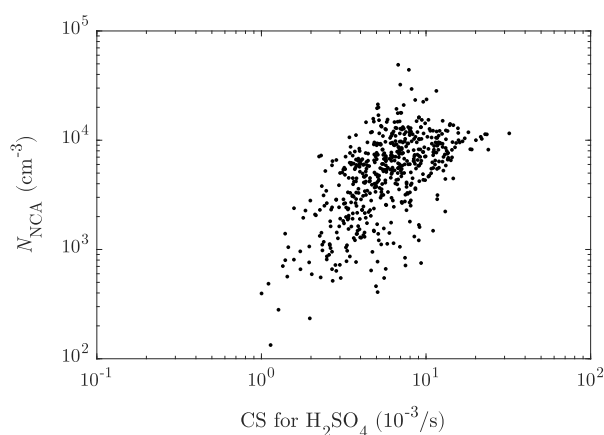


Figure FR4. Correlation of the NCA concentration and CS for H_2SO_4 .

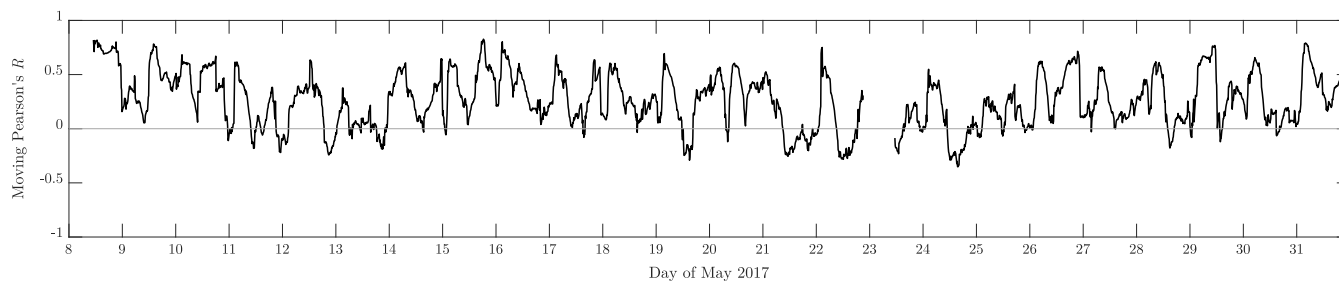


Figure FR5. Moving (time window of 8 hours) Pearson's R for the NCA concentration versus CS for H_2SO_4 .

4) The authors argue that NO_x provides a good proxy for traffic flow. This claim is moderately supported by averaged trend data provided in Figure 3. My concerns are twofold. First, although the variance in the profiles appear to co-vary, why not simply correlate NO_x and traffic profiles (separating weekends and weekdays). As a side note, I do not understand the decision to take the geometric mean opposed to the arithmetic mean. Second, the authors do not state the significance for using NO_x as a proxy for traffic. It is strange to me as the authors have a direct measure of traffic 600 m up the road which they use for justifying NO_x as a tracer for traffic.

Whereas we claim that NO_x is a good tracer for traffic, we are not claiming that the NO_x concentration and traffic density are correlated due to different dilution ratios of the air parcels when measured at the curbside, as already discussed before. Therefore, our claim is supported only with averaged diurnal variations in Fig. 3.

Because the concentrations of the most of the pollutants cover ranges of several orders of magnitude, leading to skewed frequency distributions, arithmetic mean would weight the highest concentrations more than the lower ones. In essence, the frequency distributions are more log-normally than normally distributed. Therefore, geometric mean suits better in representing the typical value for a pollutant. This is now clarified in the manuscript.

5) Perhaps I am missing the rationale; however, I think Figure 8 should be SI vs CO_2 , where SI is not binned into separate groups. If the argument is that CO_2 does not have a diurnal profile, then the slope will be 0.

Our argument with Fig. 8 is that solar irradiance is not similarly correlated with traffic emissions like CO_2 is. If there were a remarkable (positive) slope in the SI vs. CO_2 concentration graph, that would imply that solar irradiances were higher with high CO_2 concentrations. In that case, we could have not claimed that the CO_2 -related slopes truly represent the emissions factors of vehicles; instead, the slopes could also result from photochemical production due to accelerated photochemistry with high solar irradiances. Nevertheless, there were no clear slopes in the SI vs. CO_2 concentration graph, implying that this kind of problematic co-correlation did not exist. SI was binned into the same separate groups in Fig. 8 as in Fig. 7 in order to represent the same data points consistently. These are now clarified in the manuscript and Fig. 8 is moved to the Supplement because it does not raise any new results.

6) The abstract was lacking quantitative finding. I find that statements such as, "frequently correlated" (line 6, Page 1), to be extremely vague and really should not be in abstracts.

Our main result in this manuscript is an update to the source processes of NCA and H_2SO_4 in urban areas, but as the observation is only at one site, it should be regarded as mostly qualitative; however, we have added quantitative findings on the contribution of traffic on NCA and H_2SO_4 concentrations to the abstract. The phrase "frequently correlated" was not a result from this study; instead, it was purposed to mean that traffic density in many areas is generally correlated with solar radiation, which is now clarified in the abstract.

7) There is no statement on the availability of underlying data

The time series data will be available in a FAIR-aligned open access repository IDA once the manuscript is accepted.

8) The abstract makes mention of health effects. However, this was not a major finding in this work. Although fine to mention in the introduction and conclusion, it should not be included in the abstract.

Health effects is no more mentioned in the abstract.

9) From my perspective, this is optional. The authors propose a conceptual model showing sink processes for NCA. I am generally interested in the loss rates for NCA in respect to the observed size distributions (i.e., coagulation rates). This would add a distinguishing feature from analysis presented in Hietikko et al. (2018). The authors would probably need to make assumptions about air parcels not mixing; however, this would provide an upper-bound estimate for NCA lifetime. I think this may have implications towards the authors earlier comments about potential health effects.

As NCA particles were measured at the curbside, at the same location as people walk, it is clear that NCA particles possess potential health effects. The lifetimes of the NCA particles can be estimated using coagulation sinks (CoagS) and the time constants of coagulation scavenging (τ_{CoagS}), which is the inverse of CoagS, calculated as in Kulmala et al. (2001). Assuming no other losses of the particles, such as self-coagulation and condensational growth out from the NCA size range, τ_{CoagS} represents the lifetime of the particles. Figure FR6 represents CoagS and τ_{CoagS} for the smallest (1.2 nm) and largest (3 nm) measured NCA particles in order to give idea on the lifetimes of the NCA particles. It can be seen that the lifetimes are in the scale of several minutes, resulting in a spreading possibility of the NCA particles around urban areas.

These lifetimes are upper-bound estimates for freshly-emitted aerosol; in reality, self-coagulation and condensational growth decreases the lifetimes—although with regards to condensational growth, the particles are not lost; instead, only moving out of the NCA size range (Kangasniemi et al., 2019). On the other hand, emitted aerosol mixes with background aerosol while dispersing from the streets, leading to decreasing CoagS because the background particle concentrations are usually lower compared to the curbside concentrations. Therefore, the estimated lifetimes would increase by considering also the mixing process. These views are now added to the manuscript and Fig. FR6 to the Supplement.

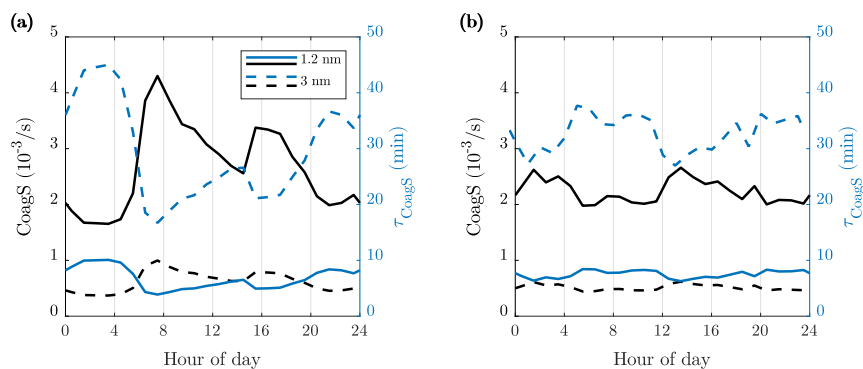


Figure FR6. Diurnal variations of coagulation sinks and coagulation time constants for 1.2 nm and 3 nm particles on (a) weekdays and on (b) weekends.

10) The authors did not outline how CS was calculated. Please include in the methods.

Equation (FR1) is now mentioned in the Supplement.

11) It is unclear what the authors mean by “weighting factor” as the authors regression analysis was not outlined in the methods. I am assuming the authors just average everything in a given bin.

Linear fitting in Figs. 6c, 6d, 7, and 8 was done in two steps. Firstly, the values of the quantity on the y -axis are averaged within arbitrary specified bins of the quantity on the x -axis. In other words, the averaging within a single bin is done across the times when the value of the quantity on the x -axis is within the range of the bin. Secondly, linear fits are output from weighted least squares fitting, in which the number of the averaged data points for a specific bin in the first step acts as a weight for the bin. This is now clarified in the manuscript.

12) The authors choice for bin widths (all regressions) may be justified but appear arbitrary without presenting a rationale. Personally, I think the data underlying regressions in Figures 6c,d Figure 7, and Figure 8 should be shown and not binned. If the data density is too high (graphical representation), the authors could possibly facet the different NOx and SI bins.

The bin widths are chosen to make the graphical presentations clear. The choice for the bin widths does not largely affect the fitted slopes. It is true that the data density is too high and the data points are also quite scattered. For that reason, the graphical representations use averaging to bins. The fitted slopes are largely affected neither by least squares fitting to the full data set instead of weighted least squares fitting to the bin-averaged values; examples are shown in Fig. FR7 and the slopes in Tab. FR1. This is now clarified in the manuscript.

Table FR1. Slopes of the linear fits in Fig. FR7.

Slope for quantity	SI range (Wm^{-2})	Fig. 4	Fig. FR7a,b (wider bins)	Fig. FR7c,d (narrower bins)	Fig. FR7e,f (no bin-averaging)
N_{NCA} ($10^{14} \text{ kg}_{\text{fuel}}^{-1}$)	< 20	5.3	5.3	5.5	4.1
	20 ... 300	6.6	6.6	6.6	5.8
	> 300	7.0	7.1	7.2	6.9
$[\text{H}_2\text{SO}_4]$ ($10^{17} \text{ kg}_{\text{fuel}}^{-1}$)	< 20	3.0	3.0	3.1	3.1
	20 ... 300	10.0	10.0	10.1	8.2
	> 300	13.6	13.5	13.7	21.0

13) Figures 6c,d-8 should have confidence intervals for the intercepts so readers can evaluate the robustness in the intercepts (really relevant to 6c).

The intercepts with the confidence intervals in Figs. 6c, 6d, and 7 are now added to the figure captions. In Fig. 8, the intercepts are irrelevant and are thus not shown.

14) Line 18, Page 9: How many instances of NCA events occurred during cloudy weather? Was this the only time? This could be highlighted on the timeseries mentioned in main comment 3.

There were several days during the campaign when cloudiness decreased solar irradiance. In all of those days, NCA formation with high traffic can be seen; however, the example day in Fig. 5c was the day with the most clear effect of cloudiness on solar irradiance and the reduction of solar irradiance coincides with morning rush hours, displaying high NCA concentrations. Additionally, the wind direction remained unchanged during the day. Therefore, only this day was shown separately. This is now clarified in the manuscript.

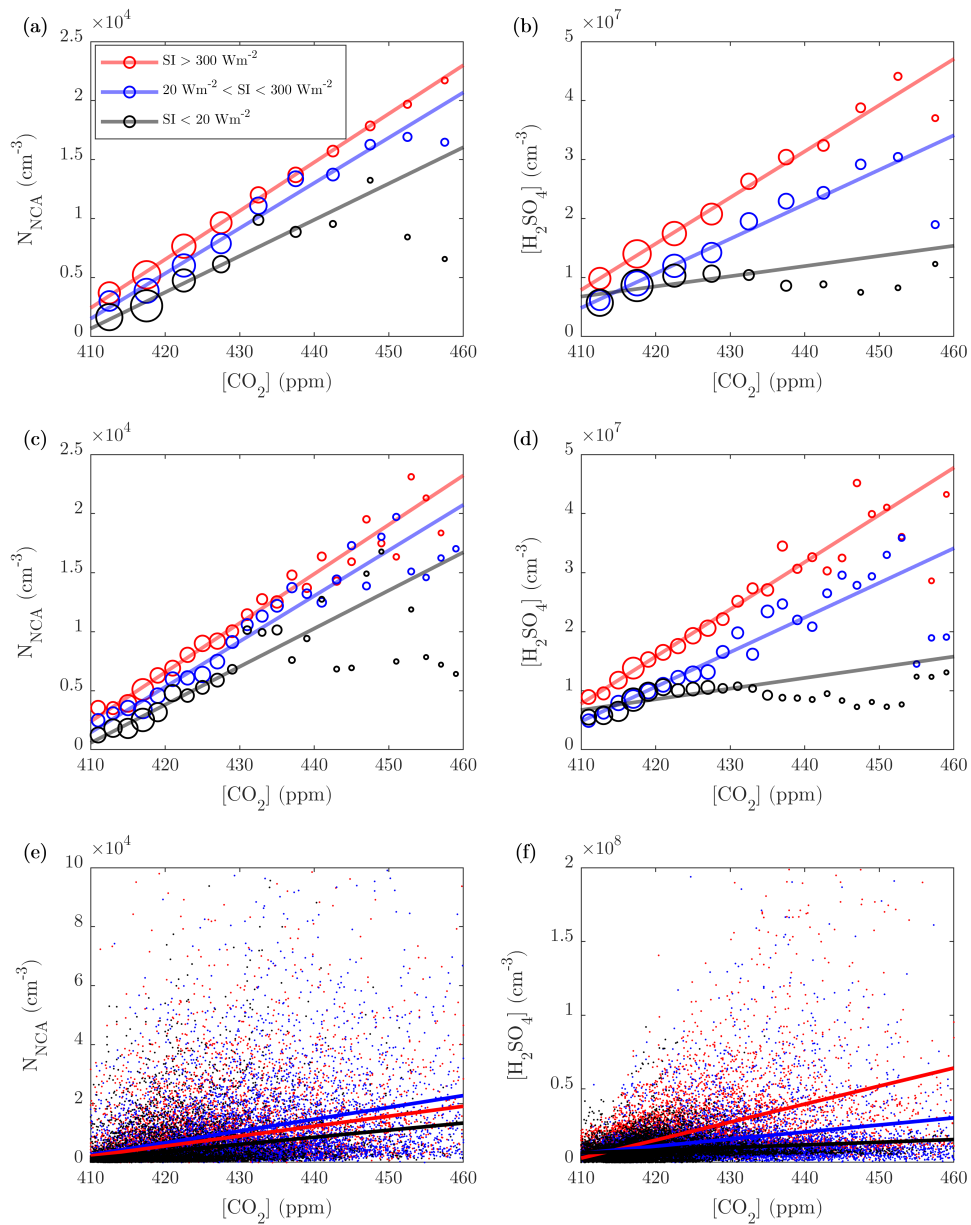


Figure FR7. Comparison of different bin widths in bin-averaging of Fig. 4. (a,b) Wider bins as in Fig. 4, (c,d) narrower bins as in Fig. 4, (e,f) no bin-averaging; instead, least squares fitting is done to the full data sets. The slopes of the linear fits are shown in Tab. FR1.

15) Line 2, Page 10: *I am not familiar with momentary concentrations.*

It was meant to represent the concentrations at the same moment, but because the sentence is clear also without the word “momentary”, it is now removed from the text.

16) Line 4, Page 10: *The use of relating NCA/H₂SO₄ to CO₂ appears be creating an annual estimate of NCA. I did not think this was clearly articulated. Furthermore, on line 28, Page 5, the authors state: “because traffic does not cause a clear signal on the measured CO₂ concentration due to a high and varying CO₂ background level, the NO_x concentration was selected to represent the traffic-originated emissions overall.”*

Please refer to the third reply.

Technical Comments: 1) Line 21, Page 2: “an evidence” should just be “evidence”

The word “an” is now removed from the text.

2) Line 10, Page 17: *two doi’s*

The extra doi is now removed.

References

- Arnold, F., Pirjola, L., Rönkkö, T., Reichl, U., Schlager, H., Lähde, T., Heikkilä, J., and Keskinen, J.: First online measurements of sulfuric acid gas in modern heavy-duty diesel engine exhaust: Implications for nanoparticle formation, *Environ. Sci. Technol.*, 46, 11 227–11 234, <https://doi.org/10.1021/es302432s>, 2012.
- Clapp, L. J. and Jenkin, M. E.: Analysis of the relationship between ambient levels of O₃, NO₂ and NO as a function of NO_x in the UK, *Atmos. Environ.*, 35, 6391–6405, [https://doi.org/10.1016/S1352-2310\(01\)00378-8](https://doi.org/10.1016/S1352-2310(01)00378-8), 2001.
- Ehn, M., Thornton, J., Kleist, E., Sipilä, M., Junninen, H., Pullinen, I., Springer, M., Rubach, F., Tillmann, R., Lee, B., Lopez-Hilfiker, F., Andres, S., Acir, I.-H., Rissanen, M., Jokinen, T., Schobesberger, S., Kangasluoma, J., Kontkanen, J., Nieminen, T., Kurtén, T., Nielsen, L., Jørgensen, S., Kjaergaard, H., Canagaratna, M., Maso, M., Berndt, T., Petäjä, T., Wahner, A., Kerminen, V.-M., Kulmala, M., Worsnop, D., Wildt, J., and Mentel, T.: A large source of low-volatility secondary organic aerosol, *Nature*, 506, 476–479, <https://doi.org/10.1038/nature13032>, 2014.
- Hietikko, R., Kuuluvainen, H., Harrison, R. M., Portin, H., Timonen, H., Niemi, J. V., and Rönkkö, T.: Diurnal variation of nanocluster aerosol concentrations and emission factors in a street canyon, *Atmos. Environ.*, 189, 98–106, <https://doi.org/10.1016/j.atmosenv.2018.06.031>, 2018.
- Kangasniemi, O., Kuuluvainen, H., Heikkilä, J., Pirjola, L., Niemi, J. V., Timonen, H., Saarikoski, S., Rönkkö, T., and Dal Maso, M.: Dispersion of a Traffic Related Nanocluster Aerosol Near a Major Road, *Atmosphere*, 10, 309, <https://doi.org/10.3390/atmos10060309>, 2019.
- Kerminen, V.-M., Chen, X., Vakkari, V., Petäjä, T., Kulmala, M., and Bianchi, F.: Atmospheric new particle formation and growth: review of field observations, *Environ. Res. Lett.*, 13, 103 003, <https://doi.org/10.1088/1748-9326/aadf3c>, 2018.
- Kulmala, M., Dal Maso, M., Mäkelä, J. M., Pirjola, L., Väkevä, M., Aalto, P., Miiikkulainen, P., Hämeri, K., and O'Dowd, C. D.: On the formation, growth and composition of nucleation mode particles, *Tellus B*, 53, 479–490, <https://doi.org/10.1034/j.1600-0889.2001.530411.x>, 2001.
- Lehtinen, K. E. J., Dal Maso, M., Kulmala, M., and Kerminen, V.-M.: Estimating nucleation rates from apparent particle formation rates and vice versa: Revised formulation of the Kerminen-Kulmala equation, *J. Aerosol Sci.*, 38, 988–994, <https://doi.org/10.1016/j.jaerosci.2007.06.009>, 2007.
- Rönkkö, T., Lähde, T., Heikkilä, J., Pirjola, L., Bauschke, U., Arnold, F., Schlager, H., Rothe, D., Yli-Ojanperä, J., and Keskinen, J.: Effects of gaseous sulphuric acid on diesel exhaust nanoparticle formation and characteristics, *Environ. Sci. Technol.*, 47, 11 882–11 889, <https://doi.org/10.1021/es402354y>, 2013.
- Rönkkö, T., Kuuluvainen, H., Karjalainen, P., Keskinen, J., Hillamo, R., Niemi, J. V., Pirjola, L., Timonen, H. J., Saarikoski, S., Saukko, E., Järvinen, A., Silvennoinen, H., Rostedt, A., Olin, M., Yli-Ojanperä, J., Nousiainen, P., Kousa, A., and Dal Maso, M.: Traffic is a major source of atmospheric nanocluster aerosol, *P. Natl. Acad. Sci. USA*, 114, 7549–7554, <https://doi.org/10.1073/pnas.1700830114>, 2017.
- Yli-Tuomi, T., Aarnio, P., Pirjola, L., Mäkelä, T., Hillamo, R., and Jantunen, M.: Emissions of fine particles, NO_x, and CO from on-road vehicles in Finland, *Atmos. Environ.*, 39, 6696–6706, <https://doi.org/10.1016/j.atmosenv.2005.07.049>, 2005.

Traffic-originated nanocluster emission exceeds H₂SO₄-driven photochemical new particle formation in an urban area

Miska Olin¹, Heino Kuuluvainen¹, Minna Aurela², Joni Kalliokoski¹, Niina Kuittinen¹, Mia Isotalo¹, Hilikka J. Timonen², Jarkko V. Niemi³, Topi Rönkkö¹, and Miikka Dal Maso¹

¹Aerosol Physics Laboratory, Physics Unit, Tampere University, FI-33014 Tampere, Finland

²Atmospheric Composition Research, Finnish Meteorological Institute, FI-00101 Helsinki, Finland

³Helsinki Region Environmental Services Authority (HSY), FI-00066 HSY, Finland

Correspondence: Miska Olin (miska.olin@tuni.fi)

Abstract. Elevated ambient concentrations of sub-3 nm particles (nanocluster aerosol, NCA) are generally related to atmospheric new particle formation events, usually linked with gaseous sulfuric acid (H₂SO₄) produced via photochemical oxidation of sulfur dioxide. According to our measurement results of H₂SO₄ and NCA concentrations, traffic density, and solar irradiance at an urban traffic site in Helsinki, Finland, the view of aerosol formation in traffic-influenced environments is updated by presenting two separate and independent pathways of traffic affecting the atmospheric NCA concentrations: by acting as a direct nanocluster source, and by influencing the production of H₂SO₄. As traffic density is frequently in many areas is generally correlated with solar radiation, it is likely that the influence of traffic-related nanoclusters has been hidden in the diurnal variation, and is thus underestimated because new particle formation events also follow the diurnal cycle of sunlight. Urban aerosol formation studies should, therefore, be updated to include the proposed formation mechanisms. ~~Additionally, the directly emitted NCA poses a potentially elevated health risk, highlighting the need for quantifying the source and loadings in populated areas.~~ The formation of H₂SO₄ in urban environments is here separated in two routes: primary H₂SO₄ is formed in hot vehicle exhaust and is converted rapidly to particle phase; secondary H₂SO₄ results from the combined effect of emitted gaseous precursors and available solar radiation. A rough estimation demonstrates that ~ 85 % of the total NCA and ~ 68 % of the total H₂SO₄ in urban air at noontime at the measurement site are contributed by traffic, indicating the importance of traffic emissions.

Copyright statement.

1 Introduction

Urban environments exhibit some of the highest aerosol particle concentrations encountered in the Earth's atmosphere. Elevated particle concentrations are related to adverse health effects (Dockery et al., 1993; Pope et al., 2002; Beelen et al., 2014) and various effects on climate (Arneth et al., 2009). Recent studies on urban aerosol particles have focused attention on the formation process of sub-3 nm particles (Zhao et al., 2011; Kulmala et al., 2013; Kontkanen et al., 2017) also called

nanocluster aerosol (NCA) (Rönkkö et al., 2017). The importance of photochemical formation mechanisms, involving, e.g., sulfuric acid (H_2SO_4) and ammonia (Yao et al., 2018) or other photochemically produced vapors (Lehtipalo et al., 2018), has been highlighted. However, these studies omit the important role of direct emission of NCA-sized particles in their analysis, despite recent findings that traffic is a major source of such particles (Rönkkö et al., 2017). The proposed mechanisms also
5 assume that key precursor vapors are formed via photochemical oxidation (Paasonen et al., 2010; Lehtipalo et al., 2018).

The most important gaseous species forming new particles in the atmosphere is H_2SO_4 , the main source of which is usually considered to be sulfur dioxide (SO_2). SO_2 is photochemically oxidized in the atmosphere by an oxidizing agent produced by solar radiation, such as hydroxyl radical (OH) (Kulmala et al., 2014). H_2SO_4 produced via this route is here termed *secondary H_2SO_4* . Sources of regional SO_2 include shipping, power generation, atmospheric oxidation of dimethyl sulfide,
10 and volcanic activity. Additionally, motor vehicles emit SO_2 due to sulfur-containing fuels and lubricant oils; hence, also traffic can contribute to the secondary H_2SO_4 levels. A part of SO_2 formed during combustion is oxidized to H_2SO_4 already in vehicles' oxidative exhaust after-treatment systems (Arnold et al., 2012), which makes vehicles direct H_2SO_4 emitters. In contrast to the secondary H_2SO_4 formed via photochemistry, H_2SO_4 formed in hot exhaust without the need of solar radiation is here termed *primary H_2SO_4* . In principle, primary H_2SO_4 can also contribute to the atmospheric H_2SO_4 concentrations, at
15 least in the vicinity of traffic.

Ambient aerosol particles are either emitted directly into the atmosphere as primary particles or new particles are formed from atmospheric precursor gases in a new particle formation (NPF) process. NPF processes have been shown to occur in a variety of environments, and their occurrence is believed to be controlled by, on one hand, by the availability of particle-forming vapors and, on the other hand, by the reduction of the vapors and fresh cluster-sized nuclei due to pre-existing aerosol surface
20 area acting as a condensation sink (CS) (McMurry and Friedlander, 1979; Kerminen et al., 2018). The observations that many urban areas display high numbers of NCA particles have been puzzling because aerosol in this size range has generally been associated with NPF processes, which are unexpected due to high CS in urban areas.

Simultaneously, an evidence has been mounting that the exhaust of road vehicles often contains high numbers of particles in the nucleation mode size range (5–50 nm) (Kittelson, 1998) and, recently, that traffic is a direct source of NCA-sized particles
25 (Rönkkö et al., 2017). A recent study by Yao et al. (2018) presented data of high NCA concentrations in a highly polluted urban area, with an interpretation that they are formed in a regional NPF process. Here, this view is contrasted and complemented by presenting data from a one-month measurement campaign performed in May 2017 at curbside of a densely trafficked street in an urban area of Helsinki, Finland. NCA concentration data from this curbside measurement have already been analyzed by Hietikko et al. (2018) with the conclusion of traffic inducing a dominant signal on NCA concentrations, according to diurnal
30 variation and wind direction. Here, we extend the analysis with the data of H_2SO_4 concentrations and solar irradiances (SI) to distinguish interfering processes of traffic and regional NPF on NCA concentrations. [The \$H_2SO_4\$ measurement at the curbside connects urban \$H_2SO_4\$ concentrations to traffic sources quantitatively, for the first time. The data provide reference data for primary \$H_2SO_4\$ emission data and the ability to determine emission factors of vehicles in a real-world driving situation.](#)

Prescribed primary emissions in current regional and global aerosol models do not include particles in the smallest size
35 range (Paasonen et al., 2016). The NCA-sized particle concentrations in models are therefore mainly driven by photochem-

ical NPF processes, omitting the directly emitted NCA-sized particles. Due to the unknown chemical composition of the traffic-originated NCA-sized particles, significant NCA-related health risks cannot be excluded. Especially for solid NCA, their behavior inside the body, such as penetrating directly into brains through the olfactory nerve (Maher et al., 2016), may have hitherto unknown adverse effects. Measuring the composition of NCA particles directly is very challenging with current technologies due to very small particle size and thus very low mass of NCA particles. An alternative way to study particle composition is to study the formation mechanism of the particles, which is one objective of this study.

2 Methods

2.1 Measurement site

The measurement site was located at a street canyon at Mäkelänkatu about 3 km north of the city center of Helsinki, Finland (Fig. 1). The devices for gas and aerosol measurements were installed in two containers next to each other (Fig. 2) located at the curbside of the street canyon.

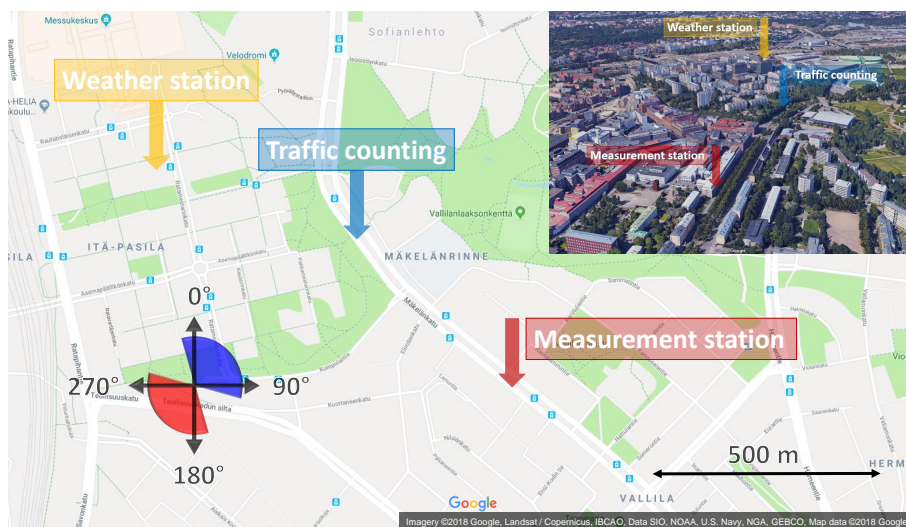


Figure 1. The map of the measurement site. Red and blue sectors denote the wind directions which result in the flow field coming from the street direction and from the background direction, respectively, towards the measurement container.

Traffic count was measured in 15 min time resolution by the City of Helsinki at the same street but 600 m north of the measurement containers. Environmental parameters, such as wind velocity, wind direction, SI, air temperature, pressure, relative humidity, and precipitation, were measured at a weather station on the rooftop of a 53 m high building 900 m northwest of the measurement containers. The location of the weather station provided measurement data which are undisturbed by other buildings but the location was still sufficiently near to the measurement containers to provide representative values.

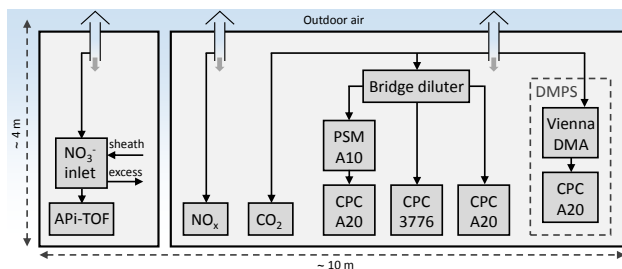


Figure 2. The measurement setup inside the containers at the curbside of the street canyon.

The street canyon consists of three lanes for cars to both directions, two rows of trees, two tramlines, and two pavements, resulting in total width of 42 m and height of 17 m (Kuuluvainen et al., 2018). Due to the vortex affecting the flow field in a street canyon, the wind direction at the measurement containers was considered opposite to the direction above the roofs (Ahmad et al., 2005). Therefore, the wind direction diagram in Fig. 1 is mirrored by the street canyon axis. However, the street canyon in this case is not a regular street canyon but a wide avenue canyon and it has a displaced building near the measurement location. This can cause some errors to the actual flow field interpreted using the mirrored wind direction, and the effect of wind direction on the measured emissions is not seen as clearly as in an open environment or in a regular street canyon.

The measurement setup inside the containers is shown in Fig. 2. Outdoor air samples to the measurement devices were drawn through the roof of the containers 4 m above the ground, using vertical probes having diameters of 50 mm and flow rates higher than 200 lpm to minimize losses onto the walls of the sampling lines.

2.2 Sulfuric acid measurements

H_2SO_4 was measured in the gas phase using a nitrate-ion-based (NO_3^- -based) chemical ionization atmospheric pressure interface time-of-flight mass spectrometer (CI-API-TOF; Aerodyne Research Inc.; USA and ToFwerk AG, Switzerland; Jokinen et al., 2012). It consists of a chemical ionization (CI) inlet (Eisele and Tanner, 1993) and an API-TOF mass spectrometer (Junninen et al., 2010).

The CI-inlet was operated by ionizing small concentration of nitric acid (HNO_3) vapor in the sheath air using X-ray to produce NO_3^- ions. The sheath air flow rate to the CI-inlet was 20 lpm and it was generated in two ways: during the first two weeks, a small pump followed by an HEPA filter was used; and during the last two weeks, an oil-lubricated compressor followed by a coarse particle, an oil, a water droplet, an HEPA, and an activated carbon filters was used. The excess flow from the CI-inlet using a vacuum pump had a flow rate of 30 lpm, resulting in the sample flow rate of 10 lpm to the inlet.

H_2SO_4 is detected in the CI-API-TOF as bisulfate ions (HSO_4^-) and as HSO_4^- ions clustered with HNO_3 through the following reactions:





where $n = 0, 1, \dots$. The H_2SO_4 concentrations are calculated with the equation:

$$[\text{H}_2\text{SO}_4] = \quad (1)$$

$$5 \quad \frac{C}{P} \cdot \frac{\{\text{HSO}_4^-\} + \{\text{HSO}_4^- \cdot \text{HNO}_3\} + \{\text{HSO}_4^- \cdot \text{H}_2\text{SO}_4\}}{\{\text{NO}_3^-\} + \{\text{NO}_3^- \cdot \text{HNO}_3\} + \{\text{NO}_3^- \cdot (\text{HNO}_3)_2\}}$$

where C is the calibration coefficient for H_2SO_4 , P is the penetration efficiency of H_2SO_4 in the sampling lines, and the $\{\}$ -braces denote the areas of the peaks at corresponding mass-to-charge ratios in the high-resolution spectra measured by the TOF mass spectrometer. The calibration coefficient was determined by generating known concentrations of H_2SO_4 using the oxidation of SO_2 by OH radical (Kürten et al., 2012). The calibration coefficient was determined for the both sheath air generations: the values are $C = 1.3 \times 10^9 \text{ cm}^{-3}$ for the pump-based sheath air and $C = 9.1 \times 10^9 \text{ cm}^{-3}$ for the compressor-based sheath air. The values differ due to different purities of the sheath air.

The diffusional losses (Brockmann, 2005) of H_2SO_4 in the sampling lines were calculated with the diffusion coefficient of $0.071 \text{ cm}^2/\text{s}$ representing the diffusion coefficient of a hydrated H_2SO_4 molecule in the relative humidity of 60% and temperature of 283 K (Chapman and Cowling, 1954; Hanson and Eisele, 2000). The calculated penetrations are $P = 0.30$ when pump-based sheath air was used and $P = 0.22$ when compressor-based sheath air was used. These values differ because minor changes to the sampling lines were also done when the compressor was installed.

The H_2SO_4 concentrations from zero measurements are subtracted from the measured H_2SO_4 concentrations. The zero measurements were done by using the sheath air as a sample to obtain the H_2SO_4 concentration originated from the sheath air generation. The H_2SO_4 concentrations during the zero measurements were $3.7 \times 10^5 \text{ cm}^{-3}$ with the pump-based sheath air and $1.8 \times 10^6 \text{ cm}^{-3}$ with the compressor-based sheath air. Due to the limitations of space inside the containers, higher level of purification for the sheath air was not available.

The data from the API-TOF was recorded with the time resolution of 2 s, but at least 1 min of the raw data is required for averaging to obtain feasible high-resolution spectra.

2.3 Gas measurements

25 Nitric oxide (NO) and nitrogen dioxide (NO_2) concentrations were measured using Horiba APNA-370 and the data were recorded with a time resolution of 1 min. In this study, only the sum of NO and NO_2 concentrations, denoted as NO_x concentration, is used in the analysis. Carbon dioxide (CO_2) concentration was measured using LI-COR LI-7000 analyzer with a time resolution of 1 s.

30 The Because traffic density and the concentrations of emissions at the curbside are not directly correlated due to turbulent flow field and variable wind directions causing the emissions to be diluted in a different extent at the measurement location, a traffic-originated tracer is needed to connect the observed concentrations quantitatively to traffic emissions. An ideal tracer is

one that is universally emitted by all vehicles and is not altered in the atmosphere during the time scale of the exhaust plume dilution process. CO_2 is emitted by all combustion engines, with the emission rate proportional to the fuel consumption; thus, it is used as a tracer in determining emission factors of traffic. The drawback of CO_2 as a traffic tracer is its varying background concentration due to regional-level phenomena. The background concentration is also higher than the concentration increase of traffic. As the main source of NO_x concentration is used to represent the concentration of in urban areas is traffic (Clapp and Jenkin, 2001), the background concentration is low and causes thus no significant uncertainty to the traffic-originated emissions overall, because it traffic contribution. However, the drawback of NO_x is its varying emission rates across the whole vehicle fleet (Yli-Tuomi et al., 2005). Concluding, we decided to use NO_x as the traffic tracer, except in the emission factor analysis where CO_2 is used due to its direct connection to the fuel consumption.

The NO_x concentration ($[\text{NO}_x]$) correlates well with the traffic density on weekdays (Fig. 3). However, on weekends, much stronger dilution conditions during daytime compared to nighttime are seen. During nighttime, there is a peak in the NO_x concentration though it is nonexistent in traffic density, which suggests stagnant weather conditions coincided at nighttime on weekends for the considered time range. The concentration would represent the amount of combusted fuel better than the NO_x concentration; however, because traffic does not cause a clear signal on the measured concentration due to a high and varying background level, the NO_x concentration was selected to represent the traffic-originated emissions overall. The NO_x concentrations were higher during the morning rush hours than during the afternoon rush hours on weekdays although the traffic density behaved oppositely, which occurs because, during the morning rush hours, traffic was concentrated on the same side of the street as the measurement containers located providing a shorter distance, and thus less dilution, for the emissions to travel to the measurement devices.

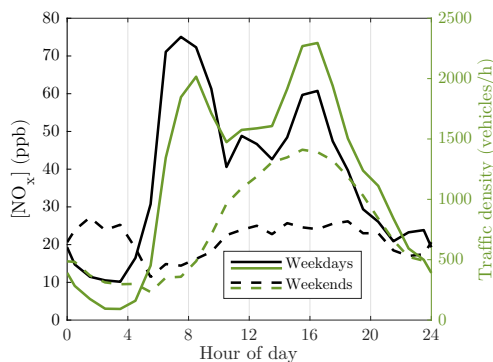


Figure 3. Average diurnal variations of nitrogen oxides (NO_x) concentration, representing the concentration of the traffic-originated emissions overall, and traffic density. The NO_x concentration data measured with 1 min time resolution are firstly averaged to 1 h time-resolution; secondly, the averaged data from different days are averaged geometrically due to for the specific hours. Geometric averages are used for emissions, instead of arithmetic averages, because the logarithmic nature of the concentrations would cause skewed frequency distributions; thus, the highest concentrations would be weighted more than the lower ones. Arithmetic averaging is used for the traffic density.

2.4 Particle measurements

The number concentration of particles with the diameters larger than approximately 1.2 nm were measured using an Airmodus A10 Particle Size Magnifier (PSM A10) (Vanhanen et al., 2011) with a diethylene glycol saturator flow rate of 1.3 lpm followed by an Airmodus A20 Condensation Particle Counter (CPC A20). Particles larger than 3 and 7 nm were measured using a TSI 5 3776 Condensation Particle Counter (CPC 3776) and another Airmodus CPC A20, respectively. The particle size distribution between 6 and 800 nm was measured using a Differential Mobility Particle Sizer (DMPS) consisting of a Vienna-type Differential Mobility Analyzer (DMA) followed by a CPC A20. Due to high particle concentrations at the street canyon, the sample to CPCs was diluted using a bridge diluter having a dilution ratio of 8.2. The dilution ratio for the specific diluter is, however, measured for larger particle sizes only, and because the diluter is based on diffusional losses of the particles, the dilution ratio 10 for NCA-sized particles is higher. Therefore, the NCA concentrations reported here represent the lower limits of the actual concentrations.

The number concentration of nanocluster aerosol (NCA), particles within the diameter range between 1.2 and 3 nm, can be calculated by subtracting the concentration measured by the CPC 3776 from the concentration measured by the PSM. The particle size distribution between 1.2 nm and 800 nm can be calculated with the data from all these aerosol measurement 15 devices by taking the cut diameters of the CPCs and the dilution ratio of the bridge diluter into account. The NCA concentration was measured with a time resolution of 1 s and the size distribution with a time resolution of 9 min.

3 Results and discussion

The data from the off-site measurements of traffic count and environmental parameters are available for the whole four-week measurement campaign starting on 4 May 2017 and ending on 31 May 2017 (see the Supplement for the time series). This 20 time range provided adequate data for examining NCA and H_2SO_4 formation respect to solar irradiance, because there were sufficient amounts of days both with clear sky and with cloud cover, yet without too many rainy days. There are some gaps in the NCA and H_2SO_4 data during the four weeks due to unavailability of the measurement devices. The data analysis considers only the time ranges for which all the measurement data are available, resulting in three weeks of data.

Figure 4 presents our proposal for the updated mechanism of H_2SO_4 and particle formation in traffic-influenced areas, 25 based on our measurement results. The most noteworthy details are illustrated with red crosses indicating H_2SO_4 routes which were observed to occur barely only, or not at all. As shown later in this section, our measurement at the curbside displays no clear increase in gaseous H_2SO_4 concentrations with increasing traffic volumes, ~~indicating~~. With the fact that vehicles do emit primary H_2SO_4 (Arnold et al., 2012; Rönkkö et al., 2013), it is evident that the majority of primary H_2SO_4 ~~is~~ must be converted to the particle phase via nucleation ~~and condensation~~ (route 1A) and condensation (1B) rapidly after emission. Conversely, secondary H_2SO_4 potentially remains longer in urban atmosphere because it does not experience conditions favoring such a rapid gas-to-particle conversion, i.e., rapid temperature decrease, high precursor concentrations, and high pre-existing CS. Therefore, the signal of H_2SO_4 measured from the curbside of the street is mainly due to secondary H_2SO_4 only. 30

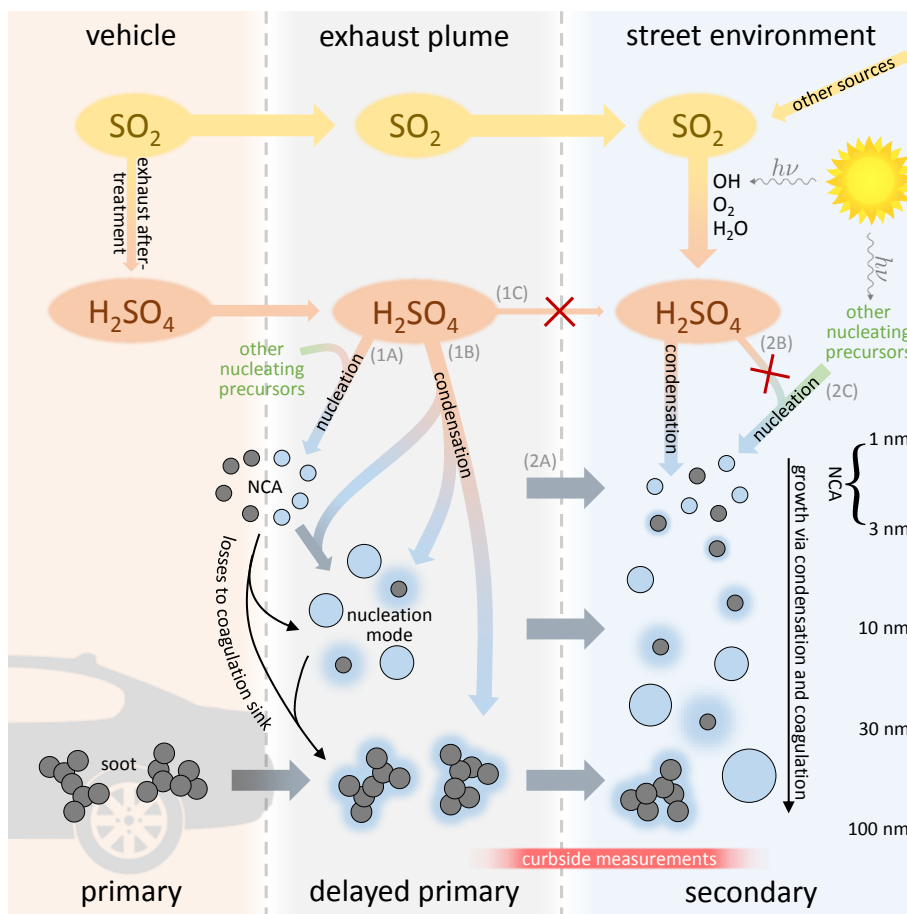


Figure 4. Proposed mechanism of sulfuric acid and particle formation in traffic-influenced areas. The route of primary H_2SO_4 to urban atmosphere (route 1C) is largely terminated to particle phase rapidly after the emission (routes 1A and 1B). Conversely, secondary H_2SO_4 remains in urban atmosphere because it does not experience such a rapid gas-to-particle conversion. NCA presence in urban atmosphere is majorly controlled by traffic emissions (route 2A) and only marginally by nucleation from secondary precursors (routes 2B and 2C), especially the contribution of nucleation from secondary H_2SO_4 (route 2B) is noticeably overridden by traffic emissions (route 2A).

Our results show that both traffic and regional NPF influence NCA concentrations at the urban traffic site, with direct NCA emission from traffic dominating. Comparison of the NCA and H_2SO_4 concentrations with SI and traffic density suggests that while solar radiation favors higher NCA concentrations, the photochemically produced H_2SO_4 may not be the key compound in the presence of NCA in urban areas. Traffic-originated NCA particles may be formed via a delayed primary emission route by rapid nucleation of low-volatile gaseous compounds emitted by vehicles during exhaust cooling after releasing from the tailpipe (1A). On the other hand, they may be solid particles emitted directly by engines, via a primary emission route (Sgro et al., 2012; Alanen et al., 2015). Although it is likely that both nucleation (1A) and condensation (1B) routes from primary H_2SO_4 exist because nucleation mode particle number concentrations and particle sizes are correlated with the H_2SO_4 concentration in exhaust (Arnold et al., 2012; Rönkkö et al., 2013), the ratio of the routes at our measurement site is not determined. Neither is the ratio of NCA particles emitted primarily and through the nucleation route (1A) determined. Therefore, the relative proportion of H_2SO_4 in traffic-originated NCA particles remains unknown, leading to the possibility of solid NCA emissions.

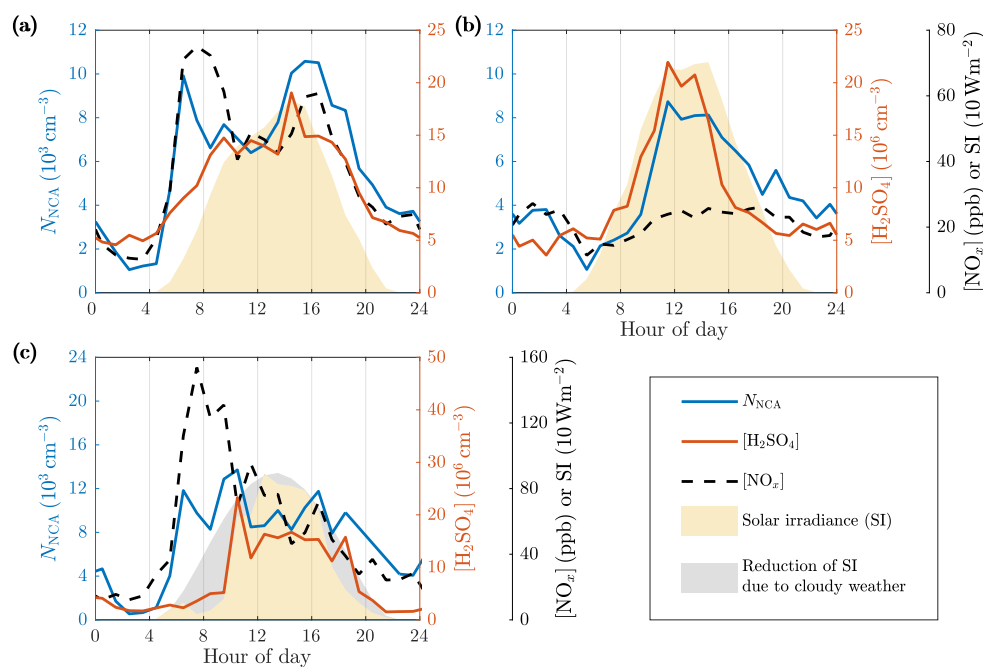


Figure 5. Average diurnal variations of the NCA, H_2SO_4 , and NO_x concentrations and solar irradiance (SI) on (a) weekdays, (b) weekends, and (c) example day 5/22/2017 with cloudy morning and evening. The concentration data are firstly averaged to 1 h time resolution; secondly, the data from different days are averaged geometrically (except SI) due to the logarithmic nature of the concentrations of the emissions as described in Fig. 3.

The first evidence for traffic-contributed concentrations of NCA (N_{NCA}) and H_2SO_4 was found in the diurnal variations of the NCA, H_2SO_4 , and NO_x concentrations and SI (Fig. 5). The diurnal variations on weekdays (Fig. 5a) differ from the diurnal variations on weekends (Fig. 5b). The main difference between weekdays and weekends are traffic volumes; therefore, such a difference in the concentrations of NCA and H_2SO_4 should only be expected if their formation are in some manner connected to traffic. The connection of NCA to traffic is further strengthened by comparing it to the NO_x concentrations, which are directly linked to traffic densities and traffic-related emissions (Fig. 3). On weekdays, the NCA concentration increased in tandem with the NO_x concentration during the morning rush hours. On weekends, the NCA concentration increased at noontime much more clearly than the NO_x concentration. This can be interpreted as a sign of an ongoing regional NPF process producing NCA particles with high SI. On weekdays, the regional NPF process should only produce higher NCA concentration during afternoon rush hours having higher SI compared to morning. The increased NCA concentrations during the morning rush hours suggest that the traffic-originated NCA does not require solar radiation to form.

We observed that, traffic levels influence the H_2SO_4 concentrations, but they are still mainly controlled by solar radiation. In contrast to the NCA concentration, the H_2SO_4 concentration traced SI much more closely, with a maximum at noontime and minimum at night. On weekdays, a peak in the H_2SO_4 concentration during afternoon rush hours suggests that traffic might also influence the formation of H_2SO_4 . Further evidence for this is found by comparing the diurnal variation of H_2SO_4 between weekdays and weekends. On weekends, the H_2SO_4 concentration increased not until the traffic density and the NO_x concentration were also increased, whereas on weekdays, the traffic density was already high when SI and the H_2SO_4 concentration began to increase. Furthermore, higher irradiances were required on weekends before the rise in the H_2SO_4 concentration and, additionally, the order of the increase in the NCA and H_2SO_4 concentrations was switched.

The time series show that NCA is not similarly controlled by solar radiation but rather by traffic. This is clearly showcased in Fig. 5c which presents data from a day with cloudy weather reducing SI in the morning and in the evening but still with a constant wind direction. The NCA concentration closely traced traffic levels in the morning, whereas the H_2SO_4 concentration only increased when SI increased hours later. This clearly shows that the formation of NCA, in this case, is independent of SI and the H_2SO_4 concentration. It is also noteworthy that no increase in the NCA concentration is observed when SI increased, suggesting that traffic dominated in the NCA formation. There were also other days with cloudiness decreasing SI with similar observations; however, the example day in Fig. 5c was the day with the most clear effect of cloudiness on SI and the reduction of SI coincides with morning rush hours, displaying high NCA concentrations.

The data suggest that the formation of atmospheric H_2SO_4 is strongly enhanced in the presence of both traffic and sunlight. While a strong correlation between the NCA and NO_x concentrations (Fig. 6a, b: Pearson's $R = 0.84$) confirms the connection between NCA and traffic, a remarkably weaker, but also positive, correlation between the H_2SO_4 and NO_x concentrations ($R = 0.50$) was observed, revealing the connection between H_2SO_4 and traffic. The effect of SI at different traffic densities (data averaged to 17 different SI bins for three different x -concentration ranges) shows differing patterns for NCA (Fig. 6c) and H_2SO_4 (Fig. 6d). While high SI is associated with higher NCA and H_2SO_4 levels, traffic density determines the base level for both (the concentrations at zero SI). For H_2SO_4 , the influence of traffic causes a marked increase in the slope of the H_2SO_4 concentration-SI-line. The slope can be interpreted as the production efficiency of H_2SO_4 via photochemistry. It is evident that

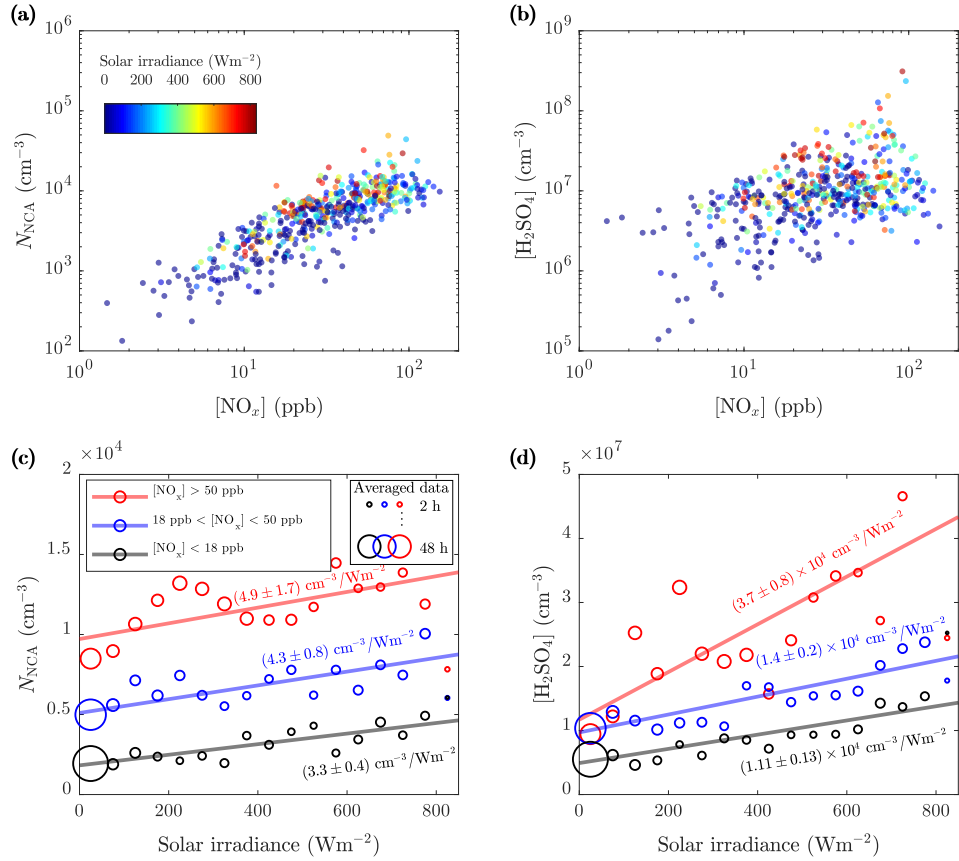


Figure 6. One-hour-averages-1-hour-averages of the (a) NCA and (b) H₂SO₄ concentrations as a function of the NO_x concentration colored by the solar irradiance (SI) and 10-min-averages of the (c) NCA and (d) H₂SO₄ concentrations further averaged to 17 different SI bins (bin width is chosen to provide clear graphical representation) for three NO_x concentration ranges. The slopes of Weighted least squares fitting, with data point count in bin-averaging (shown with the circle diameters) as weighs, for the bin-averaged values was done to output linear fits. The slopes are marked in the figure and are not largely affected by the chosen bin width. The amount of the averaged data to specific bins intercepts are shown with (c) $(0.182 \pm 0.013) \times 10^4 \text{ cm}^{-3}$, $(0.51 \pm 0.03) \times 10^4 \text{ cm}^{-3}$, and $(0.97 \pm 0.07) \times 10^4 \text{ cm}^{-3}$; and (d) $(0.49 \pm 0.04) \times 10^7 \text{ cm}^{-3}$, $(0.97 \pm 0.06) \times 10^7 \text{ cm}^{-3}$, and $(1.2 \pm 0.3) \times 10^7 \text{ cm}^{-3}$, for the radii of lowest, the circles mid-ranged, and are also used as weighting factors for the linear fitting highest NO_x concentration range, respectively.

for NCA, the influence of traffic dominates in comparison to SI, as the traffic-influenced NCA concentration (red data) exceeds the non-traffic concentrations (black data) even during dark times. For H_2SO_4 , the situation is different, as all dark-period H_2SO_4 concentrations are close to equal levels. These differing patterns suggest that the majority of NCA in traffic-influenced areas is formed independently of secondary H_2SO_4 , in contrast to the findings of Yao et al. (2018).

5 Even more compelling evidence for traffic-originated NCA and H_2SO_4 can be found by comparing the observed concentrations to ~~momentary~~ CO_2 concentrations ~~-. Such a comparison for measurements near emission sources has been shown to directly represent a fuel-based emission factor using the emission factor of ,3.14 kg per 1 kg of fuel combusted (Yli-Tuomi et al., 2005)([CO₂]).~~ In Fig. 7, no apparent difference in the emission factors of NCA for different SI are seen; however, in the case of H_2SO_4 , higher SI lead to noticeably higher emission factors of H_2SO_4 . We tested for potential correlations between SI and traffic density to examine potential traffic level increase with simultaneous SI increase due to their almost similar diurnal cycles. We found no clear correlation between CO_2 concentration and SI (Fig. 8)~~that would have led to the misinterpretation of NCA and formation via traffic instead of solar radiation. This result again supports S5). In a case of a found correlation, the slopes in Fig. 7 could not have been interpreted as emission factors, but as photochemical production due to accelerated photochemistry with higher SI values. Although the varying background concentration of CO_2 causes uncertainty in analyzing the contribution of traffic on emissions, linear dependencies are still observed in Fig. 7. These results again support~~ the finding that solar radiation is required for the formation of H_2SO_4 from traffic emissions and demonstrates clearly that both NCA and H_2SO_4 originate from traffic. This is further supported by examining the concentrations in different wind directions (Figs. 9 and 10) which shows that the highest concentrations ~~are~~ were measured when the wind blew from the street.

20 While the emission factors can depend markedly on vehicle, engine, fuel, and after-treatment system types, the emission factors obtained here represent the average fleet-level values and can thus be moderately applicable in regional and global aerosol models at least for areas with the same average fleet composition as in our measurement site in Helsinki. However, more research is needed to obtain emission factors separated into the different types.

The annual CO_2 emission rate from traffic in Helsinki in 2017 was $5.38 \times 10^8 \text{ kgCO}_2 \cdot \text{a}^{-1}$ (VTT Technical Research Centre of Finland Ltd, 2017). Using the average NCA emission factor versus CO_2 emission, $2.21 \times 10^{14} \text{ kgCO}_2^{-1}$, a rough estimation on the annual NCA emission from traffic in Helsinki becomes $1.19 \times 10^{23} \text{ a}^{-1}$. The annual NCA formation rate via photochemical NPF in Helsinki can be approximated using estimates of nucleation rate, from 1 to $10 \text{ cm}^{-3}\text{s}^{-1}$, NPF event day count per year, from 30 to 120 a^{-1} , NPF duration, from 2 to 4 h, measured in a rural area in Hyytiälä, Finland (Dal Maso et al., 2005; Kulmala and Kerminen, 2008) and in an urban area in Helsinki (Hussein et al., 2008), the total area of Helsinki, 30 214 km^2 , and a rough estimate for the boundary layer height, 500 m. Multiplying these gives the estimation of the annual NCA formation rate from 0.23×10^{23} to $18.5 \times 10^{23} \text{ a}^{-1}$. Comparison of these annual rates suggests that in minimum of 6 % but even up to 84 % of NCA particles ~~originates~~ are estimated to originate from traffic in Helsinki on an annual basis. Although this range is wide, the contribution of traffic-originated NCA is significant.

Another estimation for the traffic contribution on NCA (and also on H_2SO_4) in urban air can be performed using the linear fits from Fig. 6. Considering typical weekday noontime at our measurement location and assuming the annual mean of the

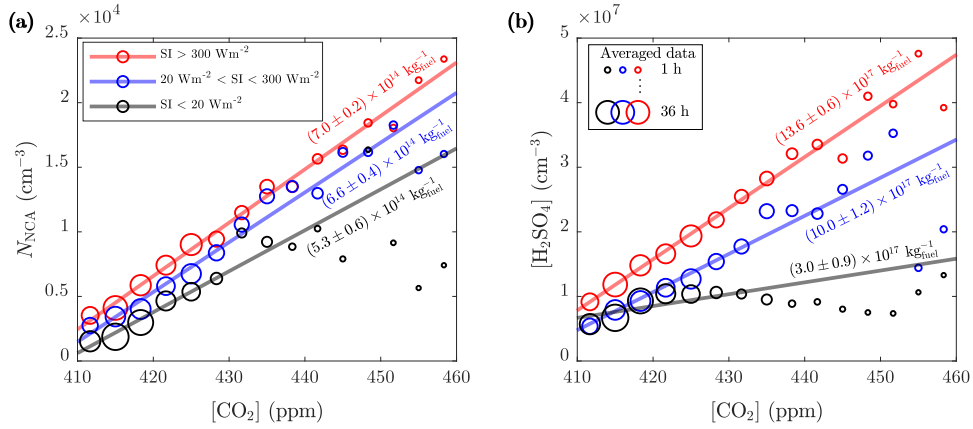


Figure 7. 1-min-averages of the (a) NCA and (b) H_2SO_4 concentrations further averaged to CO_2 concentration bins for three SI ranges (see Fig. 6 for the details in averaging and linear regression). The slopes of the linear fits converted to kilograms of fuel combusted (using the emission factor of CO_2 , 3.14 kg per 1 kg of fuel combusted (Yli-Tuomi et al., 2005)) are marked in the figure. The amount intercepts of the averaged data to specific bins fits at 410 ppm are shown with (a) $(0.07 \pm 0.04) \times 10^4 \text{ cm}^{-3}$, $(0.15 \pm 0.05) \times 10^4 \text{ cm}^{-3}$ and $(0.25 \pm 0.03) \times 10^4 \text{ cm}^{-3}$; and (b) $(0.67 \pm 0.07) \times 10^7 \text{ cm}^{-3}$, $(0.49 \pm 0.15) \times 10^7 \text{ cm}^{-3}$, and $(0.79 \pm 0.06) \times 10^7 \text{ cm}^{-3}$, for the radii of lowest, the circles mid-ranged, and are also used as weighting factors for the linear fitting highest SI range, respectively.

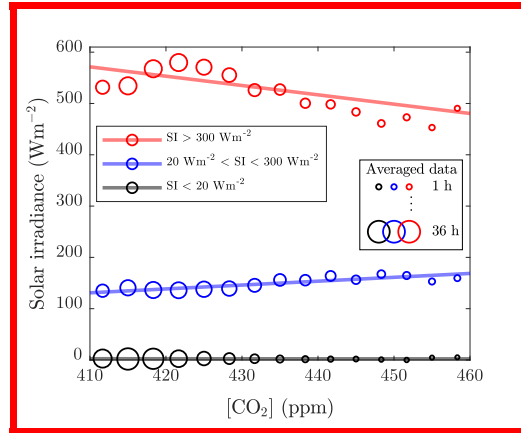


Figure 8. moved to the Supplement. 1-min-averages of the solar irradiances (SI) as a function of concentration for the SI ranges used in Fig. 7. The amount of the averaged data to specific bins are shown with the radii of the circles and are also used as weighting factors for the linear fitting.

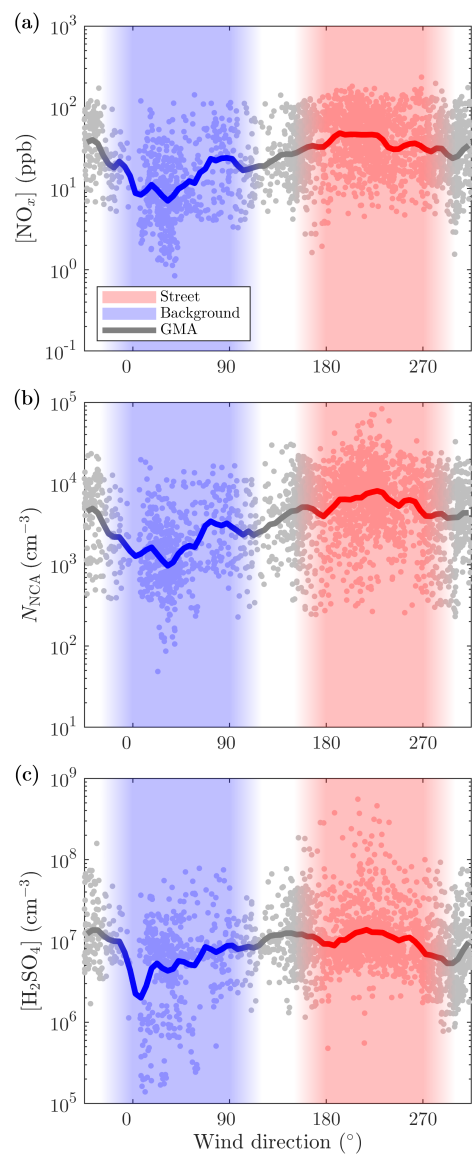


Figure 9. 10-min-averages of the (a) NO_x , (b) NCA, and (c) H_2SO_4 concentrations measured with different wind directions. Wind velocities smaller than 0.5 m/s are excluded. GMA denotes geometric moving average.

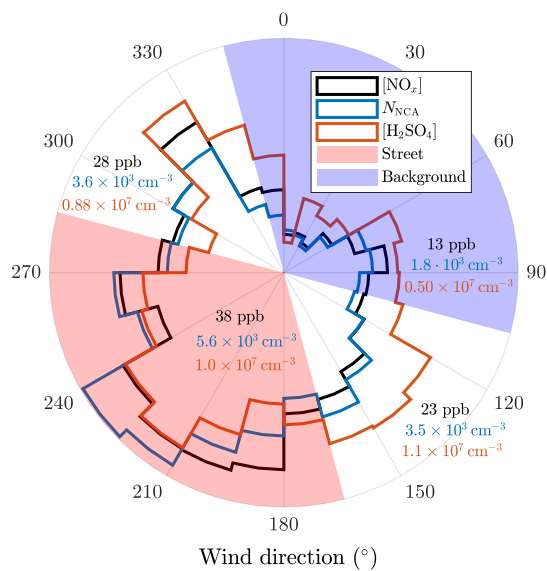


Figure 10. 10-min-averages of the NO_x, NCA, and H₂SO₄ concentrations further averaged to different wind direction sectors. Wind velocities smaller than 0.5 m/s are excluded. The geometric averages of the concentrations across the sectors are shown in the figure.

daytime maximum SI in Helsinki, 500 Wm^{-2} , the NCA concentration due to traffic is $\sim 9.5 \times 10^3 \text{ cm}^{-3} \sim 9.7 \times 10^3 \text{ cm}^{-3}$ (the value of the high NO_x line at zero irradiance in Fig. 6) and the increase of the NCA concentration due to photochemistry is $\sim 1.7 \times 10^3 \text{ cm}^{-3}$ (calculated with the slope of the low NO_x line in Fig. 6). These concentrations indicate that approximately 85 % of the total NCA concentration at the street canyon is originated from traffic at noontime. Considering midsummer and midwinter, the daytime maximum SI are 850 Wm^{-2} and 100 Wm^{-2} , giving the contributions of $\sim 78 \%$ and $\sim 97 \%$, respectively. Therefore, it is evident that the major fraction of NCA originated from traffic at our measurement location, even with the highest available SI values in midsummer.

For H₂SO₄, the concentration due to traffic at our measurement location at typical weekday noontime is $\sim 12 \times 10^6 \text{ cm}^{-3}$ and the increase of the concentration due to photochemistry is $\sim 5.6 \times 10^6 \text{ cm}^{-3}$, indicating approximately 68 % of the total H₂SO₄ concentration at the street canyon is originating from local traffic at noontime. For midsummer and midwinter, the contributions become $\sim 56 \%$ and $\sim 92 \%$, respectively. These values signify that also the major fraction of H₂SO₄ originated from traffic even though it cannot be seen as clearly from the diurnal variation as is seen in the case of NCA.

Because regional NPF events are frequently suppressed by high condensation sinks (Kerminen et al., 2018), decreasing condensation sink can lead to a NPF event, resulting in particle number concentration increase. However, our data display no clear anticorrelations of this kind (see Fig. S6). This again implies that regional NPF events cannot clearly be distinguished from the data measured in a vicinity of dense traffic.

Traffic-emitted NCA poses a potential health risk because the observed NCA concentrations are valid at the curbside of the street, which is the location where pedestrians spend time in traffic. Spreading of the NCA particles emitted on the streets can be approximated with particle lifetimes. The lifetimes can be estimated using coagulation sinks (CoagS) and the time constants of coagulation scavenging (τ_{CoagS}), which is the inverse of CoagS, calculated as in Kulmala et al. (2001). Assuming no other losses of the particles, such as self-coagulation and condensational growth out from the NCA size range, and no mixing of the emitted aerosol with the background aerosol, τ_{CoagS} represents the lifetime of the particles. The estimated lifetimes were in the scale of several minutes, resulting in a spreading possibility of the NCA particles around urban areas. The diurnal variations of CoagS and τ_{CoagS} are presented in Fig. S2.

Our data clearly demonstrate that NCA-sized particle concentrations in a traffic-influenced environment is controlled by NCA directly emitted by traffic. The data also demonstrate that while generally NCA and photochemically produced nucleating vapor concentrations correlate, this correlation is likely, firstly, due to increased traffic volumes at daytime and, secondly, due to traffic-originated H_2SO_4 and other nucleating vapors. We also showed that H_2SO_4 formation is driven by both solar radiation and a traffic-related source.

4 Conclusions

Our results have several implications on our understanding of aerosol particle formation in traffic-influenced areas. Firstly, because current regional and global air quality models do not include particles in the sub-3 nm size range as primary emissions (Paasonen et al., 2016), the modelled NCA-sized particle concentrations are mainly driven by photochemical NPF processes, neglecting their origin from traffic as primary sources. Thus, our results show an urgent need to update these emissions. In light of our results, it seems evident that there will be areas in which direct emissions dominate the formation of new aerosol.

A rough calculation gives that, on an annual basis, up to 84 % of NCA can originate from traffic in Helsinki; and according to the measured NCA concentrations, on typical weekday noontime, ~85 % of the total NCA concentration was contributed by traffic at our studied site. In wintertime, this contribution may reach ~97 % due to lower SI, which highlights the need for updating the annual particle formation cycles in the models. Secondly, our results also show that both traffic emission and regional NCA formation signals can be distinguished for the most of the times, and that traffic also influences the formation of

H_2SO_4 . Together with the findings of Yao et al. (2018), this presents a significant update on the particle formation mechanisms in urban areas. As illustrated in Fig. 4, the particle concentration is controlled by the interplay of the two processes, with varying importance depending on the proximity of the emission source. Our results call for reconsideration and re-analysis of observations of NPF events observed in traffic-influenced areas. In many cases, there is covariance between traffic volumes and SI, and care should be taken to separate these two variables in the analysis, e.g., by considering CO_2 or NO_x as tracers

for traffic volumes. Finally, potential health effects of traffic emissions in urban areas should also be considered more carefully because the composition of the emitted NCA particles is still unknown, especially as some clues for their non-volatility exist.

Data availability. The time series data are freely available at: (the link will be shown when the manuscript is accepted)

Author contributions. MD, TR, JVN, and HJT. designed the research. MO, HK, MA, JK, NK, and MI, performed the measurements. MO, HK, NK, and MI analyzed the data. MO prepared the manuscript with contribution from all co-authors.

Competing interests. The authors declare no conflict of interest.

- 5 *Acknowledgements.* We thank the tofTools team for providing tools for mass spectrometry analysis and Prof. Mikko Sipilä from the University of Helsinki for lending the chemical ionization inlet for the atmospheric pressure interface time-of-flight mass spectrometer. Dr. Harri Portin and Dr. Anu Kousa from Helsinki Region Environmental Services Authority (HSY) as well as the HSY's AQ measurement team are acknowledged for their valuable work related to the data quality control and measurements at the Mäkelänkatu supersite. Mr. Petri Blomqvist from the City of Helsinki is acknowledged for the traffic count data. The research has received funding from Tekes - the Finnish Funding Agency for Innovation (Grant no. 2883/31/2015), HSY, and Pegasor Oy, who funded the research through the Cityzer project, the graduate school of Tampere University of Technology, and Academy of Finland for Profi 4 (Grant no. 318940) and infrastructure funding (Grant no. 273010).
- 10

References

- Ahmad, K., Khare, M., and Chaudhry, K.: Wind tunnel simulation studies on dispersion at urban street canyons and intersections—a review, *J. Wind Eng. Ind. Aerod.*, 93, 697–717, <https://doi.org/10.1016/j.jweia.2005.04.002>, 2005.
- Alanen, J., Saukko, E., Lehtoranta, K., Murtonen, T., Timonen, H., Hillamo, R., Karjalainen, P., Kuuluvainen, H., Harra, J., Keskinen, J., and Rönkkö, T.: The formation and physical properties of the particle emissions from a natural gas engine, *Fuel*, 162, 155–161, <https://doi.org/10.1016/j.fuel.2015.09.003>, 2015.
- Arnth, A., Unger, N., Kulmala, M., and Andreae, M.: Clean the air, heat the planet?, *Science*, 326, 672–673, <https://doi.org/10.1126/science.1181568>, 2009.
- Arnold, F., Pirjola, L., Rönkkö, T., Reichl, U., Schlager, H., Lähde, T., Heikkilä, J., and Keskinen, J.: First online measurements of sulfuric acid gas in modern heavy-duty diesel engine exhaust: Implications for nanoparticle formation, *Environ. Sci. Technol.*, 46, 11 227–11 234, <https://doi.org/10.1021/es302432s>, 2012.
- Beelen, R., Raaschou-Nielsen, O., Stafoggia, M., Andersen, Z., Weinmayr, G., Hoffmann, B., Wolf, K., Samoli, E., Fischer, P., Nieuwenhuijsen, M., Vineis, P., Xun, W., Katsouyanni, K., Dimakopoulou, K., Oudin, A., Forsberg, B., Modig, L., Havulinna, A., Lanki, T., Turunen, A., Oftedal, B., Nystad, W., Nafstad, P., De Faire, U., Pedersen, N., Östenson, C.-G., Fratiglioni, L., Penell, J., Korek, M., Pershagen, G., Eriksen, K., Overvad, K., Ellermann, T., Eeftens, M., Peeters, P., Meliefste, K., Wang, M., Bueno-De-Mesquita, B., Sugiri, D., Krämer, U., Heinrich, J., De Hoogh, K., Key, T., Peters, A., Hampel, R., Concin, H., Nagel, G., Ineichen, A., Schaffner, E., Probst-Hensch, N., Künzli, N., Schindler, C., Schikowski, T., Adam, M., Phuleria, H., Vilier, A., Clavel-Chapelon, F., Declercq, C., Grioni, S., Krogh, V., Tsai, M.-Y., Ricceri, F., Sacerdote, C., Galassi, C., Migliore, E., Ranzi, A., Cesaroni, G., Badaloni, C., Forastiere, F., Tamayo, I., Amiano, P., Dorronsoro, M., Katsoulis, M., Trichopoulou, A., Brunekreef, B., and Hoek, G.: Effects of long-term exposure to air pollution on natural-cause mortality: An analysis of 22 European cohorts within the multicentre ESCAPE project, *Lancet*, 383, 785–795, [https://doi.org/10.1016/S0140-6736\(13\)62158-3](https://doi.org/10.1016/S0140-6736(13)62158-3), 2014.
- Brockmann, J. E.: Sampling and Transport of Aerosols, in: *Aerosol Measurement: Principles, Techniques, and Applications*, edited by Baron, P. A. and Willeke, K., pp. 143–195, John Wiley & Sons, Hoboken, USA, 2nd edn., 2005.
- Chapman, S. and Cowling, T.: *The Mathematical Theory of Non-uniform Gases. An account of the kinetic theory of viscosity, thermal conduction, and diffusion in gases*, Cambridge University Press, Cambridge, UK, 2nd edn., 1954.
- Clapp, L. J. and Jenkin, M. E.: Analysis of the relationship between ambient levels of O₃, NO₂ and NO as a function of NO_x in the UK, *Atmos. Environ.*, 35, 6391–6405, [https://doi.org/10.1016/S1352-2310\(01\)00378-8](https://doi.org/10.1016/S1352-2310(01)00378-8), 2001.
- Dal Maso, M., Kulmala, M., Riipinen, I., Wagner, R., Hussein, T., Aalto, P., and Lehtinen, K.: Formation and growth of fresh atmospheric aerosols: eight years of aerosol size distribution data from SMEAR II, Hyytiälä, Finland, *Bor. Env. Res.*, 10, 323–336, 2005.
- Dockery, D., Pope III, C., Xu, X., Spengler, J., Ware, J., Fay, M., Ferris Jr., B., and Speizer, F.: An association between air pollution and mortality in six U.S. cities, *New Engl. J. Med.*, 329, 1753–1759, <https://doi.org/10.1056/NEJM199312093292401>, 1993.
- Eisele, F. L. and Tanner, D. J.: Measurement of the gas phase concentration of H₂SO₄ and methane sulfonic acid and estimates of H₂SO₄ production and loss in the atmosphere, *J. Geophys. Res. Atmos.*, 98, 9001–9010, <https://doi.org/10.1029/93JD00031>, 1993.
- Hanson, D. R. and Eisele, F.: Diffusion of H₂SO₄ in Humidified Nitrogen: Hydrated H₂SO₄, *J. Phys. Chem. A*, 104, 1715–1719, <https://doi.org/10.1021/jp993622j>, 2000.

- Hietikko, R., Kuuluvainen, H., Harrison, R. M., Portin, H., Timonen, H., Niemi, J. V., and Rönkkö, T.: Diurnal variation of nanocluster aerosol concentrations and emission factors in a street canyon, *Atmos. Environ.*, 189, 98–106, <https://doi.org/10.1016/j.atmosenv.2018.06.031>, 2018.
- Hussein, T., Martikainen, J., Junninen, H., Sogacheva, L., Wagner, R., Dal Maso, M., Riipinen, I., Aalto, P., and Kulmala, M.: Observation of regional new particle formation in the urban atmosphere, *Tellus*, 60, 509–521, <https://doi.org/10.1111/j.1600-0889.2008.00365.x>, 2008.
- Jokinen, T., Sipilä, M., Junninen, H., Ehn, M., Lönn, G., Hakala, J., Petäjä, T., Mauldin III, R. L., Kulmala, M., and Worsnop, D. R.: Atmospheric sulphuric acid and neutral cluster measurements using CI-API-TOF, *Atmos. Chem. Phys.*, 12, 4117–4125, <https://doi.org/10.5194/acp-12-4117-2012>, 2012.
- Junninen, H., Ehn, M., Petäjä, T., Luosujärvi, L., Kotiaho, T., Kostianen, R., Rohner, U., Gonin, M., Fuhrer, K., Kulmala, M., and Worsnop, D. R.: A high-resolution mass spectrometer to measure atmospheric ion composition, *Atmos. Meas. Tech.*, 3, 1039–1053, <https://doi.org/10.5194/amt-3-1039-2010>, 2010.
- Kerminen, V.-M., Chen, X., Vakkari, V., Petäjä, T., Kulmala, M., and Bianchi, F.: Atmospheric new particle formation and growth: review of field observations, *Environ. Res. Lett.*, 13, 103 003, <https://doi.org/10.1088/1748-9326/aadf3c>, 2018.
- Kittelson, D.: Engines and nanoparticles: A review, *J. Aerosol Sci.*, 29, 575–588, [https://doi.org/10.1016/S0021-8502\(97\)10037-4](https://doi.org/10.1016/S0021-8502(97)10037-4), 1998.
- Kontkanen, J., Lehtipalo, K., Ahonen, L., Kangasluoma, J., Manninen, H. E., Hakala, J., Rose, C., Sellegri, K., Xiao, S., Wang, L., Qi, X., Nie, W., Ding, A., Yu, H., Lee, S., Kerminen, V.-M., Petäjä, T., and Kulmala, M.: Measurements of sub-3 nm particles using a particle size magnifier in different environments: from clean mountain top to polluted megacities, *Atmos. Chem. Phys.*, 17, 2163–2187, <https://doi.org/10.5194/acp-17-2163-2017>, 2017.
- Kulmala, M. and Kerminen, V.-M.: On the formation and growth of atmospheric nanoparticles, *Atmos. Res.*, 90, 132–150, <https://doi.org/10.1016/j.atmosres.2008.01.005>, 2008.
- Kulmala, M., Dal Maso, M., Mäkelä, J. M., Pirjola, L., Väkevä, M., Aalto, P., Miikkulainen, P., Hämeri, K., and O’Dowd, C. D.: On the formation, growth and composition of nucleation mode particles, *Tellus B*, 53, 479–490, <https://doi.org/10.1034/j.1600-0889.2001.530411.x>, 2001.
- Kulmala, M., Kontkanen, J., Junninen, H., Lehtipalo, K., Manninen, H., Nieminen, T., Petäjä, T., Sipilä, M., Schobesberger, S., Rantala, P., Franchin, A., Jokinen, T., Järvinen, E., Äijälä, M., Kangasluoma, J., Hakala, J., Aalto, P., Paasonen, P., Mikkilä, J., Vanhanen, J., Aalto, J., Hakola, H., Makkonen, U., Ruuskanen, T., Mauldin III, R., Duplissy, J., Vehkamäki, H., Bäck, J., Kortelainen, A., Riipinen, I., Kurtén, T., Johnston, M., Smith, J., Ehn, M., Mentel, T., Lehtinen, K., Laaksonen, A., Kerminen, V.-M., and Worsnop, D.: Direct observations of atmospheric aerosol nucleation, *Science*, 339, 943–946, <https://doi.org/10.1126/science.1227385>, 2013.
- Kulmala, M., Petäjä, T., Ehn, M., Thornton, J., Sipilä, M., Worsnop, D., and Kerminen, V.-M.: Chemistry of Atmospheric Nucleation: On the Recent Advances on Precursor Characterization and Atmospheric Cluster Composition in Connection with Atmospheric New Particle Formation, *Annu. Rev. Phys. Chem.*, 65, 21–37, <https://doi.org/10.1146/annurev-physchem-040412-110014>, 2014.
- Kürten, A., Rondo, L., Ehrhart, S., and Curtius, J.: Calibration of a Chemical Ionization Mass Spectrometer for the Measurement of Gaseous Sulfuric Acid, *J. Phys. Chem. A*, 116, 6375–6386, <https://doi.org/10.1021/jp212123n>, 2012.
- Kuuluvainen, H., Poikkimäki, M., Järvinen, A., Kuula, J., Irjala, M., Maso, M. D., Keskinen, J., Timonen, H., Niemi, J. V., and Rönkkö, T.: Vertical profiles of lung deposited surface area concentration of particulate matter measured with a drone in a street canyon, *Environ. Pollut.*, 241, 96–105, <https://doi.org/10.1016/j.envpol.2018.04.100>, 2018.
- Lehtipalo, K., Yan, C., Dada, L., Bianchi, F., Xiao, M., Wagner, R., Stolzenburg, D., Ahonen, L. R., Amorim, A., Baccarini, A., Bauer, P. S., Baumgartner, B., Bergen, A., Bernhammer, A.-K., Breitenlechner, M., Brilke, S., Buchholz, A., Mazon, S. B., Chen, D., Chen, X., Dias,

- A., Dommen, J., Draper, D. C., Duplissy, J., Ehn, M., Finkenzeller, H., Fischer, L., Frege, C., Fuchs, C., Garmash, O., Gordon, H., Hakala, J., He, X., Heikkinen, L., Heinritzi, M., Helm, J. C., Hofbauer, V., Hoyle, C. R., Jokinen, T., Kangasluoma, J., Kerminen, V.-M., Kim, C., Kirkby, J., Kontkanen, J., Kürten, A., Lawler, M. J., Mai, H., Mathot, S., Mauldin, R. L., Molteni, U., Nichman, L., Nie, W., Nieminen, T., Ojdanic, A., Onnela, A., Passananti, M., Petäjä, T., Piel, F., Pospisilova, V., Quéléver, L. L. J., Rissanen, M. P., Rose, C., Sarnela, N., Schallhart, S., Schuchmann, S., Sengupta, K., Simon, M., Sipilä, M., Tauber, C., Tomé, A., Tröstl, J., Väisänen, O., Vogel, A. L., Volkamer, R., Wagner, A. C., Wang, M., Weitz, L., Wimmer, D., Ye, P., Ylisirniö, A., Zha, Q., Carslaw, K. S., Curtius, J., Donahue, N. M., Flagan, R. C., Hansel, A., Riipinen, I., Virtanen, A., Winkler, P. M., Baltensperger, U., Kulmala, M., and Worsnop, D. R.: Multicomponent new particle formation from sulfuric acid, ammonia, and biogenic vapors, *Sci. Adv.*, 4, eaau5363, <https://doi.org/10.1126/sciadv.aau5363>, 2018.
- 5
- 10 Maher, B. A., Ahmed, I. A. M., Karloukovski, V., MacLaren, D. A., Foulds, P. G., Allsop, D., Mann, D. M. A., Torres-Jardón, R., and Calderon-Garciduenas, L.: Magnetite pollution nanoparticles in the human brain, *P. Natl. Acad. Sci. USA*, 113, 10797–10801, <https://doi.org/10.1073/pnas.1605941113>, 2016.
- McMurry, P. and Friedlander, S.: New particle formation in the presence of an aerosol, *Atmos. Environ.*, 13, 1635–1651, [https://doi.org/10.1016/0004-6981\(79\)90322-6](https://doi.org/10.1016/0004-6981(79)90322-6), 1979.
- 15 Paasonen, P., Nieminen, T., Asmi, E., Manninen, H., Petäjä, T., Plass-Dülmer, C., Flentje, H., Birmili, W., Wiedensohler, A., Horrak, U., Metzger, A., Hamed, A., Laaksonen, A., Facchini, M., Kerminen, V.-M., and Kulmala, M.: On the roles of sulphuric acid and low-volatility organic vapours in the initial steps of atmospheric new particle formation, *Atmos. Chem. Phys.*, 10, 11223–11242, <https://doi.org/10.5194/acp-10-11223-2010>, 2010.
- Paasonen, P., Kupiainen, K., Klimont, Z., Visschedijk, A., Denier van der Gon, H. A. C., and Amann, M.: Continental anthropogenic primary particle number emissions, *Atmos. Chem. Phys.*, 16, 6823–6840, <https://doi.org/10.5194/acp-16-6823-2016>, 2016.
- 20 Pope, C., Burnett, R., Thun, M., Calle, E., Krewski, D., Ito, K., and Thurston, G.: Lung cancer, cardiopulmonary mortality, and long-term exposure to fine particulate air pollution, *J. Amer. Med. Assoc.*, 287, 1132–1141, <https://doi.org/10.1001/jama.287.9.1132>, 2002.
- Rönkkö, T., Lähde, T., Heikkilä, J., Pirjola, L., Bauschke, U., Arnold, F., Schlager, H., Rothe, D., Yli-Ojanperä, J., and Keskinen, J.: Effects of gaseous sulphuric acid on diesel exhaust nanoparticle formation and characteristics, *Environ. Sci. Technol.*, 47, 11882–11889, <https://doi.org/10.1021/es402354y>, 2013.
- 25 Rönkkö, T., Kuuluvainen, H., Karjalainen, P., Keskinen, J., Hillamo, R., Niemi, J. V., Pirjola, L., Timonen, H. J., Saarikoski, S., Saukko, E., Järvinen, A., Silvennoinen, H., Rostedt, A., Olin, M., Yli-Ojanperä, J., Nousiainen, P., Kousa, A., and Dal Maso, M.: Traffic is a major source of atmospheric nanocluster aerosol, *P. Natl. Acad. Sci. USA*, 114, 7549–7554, <https://doi.org/10.1073/pnas.1700830114>, 2017.
- Sgro, L. A., Sementa, P., Vaglieco, B. M., Rusciano, G., D’Anna, A., and Minutolo, P.: Investigating the origin of nuclei particles in GDI engine exhausts, *Combust. Flame*, 159, 1687–1692, <https://doi.org/10.1016/j.combustflame.2011.12.013>, 2012.
- 30 Vanhanen, J., Mikkilä, J., Lehtipalo, K., Sipilä, M., Manninen, H. E., Siivola, E., Petäjä, T., and Kulmala, M.: Particle size magnifier for nano-CN detection, *Aerosol Sci. Tech.*, 45, 533–542, <https://doi.org/10.1080/02786826.2010.547889>, 2011.
- VTT Technical Research Centre of Finland Ltd: LIPASTO unit emissions -database, last access: 15 January 2019, available at: <http://lipasto.vtt.fi/yksikkopaastot/>, 2017.
- 35 Yao, L., Garmash, O., Bianchi, F., Zheng, J., Yan, C., Kontkanen, J., Junninen, H., Mazon, S. B., Ehn, M., Paasonen, P., Sipilä, M., Wang, M., Wang, X., Xiao, S., Chen, H., Lu, Y., Zhang, B., Wang, D., Fu, Q., Geng, F., Li, L., Wang, H., Qiao, L., Yang, X., Chen, J., Kerminen, V.-M., Petäjä, T., Worsnop, D. R., Kulmala, M., and Wang, L.: Atmospheric new particle formation from sulfuric acid and amines in a Chinese megacity, *Science*, 361, 278–281, <https://doi.org/10.1126/science.aao4839>, 2018.

- Yli-Tuomi, T., Aarnio, P., Pirjola, L., Mäkelä, T., Hillamo, R., and Jantunen, M.: Emissions of fine particles, NO_x, and CO from on-road vehicles in Finland, *Atmos. Environ.*, 39, 6696–6706, <https://doi.org/10.1016/j.atmosenv.2005.07.049>, 2005.
- Zhao, J., Smith, J. N., Eisele, F. L., Chen, M., Kuang, C., and McMurry, P. H.: Observation of neutral sulfuric acid-amine containing clusters in laboratory and ambient measurements, *Atmos. Chem. Phys.*, 11, 10 823–10 836, <https://doi.org/10.5194/acp-11-10823-2011>, 2011.

Condensation sink calculation

Condensation sink (CS) is calculated using the function (Kulmala et al., 2001):

$$CS = 2\pi\mathcal{D} \int_0^{\infty} \beta(D_p) \cdot D_p \cdot \frac{dN}{d\log D_p}(D_p) \cdot d\log D_p \quad (\text{S1})$$

where \mathcal{D} is the diffusion coefficient of the condensing vapor and $\beta(D_p)$ and $\frac{dN}{d\log D_p}(D_p)$ are the transition regime correction factor (Fuchs and Sutugin, 1971) and particle number size distribution at particle diameter of D_p , respectively. CS is in most cases calculated only for H_2SO_4 (Lehtinen et al., 2007) but here it is calculated also for two other vapors generally participating in NPF processes (Kerminen et al., 2018): one with a high \mathcal{D} (ammonia, NH_3) and one with a low \mathcal{D} (a low volatile organic compound with a high molecular mass, $\text{C}_{19}\text{H}_{28}\text{O}_{11}$, Ehn et al., 2014). Time series of CS for H_2SO_4 is presented in Fig. S4 and the diurnal variations of CS for all three calculated condensing vapors in Fig. S1.

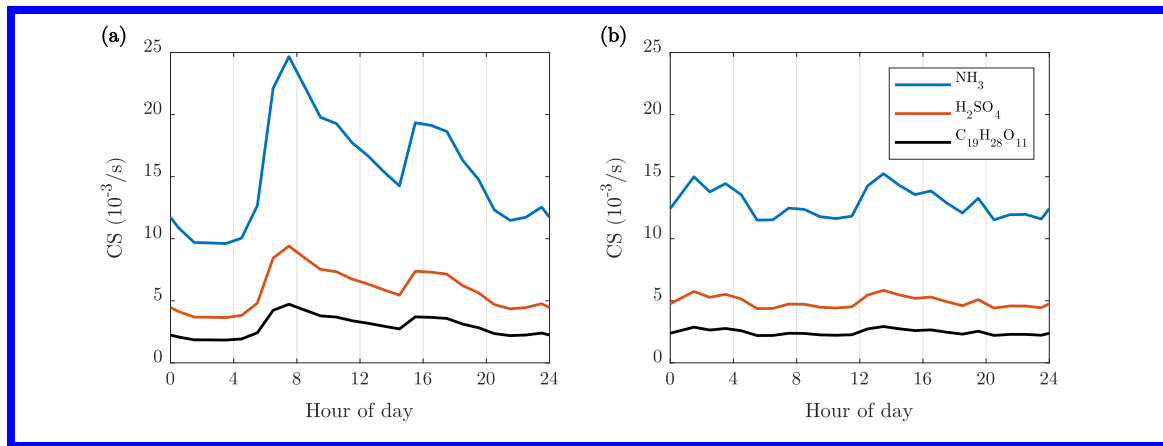


Figure S1. Diurnal variations of CS for different condensing vapors participating in NPF processes, (a) on weekdays and (b) on weekends.

Coagulation sink calculation

Coagulation sink (CoagS) for a particle diameter of D'_p is calculated using the function (Dal Maso et al., 2005):

$$\text{CoagS}(D'_p) = \int_0^{\infty} K(D_p, D'_p) \cdot \frac{dN}{d \log D_p}(D_p) \cdot d \log D_p \quad (\text{S2})$$

where $K(D_p, D'_p)$ is the coagulation coefficient of particles with the diameters of D_p and D'_p . CoagS and its inverse, coagulation time constant (τ_{CoagS}), for the smallest and largest measured NCA particles are presented in Fig. S2.

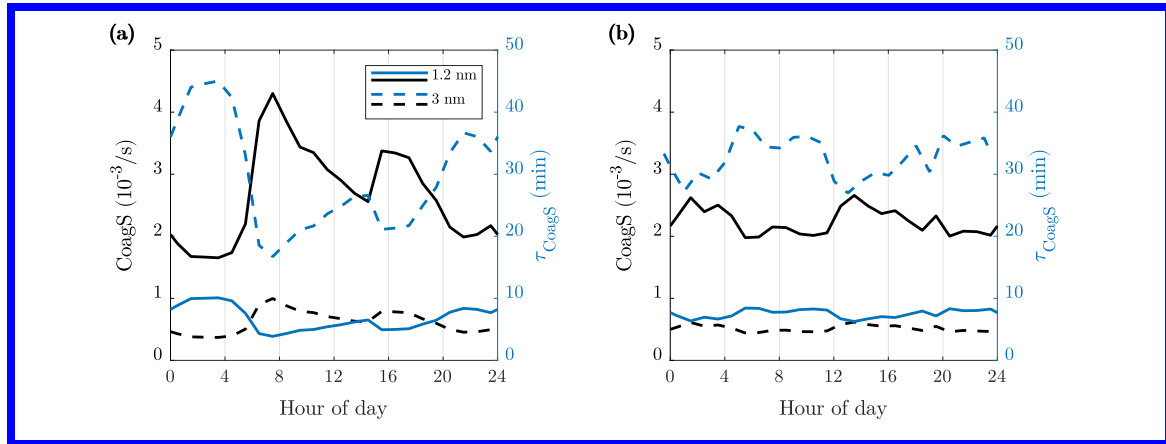


Figure S2. Diurnal variations of coagulation sinks and coagulation time constants for 1.2 nm and 3 nm particles, (a) on weekdays and (b) on weekends.

Time series

Figures S3 and S4 present the time series of all analyzed quantities.

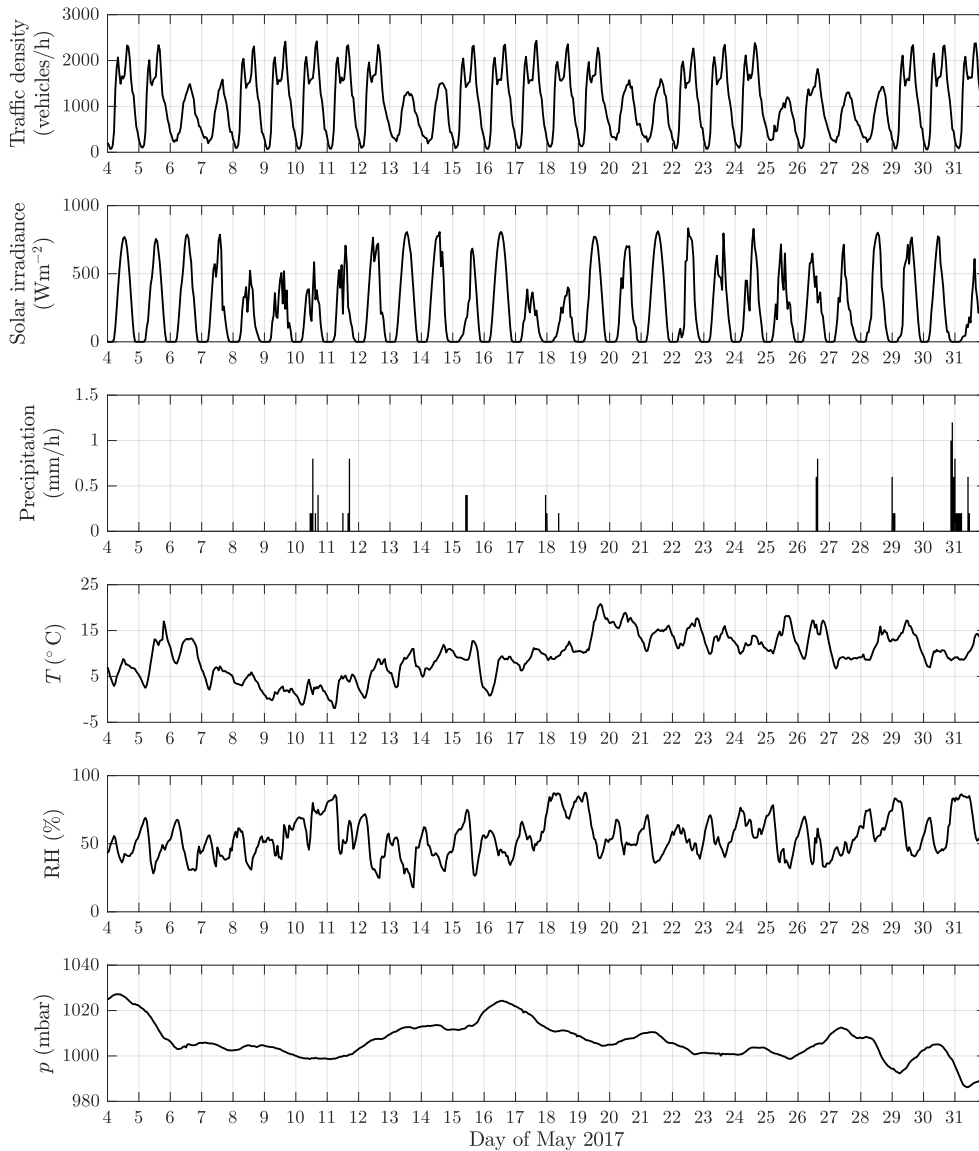


Figure S3. Time series of traffic density, solar irradiance, precipitation, temperature (T), relative humidity (RH), and atmospheric pressure (p).

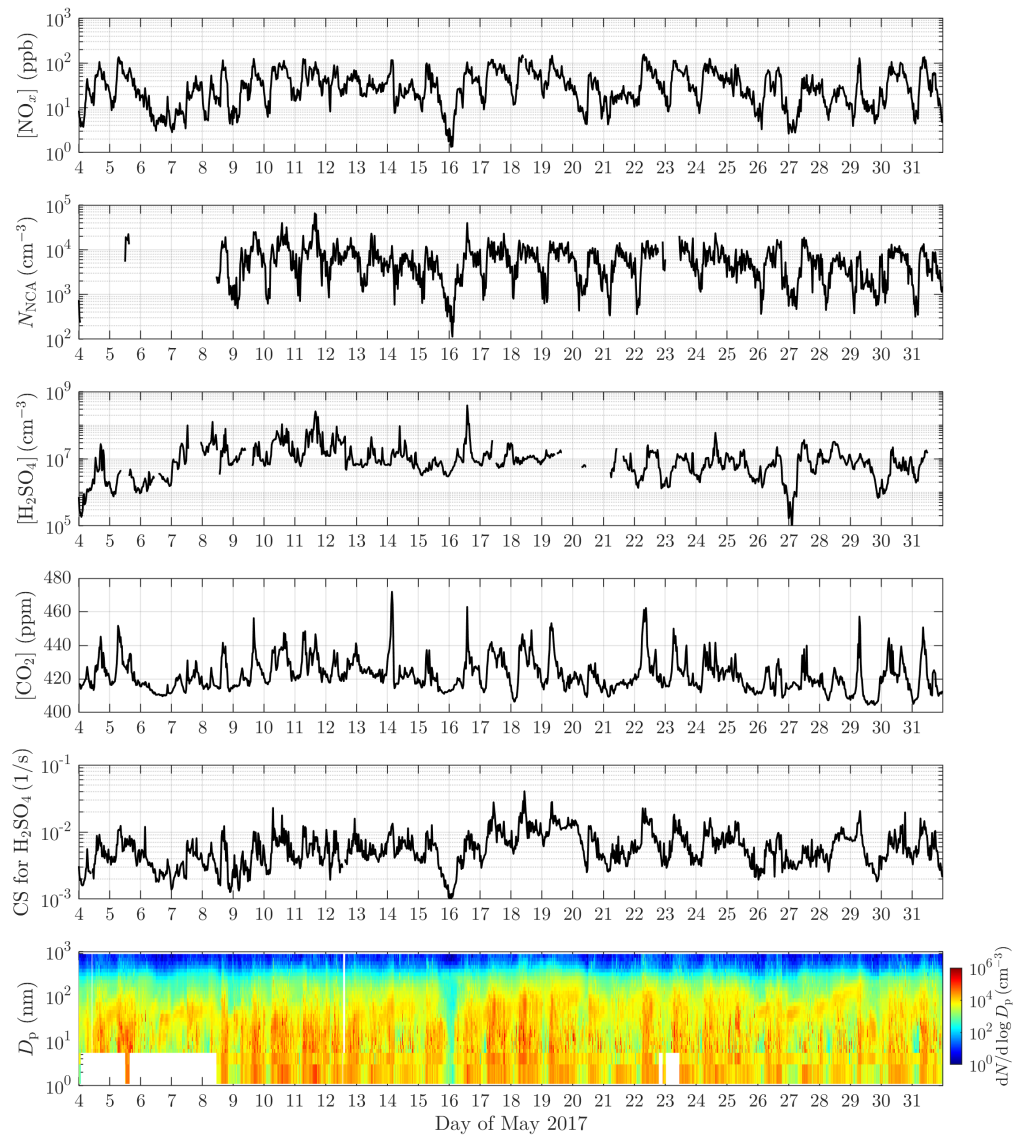


Figure S4. Time series of the NO_x , NCA, H_2SO_4 , and CO_2 concentrations, condensation sink (CS) for H_2SO_4 , and particle size distribution. The size distributions include data from PSM, CPC 3776, CPC A20, and DMPS.

Solar irradiance as a function of CO₂ concentration

Figure S5 presents solar irradiance as a function of CO₂ concentration for the same SI ranges used in Fig. 7.

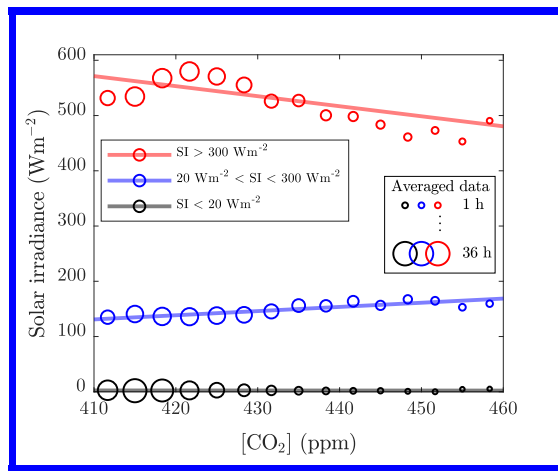


Figure S5. Moved from the manuscript. 1-min-averages of solar irradiance (SI) as a function of CO₂ concentration for the SI ranges used in Fig. 7 (see Fig. 6 for the details in averaging and linear regression).

Comparison of the NCA concentration and condensation sink time series

Figure S6 presents the time series of the NCA concentration and CS for H_2SO_4 together.

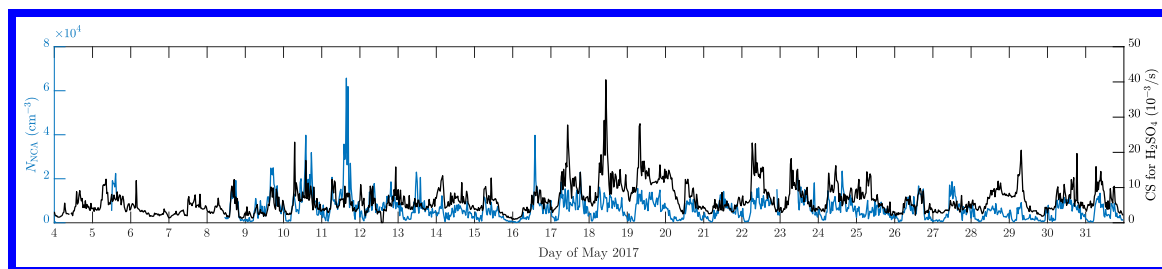


Figure S6. Time series of the NCA concentration and CS for H_2SO_4 .

References

- Dal Maso, M., Kulmala, M., Riipinen, I., Wagner, R., Hussein, T., Aalto, P., and Lehtinen, K.: Formation and growth of fresh atmospheric aerosols: eight years of aerosol size distribution data from SMEAR II, Hyytiälä, Finland, *Bor. Env. Res.*, 10, 323–336, 2005.
- Ehn, M., Thornton, J., Kleist, E., Sipilä, M., Junninen, H., Pullinen, I., Springer, M., Rubach, F., Tillmann, R., Lee, B., Lopez-Hilfiker, F., Andres, S., Acir, I.-H., Rissanen, M., Jokinen, T., Schobesberger, S., Kangasluoma, J., Kontkanen, J., Nieminen, T., Kurtén, T., Nielsen, L., Jørgensen, S., Kjaergaard, H., Canagaratna, M., Maso, M., Berndt, T., Petäjä, T., Wahner, A., Kerminen, V.-M., Kulmala, M., Worsnop, D., Wildt, J., and Mentel, T.: A large source of low-volatility secondary organic aerosol, *Nature*, 506, 476–479, <https://doi.org/10.1038/nature13032>, 2014.
- Fuchs, N. and Sutugin, A.: High-Dispersed Aerosols, in: *Topics in Current Aerosol Research*, edited by Hidy, G. and Brock, J., International Reviews in Aerosol Physics and Chemistry, p. 1, Pergamon, Oxford, UK, <https://doi.org/10.1016/B978-0-08-016674-2.50006-6>, 1971.
- Kerminen, V.-M., Chen, X., Vakkari, V., Petäjä, T., Kulmala, M., and Bianchi, F.: Atmospheric new particle formation and growth: review of field observations, *Environ. Res. Lett.*, 13, 103 003, <https://doi.org/10.1088/1748-9326/aadf3c>, 2018.
- Kulmala, M., Dal Maso, M., Mäkelä, J. M., Pirjola, L., Väkevä, M., Aalto, P., Miikkulainen, P., Hämeri, K., and O’Dowd, C. D.: On the formation, growth and composition of nucleation mode particles, *Tellus B*, 53, 479–490, <https://doi.org/10.1034/j.1600-0889.2001.530411.x>, 2001.
- Lehtinen, K. E. J., Dal Maso, M., Kulmala, M., and Kerminen, V.-M.: Estimating nucleation rates from apparent particle formation rates and vice versa: Revised formulation of the Kerminen-Kulmala equation, *J. Aerosol Sci.*, 38, 988–994, <https://doi.org/10.1016/j.jaerosci.2007.06.009>, 2007.

Traffic-originated nanocluster emission exceeds H₂SO₄-driven photochemical new particle formation in an urban area

Miska Olin¹, Heino Kuuluvainen¹, Minna Aurela², Joni Kalliokoski¹, Niina Kuittinen¹, Mia Isotalo¹, Hilikka J. Timonen², Jarkko V. Niemi³, Topi Rönkkö¹, and Miikka Dal Maso¹

¹Aerosol Physics Laboratory, Physics Unit, Tampere University, FI-33014 Tampere, Finland

²Atmospheric Composition Research, Finnish Meteorological Institute, FI-00101 Helsinki, Finland

³Helsinki Region Environmental Services Authority (HSY), FI-00066 HSY, Finland

Correspondence: Miska Olin (miska.olin@tuni.fi)

Abstract. Elevated ambient concentrations of sub-3 nm particles (nanocluster aerosol, NCA) are generally related to atmospheric new particle formation events, usually linked with gaseous sulfuric acid (H₂SO₄) produced via photochemical oxidation of sulfur dioxide. According to our measurement results of H₂SO₄ and NCA concentrations, traffic density, and solar irradiance at an urban traffic site in Helsinki, Finland, the view of aerosol formation in traffic-influenced environments is updated by presenting two separate and independent pathways of traffic affecting the atmospheric NCA concentrations: by acting as a direct nanocluster source, and by influencing the production of H₂SO₄. As traffic density in many areas is generally correlated with solar radiation, it is likely that the influence of traffic-related nanoclusters has been hidden in the diurnal variation, and is thus underestimated because new particle formation events also follow the diurnal cycle of sunlight. Urban aerosol formation studies should, therefore, be updated to include the proposed formation mechanisms. The formation of H₂SO₄ in urban environments is here separated in two routes: primary H₂SO₄ is formed in hot vehicle exhaust and is converted rapidly to particle phase; secondary H₂SO₄ results from the combined effect of emitted gaseous precursors and available solar radiation. A rough estimation demonstrates that ~ 85% of the total NCA and ~ 68% of the total H₂SO₄ in urban air at noontime at the measurement site are contributed by traffic, indicating the importance of traffic emissions.

Copyright statement.

15 1 Introduction

Urban environments exhibit some of the highest aerosol particle concentrations encountered in the Earth's atmosphere. Elevated particle concentrations are related to adverse health effects (Dockery et al., 1993; Pope et al., 2002; Beelen et al., 2014) and various effects on climate (Arneth et al., 2009). Recent studies on urban aerosol particles have focused attention on the formation process of sub-3 nm particles (Zhao et al., 2011; Kulmala et al., 2013; Kontkanen et al., 2017) also called nanocluster aerosol (NCA) (Rönkkö et al., 2017). The importance of photochemical formation mechanisms, involving, e.g., sulfuric acid (H₂SO₄) and ammonia (Yao et al., 2018) or other photochemically produced vapors (Lehtipalo et al., 2018), has

been highlighted. However, these studies omit the important role of direct emission of NCA-sized particles in their analysis, despite recent findings that traffic is a major source of such particles (Rönkkö et al., 2017). The proposed mechanisms also assume that key precursor vapors are formed via photochemical oxidation (Paasonen et al., 2010; Lehtipalo et al., 2018).

The most important gaseous species forming new particles in the atmosphere is H_2SO_4 , the main source of which is usually considered to be sulfur dioxide (SO_2). SO_2 is photochemically oxidized in the atmosphere by an oxidizing agent produced by solar radiation, such as hydroxyl radical (OH) (Kulmala et al., 2014). H_2SO_4 produced via this route is here termed *secondary H_2SO_4* . Sources of regional SO_2 include shipping, power generation, atmospheric oxidation of dimethyl sulfide, and volcanic activity. Additionally, motor vehicles emit SO_2 due to sulfur-containing fuels and lubricant oils; hence, also traffic can contribute to the secondary H_2SO_4 levels. A part of SO_2 formed during combustion is oxidized to H_2SO_4 already in vehicles' oxidative exhaust after-treatment systems (Arnold et al., 2012), which makes vehicles direct H_2SO_4 emitters. In contrast to the secondary H_2SO_4 formed via photochemistry, H_2SO_4 formed in hot exhaust without the need of solar radiation is here termed *primary H_2SO_4* . In principle, primary H_2SO_4 can also contribute to the atmospheric H_2SO_4 concentrations, at least in the vicinity of traffic.

Ambient aerosol particles are either emitted directly into the atmosphere as primary particles or new particles are formed from atmospheric precursor gases in a new particle formation (NPF) process. NPF processes have been shown to occur in a variety of environments, and their occurrence is believed to be controlled, on one hand, by the availability of particle-forming vapors and, on the other hand, by the reduction of the vapors and fresh cluster-sized nuclei due to pre-existing aerosol surface area acting as a condensation sink (CS) (McMurry and Friedlander, 1979; Kerminen et al., 2018). The observations that many urban areas display high numbers of NCA particles have been puzzling because aerosol in this size range has generally been associated with NPF processes, which are unexpected due to high CS in urban areas.

Simultaneously, evidence has been mounting that the exhaust of road vehicles often contains high numbers of particles in the nucleation mode size range (5–50 nm) (Kittelson, 1998) and, recently, that traffic is a direct source of NCA-sized particles (Rönkkö et al., 2017). A recent study by Yao et al. (2018) presented data of high NCA concentrations in a highly polluted urban area, with an interpretation that they are formed in a regional NPF process. Here, this view is contrasted and complemented by presenting data from a one-month measurement campaign performed in May 2017 at curbside of a densely trafficked street in an urban area of Helsinki, Finland. NCA concentration data from this curbside measurement have already been analyzed by Hietikko et al. (2018) with the conclusion of traffic inducing a dominant signal on NCA concentrations, according to diurnal variation and wind direction. Here, we extend the analysis with the data of H_2SO_4 concentrations and solar irradiances (SI) to distinguish interfering processes of traffic and regional NPF on NCA concentrations. The H_2SO_4 measurement at the curbside connects urban H_2SO_4 concentrations to traffic sources quantitatively, for the first time. The data provide reference data for primary H_2SO_4 emission data and the ability to determine emission factors of vehicles in a real-world driving situation.

Prescribed primary emissions in current regional and global aerosol models do not include particles in the smallest size range (Paasonen et al., 2016). The NCA-sized particle concentrations in models are therefore mainly driven by photochemical NPF processes, omitting the directly emitted NCA-sized particles. Due to the unknown chemical composition of the traffic-originated NCA-sized particles, significant NCA-related health risks cannot be excluded. Especially for solid NCA,

their behavior inside the body, such as penetrating directly into brains through the olfactory nerve (Maher et al., 2016), may have hitherto unknown adverse effects. Measuring the composition of NCA particles directly is very challenging with current technologies due to very small particle size and thus very low mass of NCA particles. An alternative way to study particle composition is to study the formation mechanism of the particles, which is one objective of this study.

5 2 Methods

2.1 Measurement site

The measurement site was located at a street canyon at Mäkelänkatu about 3 km north of the city center of Helsinki, Finland (Fig. 1). The devices for gas and aerosol measurements were installed in two containers next to each other (Fig. 2) located at the curbside of the street canyon.

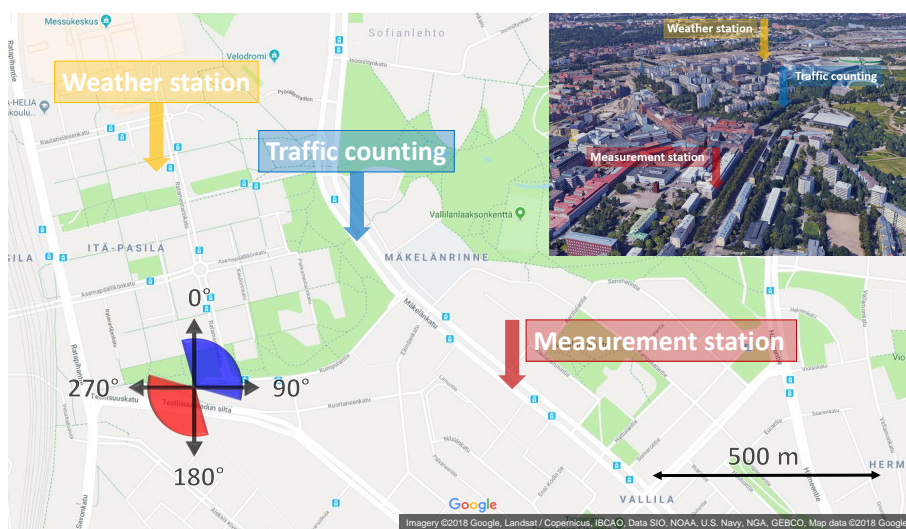


Figure 1. The map of the measurement site. Red and blue sectors denote the wind directions which result in the flow field coming from the street direction and from the background direction, respectively, towards the measurement container.

- 10 Traffic count was measured in 15 min time resolution by the City of Helsinki at the same street but 600 m north of the measurement containers. Environmental parameters, such as wind velocity, wind direction, SI, air temperature, pressure, relative humidity, and precipitation, were measured at a weather station on the rooftop of a 53 m high building 900 m northwest of the measurement containers. The location of the weather station provided measurement data which are undisturbed by other buildings but the location was still sufficiently near to the measurement containers to provide representative values.
- 15 The street canyon consists of three lanes for cars to both directions, two rows of trees, two tramlines, and two pavements, resulting in total width of 42 m and height of 17 m (Kuuluvainen et al., 2018). Due to the vortex affecting the flow field in a street canyon, the wind direction at the measurement containers was considered opposite to the direction above the roofs

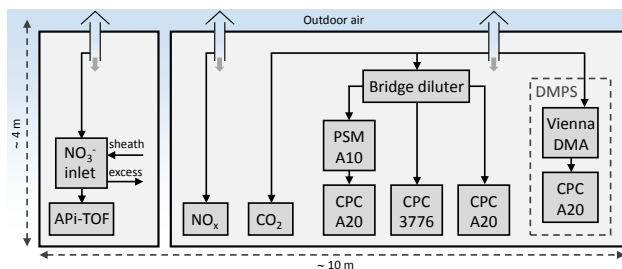


Figure 2. The measurement setup inside the containers at the curbside of the street canyon.

(Ahmad et al., 2005). Therefore, the wind direction diagram in Fig. 1 is mirrored by the street canyon axis. However, the street canyon in this case is not a regular street canyon but a wide avenue canyon and it has a displaced building near the measurement location. This can cause some errors to the actual flow field interpreted using the mirrored wind direction, and the effect of wind direction on the measured emissions is not seen as clearly as in an open environment or in a regular street canyon.

- 5 The measurement setup inside the containers is shown in Fig. 2. Outdoor air samples to the measurement devices were drawn through the roof of the containers 4 m above the ground, using vertical probes having diameters of 50 mm and flow rates higher than 200 lpm to minimize losses onto the walls of the sampling lines.

2.2 Sulfuric acid measurements

H_2SO_4 was measured in the gas phase using a nitrate-ion-based (NO_3^- -based) chemical ionization atmospheric pressure interface time-of-flight mass spectrometer (CI-API-TOF; Aerodyne Research Inc.; USA and ToFwerk AG, Switzerland; Jokinen et al., 2012). It consists of a chemical ionization (CI) inlet (Eisele and Tanner, 1993) and an API-TOF mass spectrometer (Junninen et al., 2010).

The CI-inlet was operated by ionizing small concentration of nitric acid (HNO_3) vapor in the sheath air using X-ray to produce NO_3^- ions. The sheath air flow rate to the CI-inlet was 20 lpm and it was generated in two ways: during the first two weeks, a small pump followed by an HEPA filter was used; and during the last two weeks, an oil-lubricated compressor followed by a coarse particle, an oil, a water droplet, an HEPA, and an activated carbon filters was used. The excess flow from the CI-inlet using a vacuum pump had a flow rate of 30 lpm, resulting in the sample flow rate of 10 lpm to the inlet.

H_2SO_4 is detected in the CI-API-TOF as bisulfate ions (HSO_4^-) and as HSO_4^- ions clustered with HNO_3 through the following reactions:



where $n = 0, 1, \dots$. The H_2SO_4 concentrations are calculated with the equation:

$$[\text{H}_2\text{SO}_4] = \frac{C}{P} \cdot \frac{\{\text{HSO}_4^-\} + \{\text{HSO}_4^- \cdot \text{HNO}_3\} + \{\text{HSO}_4^- \cdot \text{H}_2\text{SO}_4\}}{\{\text{NO}_3^-\} + \{\text{NO}_3^- \cdot \text{HNO}_3\} + \{\text{NO}_3^- \cdot (\text{HNO}_3)_2\}} \quad (1)$$

where C is the calibration coefficient for H_2SO_4 , P is the penetration efficiency of H_2SO_4 in the sampling lines, and the
5 $\{\}$ -braces denote the areas of the peaks at corresponding mass-to-charge ratios in the high-resolution spectra measured by the TOF mass spectrometer. The calibration coefficient was determined by generating known concentrations of H_2SO_4 using the oxidation of SO_2 by OH radical (Kürten et al., 2012). The calibration coefficient was determined for the both sheath air generations: the values are $C = 1.3 \times 10^9 \text{ cm}^{-3}$ for the pump-based sheath air and $C = 9.1 \times 10^9 \text{ cm}^{-3}$ for the compressor-based sheath air. The values differ due to different purities of the sheath air.

10 The diffusional losses (Brockmann, 2005) of H_2SO_4 in the sampling lines were calculated with the diffusion coefficient of $0.071 \text{ cm}^2/\text{s}$ representing the diffusion coefficient of a hydrated H_2SO_4 molecule in the relative humidity of 60% and temperature of 283 K (Chapman and Cowling, 1954; Hanson and Eisele, 2000). The calculated penetrations are $P = 0.30$ when pump-based sheath air was used and $P = 0.22$ when compressor-based sheath air was used. These values differ because minor changes to the sampling lines were also done when the compressor was installed.

15 The H_2SO_4 concentrations from zero measurements are subtracted from the measured H_2SO_4 concentrations. The zero measurements were done by using the sheath air as a sample to obtain the H_2SO_4 concentration originated from the sheath air generation. The H_2SO_4 concentrations during the zero measurements were $3.7 \times 10^5 \text{ cm}^{-3}$ with the pump-based sheath air and $1.8 \times 10^6 \text{ cm}^{-3}$ with the compressor-based sheath air. Due to the limitations of space inside the containers, higher level of purification for the sheath air was not available.

20 The data from the API-TOF was recorded with the time resolution of 2 s, but at least 1 min of the raw data is required for averaging to obtain feasible high-resolution spectra.

2.3 Gas measurements

Nitric oxide (NO) and nitrogen dioxide (NO_2) concentrations were measured using Horiba APNA-370 and the data were recorded with a time resolution of 1 min. In this study, only the sum of NO and NO_2 concentrations, denoted as NO_x concentration, is used in the analysis. Carbon dioxide (CO_2) concentration was measured using LI-COR LI-7000 analyzer with a
25 time resolution of 1 s.

Because traffic density and the concentrations of emissions at the curbside are not directly correlated due to turbulent flow field and variable wind directions causing the emissions to be diluted in a different extent at the measurement location, a traffic-originated tracer is needed to connect the observed concentrations quantitatively to traffic emissions. An ideal tracer is one that
30 is universally emitted by all vehicles and is not altered in the atmosphere during the time scale of the exhaust plume dilution process. CO_2 is emitted by all combustion engines, with the emission rate proportional to the fuel consumption; thus, it is used as a tracer in determining emission factors of traffic. The drawback of CO_2 as a traffic tracer is its varying background concentration due to regional-level phenomena. The background concentration is also higher than the concentration increase

of traffic. As the main source of NO_x in urban areas is traffic (Clapp and Jenkin, 2001), the background concentration is low and causes thus no significant uncertainty to the traffic contribution. However, the drawback of NO_x is its varying emission rates across the whole vehicle fleet (Yli-Tuomi et al., 2005). Concluding, we decided to use NO_x as the traffic tracer, except in the emission factor analysis where CO_2 is used due to its direct connection to the fuel consumption.

- 5 The NO_x concentration ($[\text{NO}_x]$) correlates well with the traffic density on weekdays (Fig. 3). However, on weekends, much stronger dilution conditions during daytime compared to nighttime are seen. During nighttime, there is a peak in the NO_x concentration though it is nonexistent in traffic density, which suggests stagnant weather conditions coincided at nighttime on weekends for the considered time range. The NO_x concentrations were higher during the morning rush hours than during the afternoon rush hours on weekdays although the traffic density behaved oppositely, which occurs because, during the morning
- 10 rush hours, traffic was concentrated on the same side of the street as the measurement containers located providing a shorter distance, and thus less dilution, for the emissions to travel to the measurement devices.

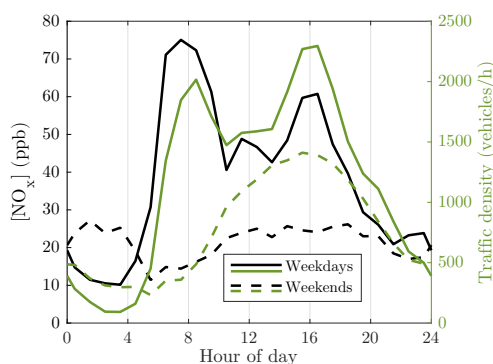


Figure 3. Average diurnal variations of nitrogen oxides (NO_x) concentration, representing the concentration of the traffic-originated emissions overall, and traffic density. The NO_x concentration data measured with 1 min time resolution are firstly averaged to 1 h resolution; secondly, the averaged data from different days are averaged geometrically for the specific hours. Geometric averages are used for emissions, instead of arithmetic averages, because the logarithmic nature of the concentrations would cause skewed frequency distributions; thus, the highest concentrations would be weighted more than the lower ones. Arithmetic averaging is used for the traffic density.

2.4 Particle measurements

- The number concentration of particles with the diameters larger than approximately 1.2 nm were measured using an Airmodus A10 Particle Size Magnifier (PSM A10) (Vanhanen et al., 2011) with a diethylene glycol saturator flow rate of 1.3 lpm followed
- 15 by an Airmodus A20 Condensation Particle Counter (CPC A20). Particles larger than 3 and 7 nm were measured using a TSI 3776 Condensation Particle Counter (CPC 3776) and another Airmodus CPC A20, respectively. The particle size distribution between 6 and 800 nm was measured using a Differential Mobility Particle Sizer (DMPS) consisting of a Vienna-type Differential Mobility Analyzer (DMA) followed by a CPC A20. Due to high particle concentrations at the street canyon, the sample to CPCs was diluted using a bridge diluter having a dilution ratio of 8.2. The dilution ratio for the specific diluter is, however,

measured for larger particle sizes only, and because the diluter is based on diffusional losses of the particles, the dilution ratio for NCA-sized particles is higher. Therefore, the NCA concentrations reported here represent the lower limits of the actual concentrations.

5 The number concentration of nanocluster aerosol, particles within the diameter range between 1.2 and 3 nm, can be calculated by subtracting the concentration measured by the CPC 3776 from the concentration measured by the PSM. The particle size distribution between 1.2 nm and 800 nm can be calculated with the data from all these aerosol measurement devices by taking the cut diameters of the CPCs and the dilution ratio of the bridge diluter into account. The NCA concentration was measured with a time resolution of 1 s and the size distribution with a time resolution of 9 min.

3 Results and discussion

10 The data from the off-site measurements of traffic count and environmental parameters are available for the whole four-week measurement campaign starting on 4 May 2017 and ending on 31 May 2017 (see the Supplement for the time series). This time range provided adequate data for examining NCA and H_2SO_4 formation respect to solar irradiance, because there were sufficient amounts of days both with clear sky and with cloud cover, yet without too many rainy days. There are some gaps in the NCA and H_2SO_4 data during the four weeks due to unavailability of the measurement devices. The data analysis considers
15 only the time ranges for which all the measurement data are available, resulting in three weeks of data.

Figure 4 presents our proposal for the updated mechanism of H_2SO_4 and particle formation in traffic-influenced areas, based on our measurement results. The most noteworthy details are illustrated with red crosses indicating H_2SO_4 routes which were observed to occur barely only, or not at all. As shown later in this section, our measurement at the curbside displays no clear increase in gaseous H_2SO_4 concentrations with increasing traffic volumes. With the fact that vehicles do emit primary
20 H_2SO_4 (Arnold et al., 2012; Rönkkö et al., 2013), it is evident that the majority of primary H_2SO_4 must be converted to the particle phase via nucleation (route 1A) and condensation (1B) rapidly after emission. Conversely, secondary H_2SO_4 potentially remains longer in urban atmosphere because it does not experience conditions favoring such a rapid gas-to-particle conversion, i.e., rapid temperature decrease, high precursor concentrations, and high pre-existing CS. Therefore, the signal of H_2SO_4 measured from the curbside of the street is mainly due to secondary H_2SO_4 only.

25 Our results show that both traffic and regional NPF influence NCA concentrations at the urban traffic site, with direct NCA emission from traffic dominating. Comparison of the NCA and H_2SO_4 concentrations with SI and traffic density suggests that while solar radiation favors higher NCA concentrations, the photochemically produced H_2SO_4 may not be the key compound in the presence of NCA in urban areas. Traffic-originated NCA particles may be formed via a delayed primary emission route by rapid nucleation of low-volatile gaseous compounds emitted by vehicles during exhaust cooling after releasing from the tailpipe
30 (1A). On the other hand, they may be solid particles emitted directly by engines, via a primary emission route (Sgro et al., 2012; Alanen et al., 2015). Although it is likely that both nucleation (1A) and condensation (1B) routes from primary H_2SO_4 exist because nucleation mode particle number concentrations and particle sizes are correlated with the H_2SO_4 concentration in exhaust (Arnold et al., 2012; Rönkkö et al., 2013), the ratio of the routes at our measurement site is not determined. Neither

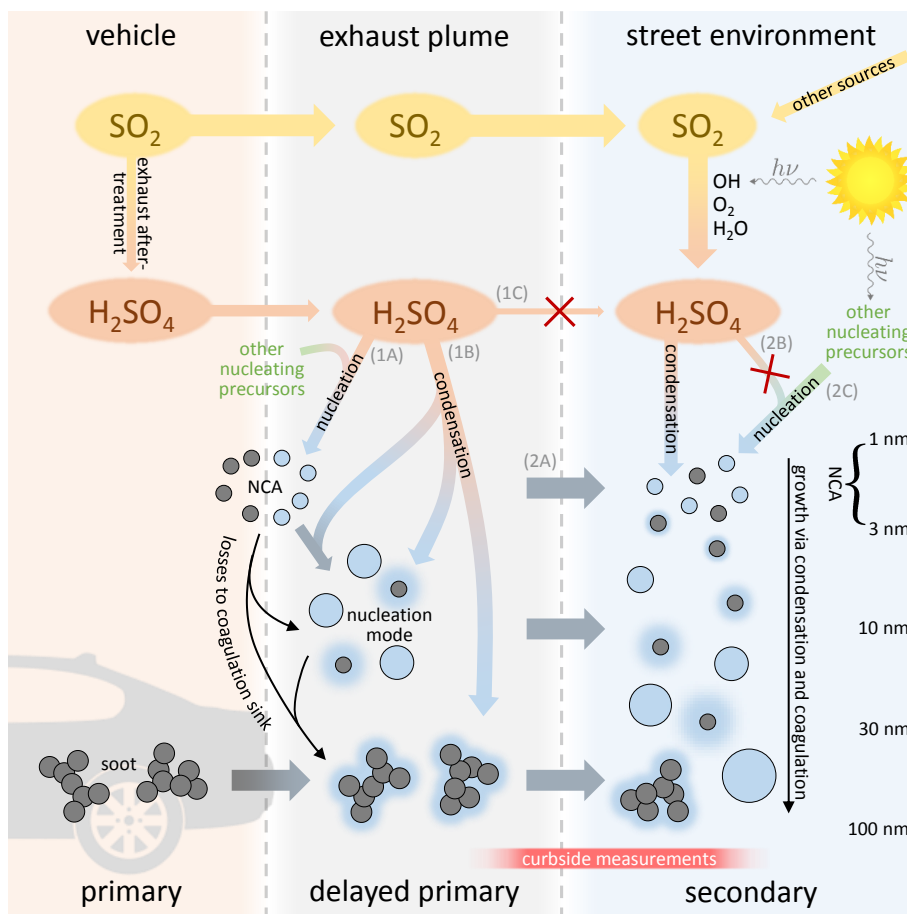


Figure 4. Proposed mechanism of sulfuric acid and particle formation in traffic-influenced areas. The route of primary H_2SO_4 to urban atmosphere (route 1C) is largely terminated to particle phase rapidly after the emission (routes 1A and 1B). Conversely, secondary H_2SO_4 remains in urban atmosphere because it does not experience such a rapid gas-to-particle conversion. NCA presence in urban atmosphere is majorly controlled by traffic emissions (route 2A) and only marginally by nucleation from secondary precursors (routes 2B and 2C), especially the contribution of nucleation from secondary H_2SO_4 (route 2B) is noticeably overridden by traffic emissions (route 2A).

is the ratio of NCA particles emitted primarily and through the nucleation route (1A) determined. Therefore, the relative proportion of H_2SO_4 in traffic-originated NCA particles remains unknown, leading to the possibility of solid NCA emissions.

The first evidence for traffic-contributed concentrations of NCA (N_{NCA}) and H_2SO_4 was found in the diurnal variations of the NCA, H_2SO_4 , and NO_x concentrations and SI (Fig. 5). The diurnal variations on weekdays (Fig. 5a) differ from the diurnal variations on weekends (Fig. 5b). The main difference between weekdays and weekends are traffic volumes; therefore, such a difference in the concentrations of NCA and H_2SO_4 should only be expected if their formation are in some manner connected to traffic. The connection of NCA to traffic is further strengthened by comparing it to the NO_x concentrations, which are directly linked to traffic densities and traffic-related emissions (Fig. 3). On weekdays, the NCA concentration increased in tandem with the NO_x concentration during the morning rush hours. On weekends, the NCA concentration increased at noontime much more clearly than the NO_x concentration. This can be interpreted as a sign of an ongoing regional NPF process producing NCA particles with high SI. On weekdays, the regional NPF process should only produce higher NCA concentration during afternoon rush hours having higher SI compared to morning. The increased NCA concentrations during the morning rush hours suggest that the traffic-originated NCA does not require solar radiation to form.

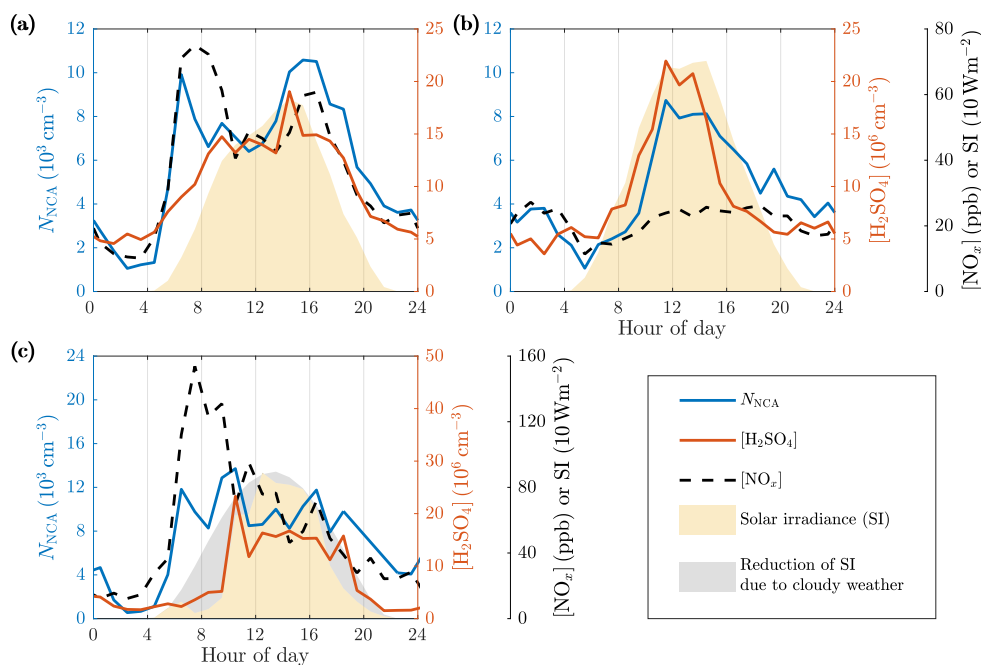


Figure 5. Average diurnal variations of the NCA, H_2SO_4 , and NO_x concentrations and solar irradiance (SI) on (a) weekdays, (b) weekends, and (c) example day 5/22/2017 with cloudy morning and evening. The concentration data firstly averaged to 1 h time resolution are averaged geometrically as described in Fig. 3.

We observed that, traffic levels influence the H_2SO_4 concentrations, but they are still mainly controlled by solar radiation. In contrast to the NCA concentration, the H_2SO_4 concentration traced SI much more closely, with a maximum at noontime and minimum at night. On weekdays, a peak in the H_2SO_4 concentration during afternoon rush hours suggests that traffic might also influence the formation of H_2SO_4 . Further evidence for this is found by comparing the diurnal variation of H_2SO_4 between weekdays and weekends. On weekends, the H_2SO_4 concentration increased not until the traffic density and the NO_x concentration were also increased, whereas on weekdays, the traffic density was already high when SI and the H_2SO_4 concentration began to increase. Furthermore, higher irradiances were required on weekends before the rise in the H_2SO_4 concentration and, additionally, the order of the increase in the NCA and H_2SO_4 concentrations was switched.

The time series show that NCA is not similarly controlled by solar radiation but rather by traffic. This is clearly showcased in Fig. 5c which presents data from a day with cloudy weather reducing SI in the morning and in the evening but still with a constant wind direction. The NCA concentration closely traced traffic levels in the morning, whereas the H_2SO_4 concentration only increased when SI increased hours later. This clearly shows that the formation of NCA, in this case, is independent of SI and the H_2SO_4 concentration. It is also noteworthy that no increase in the NCA concentration is observed when SI increased, suggesting that traffic dominated in the NCA formation. There were also other days with cloudiness decreasing SI with similar observations; however, the example day in Fig. 5c was the day with the most clear effect of cloudiness on SI and the reduction of SI coincides with morning rush hours, displaying high NCA concentrations.

The data suggest that the formation of atmospheric H_2SO_4 is strongly enhanced in the presence of both traffic and sunlight. While a strong correlation between the NCA and NO_x concentrations (Fig. 6a, b: Pearson's $R = 0.84$) confirms the connection between NCA and traffic, a remarkably weaker, but also positive, correlation between the H_2SO_4 and NO_x concentrations ($R = 0.50$) was observed, revealing the connection between H_2SO_4 and traffic. The effect of SI at different traffic densities shows differing patterns for NCA (Fig. 6c) and H_2SO_4 (Fig. 6d). While high SI is associated with higher NCA and H_2SO_4 levels, traffic density determines the base level for both (the concentrations at zero SI). For H_2SO_4 , the influence of traffic causes a marked increase in the slope of the H_2SO_4 concentration-SI-line. The slope can be interpreted as the production efficiency of H_2SO_4 via photochemistry. It is evident that for NCA, the influence of traffic dominates in comparison to SI, as the traffic-influenced NCA concentration (red data) exceeds the non-traffic concentrations (black data) even during dark times. For H_2SO_4 , the situation is different, as all dark-period H_2SO_4 concentrations are close to equal levels. These differing patterns suggest that the majority of NCA in traffic-influenced areas is formed independently of secondary H_2SO_4 , in contrast to the findings of Yao et al. (2018).

Even more compelling evidence for traffic-originated NCA and H_2SO_4 can be found by comparing the observed concentrations to CO_2 concentrations ($[\text{CO}_2]$). In Fig. 7, no apparent difference in the emission factors of NCA for different SI are seen; however, in the case of H_2SO_4 , higher SI lead to noticeably higher emission factors of H_2SO_4 . We tested for potential co-correlations between SI and traffic density to examine potential traffic level increase with simultaneous SI increase due to their almost similar diurnal cycles. We found no clear correlation between CO_2 concentration and SI (Fig. S5). In a case of a found correlation, the slopes in Fig. 7 could not have been interpreted as emission factors, but as photochemical production due to accelerated photochemistry with higher SI values. Although the varying background concentration of CO_2 causes uncer-

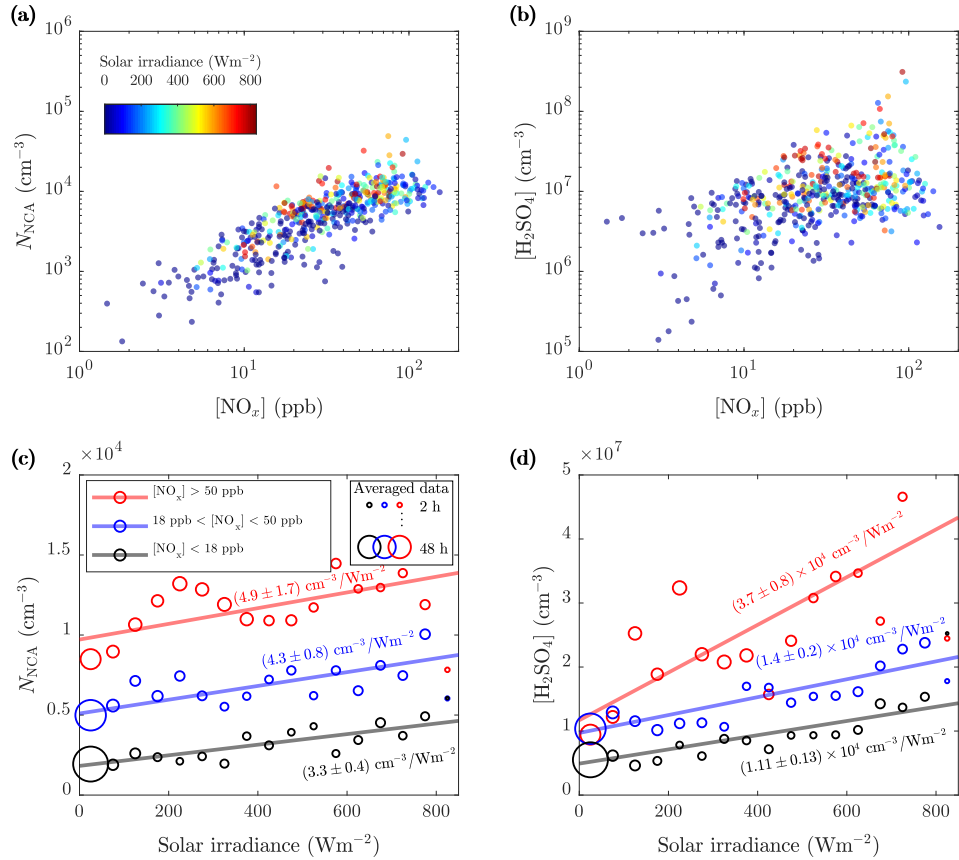


Figure 6. 1-hour-averages of the (a) NCA and (b) H_2SO_4 concentrations as a function of the NO_x concentration colored by the solar irradiance (SI) and 10-min-averages of the (c) NCA and (d) H_2SO_4 concentrations further averaged to 17 different SI bins (bin width is chosen to provide clear graphical representation) for three NO_x concentration ranges. Weighted least squares fitting, with data point count in bin-averaging (shown with the circle diameters) as weights, for the bin-averaged values was done to output linear fits. The slopes are marked in the figure and are not largely affected by the chosen bin width. The intercepts are (c) $(0.182 \pm 0.013) \times 10^4 \text{ cm}^{-3}$, $(0.51 \pm 0.03) \times 10^4 \text{ cm}^{-3}$, and $(0.97 \pm 0.07) \times 10^4 \text{ cm}^{-3}$, and (d) $(0.49 \pm 0.04) \times 10^7 \text{ cm}^{-3}$, $(0.97 \pm 0.06) \times 10^7 \text{ cm}^{-3}$, and $(1.2 \pm 0.3) \times 10^7 \text{ cm}^{-3}$, for the lowest, the mid-ranged, and the highest NO_x concentration range, respectively.

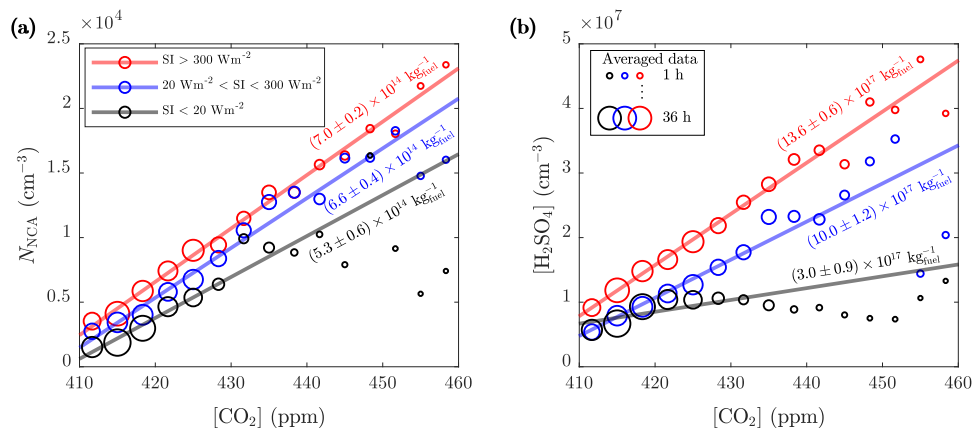


Figure 7. 1-min-averages of the (a) NCA and (b) H_2SO_4 concentrations further averaged to CO_2 concentration bins for three SI ranges (see Fig. 6 for the details in averaging and linear regression). The slopes of the linear fits converted to kilograms of fuel combusted (using the emission factor of CO_2 , 3.14 kg per 1 kg of fuel combusted (Yli-Tuomi et al., 2005)) are marked in the figure. The intercepts of the fits at 410 ppm are (a) $(0.07 \pm 0.04) \times 10^4 \text{ cm}^{-3}$, $(0.15 \pm 0.05) \times 10^4 \text{ cm}^{-3}$, and $(0.25 \pm 0.03) \times 10^4 \text{ cm}^{-3}$; and (b) $(0.67 \pm 0.07) \times 10^7 \text{ cm}^{-3}$, $(0.49 \pm 0.15) \times 10^7 \text{ cm}^{-3}$, and $(0.79 \pm 0.06) \times 10^7 \text{ cm}^{-3}$, for the lowest, the mid-ranged, and the highest SI range, respectively.

tainty in analyzing the contribution of traffic on emissions, linear dependencies are still observed in Fig. 7. These results again support the finding that solar radiation is required for the formation of H_2SO_4 from traffic emissions and demonstrates clearly that both NCA and H_2SO_4 originate from traffic. This is further supported by examining the concentrations in different wind directions (Figs. 8 and 9) which shows that the highest concentrations were measured when the wind blew from the street.

- 5 While the emission factors can depend markedly on vehicle, engine, fuel, and after-treatment system types, the emission factors obtained here represent the average fleet-level values and can thus be moderately applicable in regional and global aerosol models at least for areas with the same average fleet composition as in our measurement site in Helsinki. However, more research is needed to obtain emission factors separated into the different types.

The annual CO_2 emission rate from traffic in Helsinki in 2017 was $5.38 \times 10^8 \text{ kgCO}_2 \cdot \text{a}^{-1}$ (VTT Technical Research Centre of Finland Ltd, 2017). Using the average NCA emission factor versus CO_2 emission, $2.21 \times 10^{14} \text{ kgCO}_2^{-1}$, a rough estimation on the annual NCA emission from traffic in Helsinki becomes $1.19 \times 10^{23} \text{ a}^{-1}$. The annual NCA formation rate via photochemical NPF in Helsinki can be approximated using estimates of nucleation rate, from 1 to $10 \text{ cm}^{-3} \text{ s}^{-1}$, NPF event day count per year, from 30 to 120 a^{-1} , NPF duration, from 2 to 4 h, measured in a rural area in Hyytiälä, Finland (Dal Maso et al., 2005; Kulmala and Kerminen, 2008) and in an urban area in Helsinki (Hussein et al., 2008), the total area of Helsinki, 214 km^2 , and a rough estimate for the boundary layer height, 500 m. Multiplying these gives the estimation of the annual NCA formation rate from 0.23×10^{23} to $18.5 \times 10^{23} \text{ a}^{-1}$. Comparison of these annual rates suggests that in minimum of 6% but even up to 84% of NCA particles are estimated to originate from traffic in Helsinki on an annual basis. Although this range is wide, the contribution of traffic-originated NCA is significant.

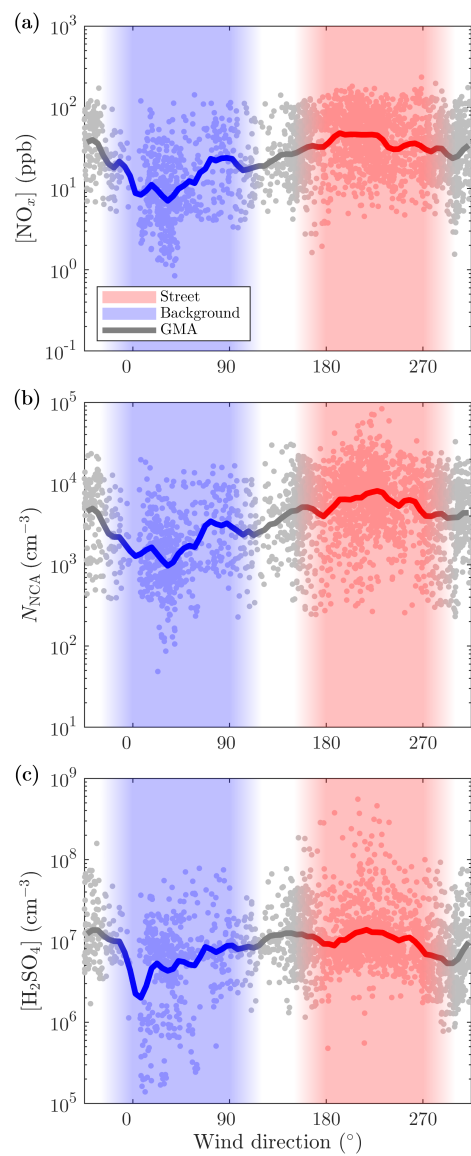


Figure 8. 10-min-averages of the (a) NO_x , (b) NCA, and (c) H_2SO_4 concentrations measured with different wind directions. Wind velocities smaller than 0.5 m/s are excluded. GMA denotes geometric moving average.

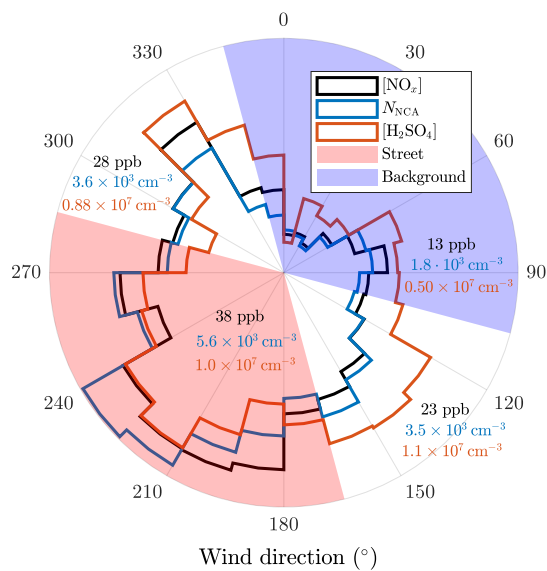


Figure 9. 10-min-averages of the NO_x , NCA, and H_2SO_4 concentrations further averaged to different wind direction sectors. Wind velocities smaller than 0.5 m/s are excluded. The geometric averages of the concentrations across the sectors are shown in the figure.

Another estimation for the traffic contribution on NCA (and also on H_2SO_4) in urban air can be performed using the linear fits from Fig. 6. Considering typical weekday noontime at our measurement location and assuming the annual mean of the daytime maximum SI in Helsinki, 500 Wm^{-2} , the NCA concentration due to traffic is $\sim 9.7 \times 10^3 \text{ cm}^{-3}$ (the value of the high NO_x line at zero irradiance) and the increase of the NCA concentration due to photochemistry is $\sim 1.7 \times 10^3 \text{ cm}^{-3}$ (calculated with the slope of the low NO_x line). These concentrations indicate that approximately 85 % of the total NCA concentration at the street canyon is originated from traffic at noontime. Considering midsummer and midwinter, the daytime maximum SI are 850 Wm^{-2} and 100 Wm^{-2} , giving the contributions of $\sim 78 \%$ and $\sim 97 \%$, respectively. Therefore, it is evident that the major fraction of NCA originated from traffic at our measurement location, even with the highest available SI values in midsummer.

For H_2SO_4 , the concentration due to traffic at our measurement location at typical weekday noontime is $\sim 12 \times 10^6 \text{ cm}^{-3}$ and the increase of the concentration due to photochemistry is $\sim 5.6 \times 10^6 \text{ cm}^{-3}$, indicating approximately 68 % of the total H_2SO_4 concentration at the street canyon is originating from local traffic at noontime. For midsummer and midwinter, the contributions become $\sim 56 \%$ and $\sim 92 \%$, respectively. These values signify that also the major fraction of H_2SO_4 originated from traffic even though it cannot be seen as clearly from the diurnal variation as is seen in the case of NCA.

Because regional NPF events are frequently suppressed by high condensation sinks (Kerminen et al., 2018), decreasing condensation sink can lead to a NPF event, resulting in particle number concentration increase. However, our data display no clear anticorrelations of this kind (see Fig. S6). This again implies that regional NPF events cannot clearly be distinguished from the data measured in a vicinity of dense traffic.

Traffic-emitted NCA poses a potential health risk because the observed NCA concentrations are valid at the curbside of the street, which is the location where pedestrians spend time in traffic. Spreading of the NCA particles emitted on the streets can be approximated with particle lifetimes. The lifetimes can be estimated using coagulation sinks (CoagS) and the time constants of coagulation scavenging (τ_{CoagS}), which is the inverse of CoagS, calculated as in Kulmala et al. (2001). Assuming no other losses of the particles, such as self-coagulation and condensational growth out from the NCA size range, and no mixing of the emitted aerosol with the background aerosol, τ_{CoagS} represents the lifetime of the particles. The estimated lifetimes were in the scale of several minutes, resulting in a spreading possibility of the NCA particles around urban areas. The diurnal variations of CoagS and τ_{CoagS} are presented in Fig. S2.

Our data clearly demonstrate that NCA-sized particle concentrations in a traffic-influenced environment is controlled by NCA directly emitted by traffic. The data also demonstrate that while generally NCA and photochemically produced nucleating vapor concentrations correlate, this correlation is likely, firstly, due to increased traffic volumes at daytime and, secondly, due to traffic-originated H_2SO_4 and other nucleating vapors. We also showed that H_2SO_4 formation is driven by both solar radiation and a traffic-related source.

4 Conclusions

Our results have several implications on our understanding of aerosol particle formation in traffic-influenced areas. Firstly, because current regional and global air quality models do not include particles in the sub-3 nm size range as primary emissions (Paasonen et al., 2016), the modelled NCA-sized particle concentrations are mainly driven by photochemical NPF processes, neglecting their origin from traffic as primary sources. Thus, our results show an urgent need to update these emissions. In light of our results, it seems evident that there will be areas in which direct emissions dominate the formation of new aerosol. A rough calculation gives that, on an annual basis, up to 84 % of NCA can originate from traffic in Helsinki; and according to the measured NCA concentrations, on typical weekday noontime, ~ 85 % of the total NCA concentration was contributed by traffic at our studied site. In wintertime, this contribution may reach ~ 97 % due to lower SI, which highlights the need for updating the annual particle formation cycles in the models. Secondly, our results also show that both traffic emission and regional NCA formation signals can be distinguished for the most of the times, and that traffic also influences the formation of H_2SO_4 . Together with the findings of Yao et al. (2018), this presents a significant update on the particle formation mechanisms in urban areas. As illustrated in Fig. 4, the particle concentration is controlled by the interplay of the two processes, with varying importance depending on the proximity of the emission source. Our results call for reconsideration and re-analysis of observations of NPF events observed in traffic-influenced areas. In many cases, there is covariance between traffic volumes and SI, and care should be taken to separate these two variables in the analysis, e.g., by considering CO_2 or NO_x as tracers for traffic volumes. Finally, potential health effects of traffic emissions in urban areas should also be considered more carefully because the composition of the emitted NCA particles is still unknown, especially as some clues for their non-volatility exist.

Data availability. The time series data are freely available at: (the link will be shown when the manuscript is accepted)

Author contributions. MD, TR, JVN, and HJT. designed the research. MO, HK, MA, JK, NK, and MI, performed the measurements. MO, HK, NK, and MI analyzed the data. MO prepared the manuscript with contribution from all co-authors.

Competing interests. The authors declare no conflict of interest.

- 5 *Acknowledgements.* We thank the tofTools team for providing tools for mass spectrometry analysis and Prof. Mikko Sipilä from the University of Helsinki for lending the chemical ionization inlet for the atmospheric pressure interface time-of-flight mass spectrometer. Dr. Harri Portin and Dr. Anu Kousa from Helsinki Region Environmental Services Authority (HSY) as well as the HSY's AQ measurement team are acknowledged for their valuable work related to the data quality control and measurements at the Mäkelänkatu supersite. Mr. Petri Blomqvist from the City of Helsinki is acknowledged for the traffic count data. The research has received funding from Tekes - the Finnish Funding Agency for Innovation (Grant no. 2883/31/2015), HSY, and Pegasor Oy, who funded the research through the Cityzer project, the graduate school of Tampere University of Technology, and Academy of Finland for Profi 4 (Grant no. 318940) and infrastructure funding (Grant no. 273010).
- 10

References

- Ahmad, K., Khare, M., and Chaudhry, K.: Wind tunnel simulation studies on dispersion at urban street canyons and intersections—a review, *J. Wind Eng. Ind. Aerod.*, 93, 697–717, <https://doi.org/10.1016/j.jweia.2005.04.002>, 2005.
- Alanen, J., Saukko, E., Lehtoranta, K., Murtonen, T., Timonen, H., Hillamo, R., Karjalainen, P., Kuuluvainen, H., Harra, J., Keskinen, J., and Rönkkö, T.: The formation and physical properties of the particle emissions from a natural gas engine, *Fuel*, 162, 155–161, <https://doi.org/10.1016/j.fuel.2015.09.003>, 2015.
- Arnth, A., Unger, N., Kulmala, M., and Andreae, M.: Clean the air, heat the planet?, *Science*, 326, 672–673, <https://doi.org/10.1126/science.1181568>, 2009.
- Arnold, F., Pirjola, L., Rönkkö, T., Reichl, U., Schlager, H., Lähde, T., Heikkilä, J., and Keskinen, J.: First online measurements of sulfuric acid gas in modern heavy-duty diesel engine exhaust: Implications for nanoparticle formation, *Environ. Sci. Technol.*, 46, 11 227–11 234, <https://doi.org/10.1021/es302432s>, 2012.
- Beelen, R., Raaschou-Nielsen, O., Stafoggia, M., Andersen, Z., Weinmayr, G., Hoffmann, B., Wolf, K., Samoli, E., Fischer, P., Nieuwenhuijsen, M., Vineis, P., Xun, W., Katsouyanni, K., Dimakopoulou, K., Oudin, A., Forsberg, B., Modig, L., Havulinna, A., Lanki, T., Turunen, A., Oftedal, B., Nystad, W., Nafstad, P., De Faire, U., Pedersen, N., Östenson, C.-G., Fratiglioni, L., Penell, J., Korek, M., Pershagen, G., Eriksen, K., Overvad, K., Ellermann, T., Eeftens, M., Peeters, P., Meliefste, K., Wang, M., Bueno-De-Mesquita, B., Sugiri, D., Krämer, U., Heinrich, J., De Hoogh, K., Key, T., Peters, A., Hampel, R., Concin, H., Nagel, G., Ineichen, A., Schaffner, E., Probst-Hensch, N., Künzli, N., Schindler, C., Schikowski, T., Adam, M., Phuleria, H., Vilier, A., Clavel-Chapelon, F., Declercq, C., Grioni, S., Krogh, V., Tsai, M.-Y., Ricceri, F., Sacerdote, C., Galassi, C., Migliore, E., Ranzi, A., Cesaroni, G., Badaloni, C., Forastiere, F., Tamayo, I., Amiano, P., Dorronsoro, M., Katsoulis, M., Trichopoulou, A., Brunekreef, B., and Hoek, G.: Effects of long-term exposure to air pollution on natural-cause mortality: An analysis of 22 European cohorts within the multicentre ESCAPE project, *Lancet*, 383, 785–795, [https://doi.org/10.1016/S0140-6736\(13\)62158-3](https://doi.org/10.1016/S0140-6736(13)62158-3), 2014.
- Brockmann, J. E.: Sampling and Transport of Aerosols, in: *Aerosol Measurement: Principles, Techniques, and Applications*, edited by Baron, P. A. and Willeke, K., pp. 143–195, John Wiley & Sons, Hoboken, USA, 2nd edn., 2005.
- Chapman, S. and Cowling, T.: *The Mathematical Theory of Non-uniform Gases. An account of the kinetic theory of viscosity, thermal conduction, and diffusion in gases*, Cambridge University Press, Cambridge, UK, 2nd edn., 1954.
- Clapp, L. J. and Jenkin, M. E.: Analysis of the relationship between ambient levels of O₃, NO₂ and NO as a function of NO_x in the UK, *Atmos. Environ.*, 35, 6391–6405, [https://doi.org/10.1016/S1352-2310\(01\)00378-8](https://doi.org/10.1016/S1352-2310(01)00378-8), 2001.
- Dal Maso, M., Kulmala, M., Riipinen, I., Wagner, R., Hussein, T., Aalto, P., and Lehtinen, K.: Formation and growth of fresh atmospheric aerosols: eight years of aerosol size distribution data from SMEAR II, Hyytiälä, Finland, *Bor. Env. Res.*, 10, 323–336, 2005.
- Dockery, D., Pope III, C., Xu, X., Spengler, J., Ware, J., Fay, M., Ferris Jr., B., and Speizer, F.: An association between air pollution and mortality in six U.S. cities, *New Engl. J. Med.*, 329, 1753–1759, <https://doi.org/10.1056/NEJM199312093292401>, 1993.
- Eisele, F. L. and Tanner, D. J.: Measurement of the gas phase concentration of H₂SO₄ and methane sulfonic acid and estimates of H₂SO₄ production and loss in the atmosphere, *J. Geophys. Res. Atmos.*, 98, 9001–9010, <https://doi.org/10.1029/93JD00031>, 1993.
- Hanson, D. R. and Eisele, F.: Diffusion of H₂SO₄ in Humidified Nitrogen: Hydrated H₂SO₄, *J. Phys. Chem. A*, 104, 1715–1719, <https://doi.org/10.1021/jp993622j>, 2000.

- Hietikko, R., Kuuluvainen, H., Harrison, R. M., Portin, H., Timonen, H., Niemi, J. V., and Rönkkö, T.: Diurnal variation of nanocluster aerosol concentrations and emission factors in a street canyon, *Atmos. Environ.*, 189, 98–106, <https://doi.org/10.1016/j.atmosenv.2018.06.031>, 2018.
- Hussein, T., Martikainen, J., Junninen, H., Sogacheva, L., Wagner, R., Dal Maso, M., Riipinen, I., Aalto, P., and Kulmala, M.: Observation of regional new particle formation in the urban atmosphere, *Tellus*, 60, 509–521, <https://doi.org/10.1111/j.1600-0889.2008.00365.x>, 2008.
- Jokinen, T., Sipilä, M., Junninen, H., Ehn, M., Lönn, G., Hakala, J., Petäjä, T., Mauldin III, R. L., Kulmala, M., and Worsnop, D. R.: Atmospheric sulphuric acid and neutral cluster measurements using CI-API-TOF, *Atmos. Chem. Phys.*, 12, 4117–4125, <https://doi.org/10.5194/acp-12-4117-2012>, 2012.
- Junninen, H., Ehn, M., Petäjä, T., Luosujärvi, L., Kotiaho, T., Kostianen, R., Rohner, U., Gonin, M., Fuhrer, K., Kulmala, M., and Worsnop, D. R.: A high-resolution mass spectrometer to measure atmospheric ion composition, *Atmos. Meas. Tech.*, 3, 1039–1053, <https://doi.org/10.5194/amt-3-1039-2010>, 2010.
- Kerminen, V.-M., Chen, X., Vakkari, V., Petäjä, T., Kulmala, M., and Bianchi, F.: Atmospheric new particle formation and growth: review of field observations, *Environ. Res. Lett.*, 13, 103 003, <https://doi.org/10.1088/1748-9326/aadf3c>, 2018.
- Kittelson, D.: Engines and nanoparticles: A review, *J. Aerosol Sci.*, 29, 575–588, [https://doi.org/10.1016/S0021-8502\(97\)10037-4](https://doi.org/10.1016/S0021-8502(97)10037-4), 1998.
- Kontkanen, J., Lehtipalo, K., Ahonen, L., Kangasluoma, J., Manninen, H. E., Hakala, J., Rose, C., Sellegri, K., Xiao, S., Wang, L., Qi, X., Nie, W., Ding, A., Yu, H., Lee, S., Kerminen, V.-M., Petäjä, T., and Kulmala, M.: Measurements of sub-3 nm particles using a particle size magnifier in different environments: from clean mountain top to polluted megacities, *Atmos. Chem. Phys.*, 17, 2163–2187, <https://doi.org/10.5194/acp-17-2163-2017>, 2017.
- Kulmala, M. and Kerminen, V.-M.: On the formation and growth of atmospheric nanoparticles, *Atmos. Res.*, 90, 132–150, <https://doi.org/10.1016/j.atmosres.2008.01.005>, 2008.
- Kulmala, M., Dal Maso, M., Mäkelä, J. M., Pirjola, L., Väkevä, M., Aalto, P., Miikkulainen, P., Hämeri, K., and O’Dowd, C. D.: On the formation, growth and composition of nucleation mode particles, *Tellus B*, 53, 479–490, <https://doi.org/10.1034/j.1600-0889.2001.530411.x>, 2001.
- Kulmala, M., Kontkanen, J., Junninen, H., Lehtipalo, K., Manninen, H., Nieminen, T., Petäjä, T., Sipilä, M., Schobesberger, S., Rantala, P., Franchin, A., Jokinen, T., Järvinen, E., Äijälä, M., Kangasluoma, J., Hakala, J., Aalto, P., Paasonen, P., Mikkilä, J., Vanhanen, J., Aalto, J., Hakola, H., Makkonen, U., Ruuskanen, T., Mauldin III, R., Duplissy, J., Vehkamäki, H., Bäck, J., Kortelainen, A., Riipinen, I., Kurtén, T., Johnston, M., Smith, J., Ehn, M., Mentel, T., Lehtinen, K., Laaksonen, A., Kerminen, V.-M., and Worsnop, D.: Direct observations of atmospheric aerosol nucleation, *Science*, 339, 943–946, <https://doi.org/10.1126/science.1227385>, 2013.
- Kulmala, M., Petäjä, T., Ehn, M., Thornton, J., Sipilä, M., Worsnop, D., and Kerminen, V.-M.: Chemistry of Atmospheric Nucleation: On the Recent Advances on Precursor Characterization and Atmospheric Cluster Composition in Connection with Atmospheric New Particle Formation, *Annu. Rev. Phys. Chem.*, 65, 21–37, <https://doi.org/10.1146/annurev-physchem-040412-110014>, 2014.
- Kürten, A., Rondo, L., Ehrhart, S., and Curtius, J.: Calibration of a Chemical Ionization Mass Spectrometer for the Measurement of Gaseous Sulfuric Acid, *J. Phys. Chem. A*, 116, 6375–6386, <https://doi.org/10.1021/jp212123n>, 2012.
- Kuuluvainen, H., Poikkimäki, M., Järvinen, A., Kuula, J., Irjala, M., Maso, M. D., Keskinen, J., Timonen, H., Niemi, J. V., and Rönkkö, T.: Vertical profiles of lung deposited surface area concentration of particulate matter measured with a drone in a street canyon, *Environ. Pollut.*, 241, 96–105, <https://doi.org/10.1016/j.envpol.2018.04.100>, 2018.
- Lehtipalo, K., Yan, C., Dada, L., Bianchi, F., Xiao, M., Wagner, R., Stolzenburg, D., Ahonen, L. R., Amorim, A., Baccarini, A., Bauer, P. S., Baumgartner, B., Bergen, A., Bernhammer, A.-K., Breitenlechner, M., Brilke, S., Buchholz, A., Mazon, S. B., Chen, D., Chen, X., Dias,

- A., Dommen, J., Draper, D. C., Duplissy, J., Ehn, M., Finkenzeller, H., Fischer, L., Frege, C., Fuchs, C., Garmash, O., Gordon, H., Hakala, J., He, X., Heikkinen, L., Heinritzi, M., Helm, J. C., Hofbauer, V., Hoyle, C. R., Jokinen, T., Kangasluoma, J., Kerminen, V.-M., Kim, C., Kirkby, J., Kontkanen, J., Kürten, A., Lawler, M. J., Mai, H., Mathot, S., Mauldin, R. L., Molteni, U., Nichman, L., Nie, W., Nieminen, T., Ojdanic, A., Onnela, A., Passananti, M., Petäjä, T., Piel, F., Pospisilova, V., Quéléver, L. L. J., Rissanen, M. P., Rose, C., Sarnela, N., Schallhart, S., Schuchmann, S., Sengupta, K., Simon, M., Sipilä, M., Tauber, C., Tomé, A., Tröstl, J., Väisänen, O., Vogel, A. L., Volkamer, R., Wagner, A. C., Wang, M., Weitz, L., Wimmer, D., Ye, P., Ylisirniö, A., Zha, Q., Carslaw, K. S., Curtius, J., Donahue, N. M., Flagan, R. C., Hansel, A., Riipinen, I., Virtanen, A., Winkler, P. M., Baltensperger, U., Kulmala, M., and Worsnop, D. R.: Multicomponent new particle formation from sulfuric acid, ammonia, and biogenic vapors, *Sci. Adv.*, 4, eaau5363, <https://doi.org/10.1126/sciadv.aau5363>, 2018.
- 5
- 10 Maher, B. A., Ahmed, I. A. M., Karloukovski, V., MacLaren, D. A., Foulds, P. G., Allsop, D., Mann, D. M. A., Torres-Jardón, R., and Calderon-Garciduenas, L.: Magnetite pollution nanoparticles in the human brain, *P. Natl. Acad. Sci. USA*, 113, 10797–10801, <https://doi.org/10.1073/pnas.1605941113>, 2016.
- McMurry, P. and Friedlander, S.: New particle formation in the presence of an aerosol, *Atmos. Environ.*, 13, 1635–1651, [https://doi.org/10.1016/0004-6981\(79\)90322-6](https://doi.org/10.1016/0004-6981(79)90322-6), 1979.
- 15 Paasonen, P., Nieminen, T., Asmi, E., Manninen, H., Petäjä, T., Plass-Dülmer, C., Flentje, H., Birmili, W., Wiedensohler, A., Horrak, U., Metzger, A., Hamed, A., Laaksonen, A., Facchini, M., Kerminen, V.-M., and Kulmala, M.: On the roles of sulphuric acid and low-volatility organic vapours in the initial steps of atmospheric new particle formation, *Atmos. Chem. Phys.*, 10, 11223–11242, <https://doi.org/10.5194/acp-10-11223-2010>, 2010.
- Paasonen, P., Kupiainen, K., Klimont, Z., Visschedijk, A., Denier van der Gon, H. A. C., and Amann, M.: Continental anthropogenic primary particle number emissions, *Atmos. Chem. Phys.*, 16, 6823–6840, <https://doi.org/10.5194/acp-16-6823-2016>, 2016.
- 20 Pope, C., Burnett, R., Thun, M., Calle, E., Krewski, D., Ito, K., and Thurston, G.: Lung cancer, cardiopulmonary mortality, and long-term exposure to fine particulate air pollution, *J. Amer. Med. Assoc.*, 287, 1132–1141, <https://doi.org/10.1001/jama.287.9.1132>, 2002.
- Rönkkö, T., Lähde, T., Heikkilä, J., Pirjola, L., Bauschke, U., Arnold, F., Schlager, H., Rothe, D., Yli-Ojanperä, J., and Keskinen, J.: Effects of gaseous sulphuric acid on diesel exhaust nanoparticle formation and characteristics, *Environ. Sci. Technol.*, 47, 11882–11889, <https://doi.org/10.1021/es402354y>, 2013.
- 25 Rönkkö, T., Kuuluvainen, H., Karjalainen, P., Keskinen, J., Hillamo, R., Niemi, J. V., Pirjola, L., Timonen, H. J., Saarikoski, S., Saukko, E., Järvinen, A., Silvennoinen, H., Rostedt, A., Olin, M., Yli-Ojanperä, J., Nousiainen, P., Kousa, A., and Dal Maso, M.: Traffic is a major source of atmospheric nanocluster aerosol, *P. Natl. Acad. Sci. USA*, 114, 7549–7554, <https://doi.org/10.1073/pnas.1700830114>, 2017.
- Sgro, L. A., Sementa, P., Vaglieco, B. M., Rusciano, G., D’Anna, A., and Minutolo, P.: Investigating the origin of nuclei particles in GDI engine exhausts, *Combust. Flame*, 159, 1687–1692, <https://doi.org/10.1016/j.combustflame.2011.12.013>, 2012.
- 30 Vanhanen, J., Mikkilä, J., Lehtipalo, K., Sipilä, M., Manninen, H. E., Siivola, E., Petäjä, T., and Kulmala, M.: Particle size magnifier for nano-CN detection, *Aerosol Sci. Tech.*, 45, 533–542, <https://doi.org/10.1080/02786826.2010.547889>, 2011.
- VTT Technical Research Centre of Finland Ltd: LIPASTO unit emissions -database, last access: 15 January 2019, available at: <http://lipasto.vtt.fi/yksikkopaastot/>, 2017.
- 35 Yao, L., Garmash, O., Bianchi, F., Zheng, J., Yan, C., Kontkanen, J., Junninen, H., Mazon, S. B., Ehn, M., Paasonen, P., Sipilä, M., Wang, M., Wang, X., Xiao, S., Chen, H., Lu, Y., Zhang, B., Wang, D., Fu, Q., Geng, F., Li, L., Wang, H., Qiao, L., Yang, X., Chen, J., Kerminen, V.-M., Petäjä, T., Worsnop, D. R., Kulmala, M., and Wang, L.: Atmospheric new particle formation from sulfuric acid and amines in a Chinese megacity, *Science*, 361, 278–281, <https://doi.org/10.1126/science.aao4839>, 2018.

- Yli-Tuomi, T., Aarnio, P., Pirjola, L., Mäkelä, T., Hillamo, R., and Jantunen, M.: Emissions of fine particles, NO_x, and CO from on-road vehicles in Finland, *Atmos. Environ.*, 39, 6696–6706, <https://doi.org/10.1016/j.atmosenv.2005.07.049>, 2005.
- Zhao, J., Smith, J. N., Eisele, F. L., Chen, M., Kuang, C., and McMurry, P. H.: Observation of neutral sulfuric acid-amine containing clusters in laboratory and ambient measurements, *Atmos. Chem. Phys.*, 11, 10 823–10 836, <https://doi.org/10.5194/acp-11-10823-2011>, 2011.

Condensation sink calculation

Condensation sink (CS) is calculated using the function (Kulmala et al., 2001):

$$CS = 2\pi\mathcal{D} \int_0^{\infty} \beta(D_p) \cdot D_p \cdot \frac{dN}{d\log D_p}(D_p) \cdot d\log D_p \quad (\text{S1})$$

where \mathcal{D} is the diffusion coefficient of the condensing vapor and $\beta(D_p)$ and $\frac{dN}{d\log D_p}(D_p)$ are the transition regime correction factor (Fuchs and Sutugin, 1971) and particle number size distribution at particle diameter of D_p , respectively. CS is in most cases calculated only for H_2SO_4 (Lehtinen et al., 2007) but here it is calculated also for two other vapors generally participating in NPF processes (Kerminen et al., 2018): one with a high \mathcal{D} (ammonia, NH_3) and one with a low \mathcal{D} (a low volatile organic compound with a high molecular mass, $\text{C}_{19}\text{H}_{28}\text{O}_{11}$, Ehn et al., 2014). Time series of CS for H_2SO_4 is presented in Fig. S4 and the diurnal variations of CS for all three calculated condensing vapors in Fig. S1.

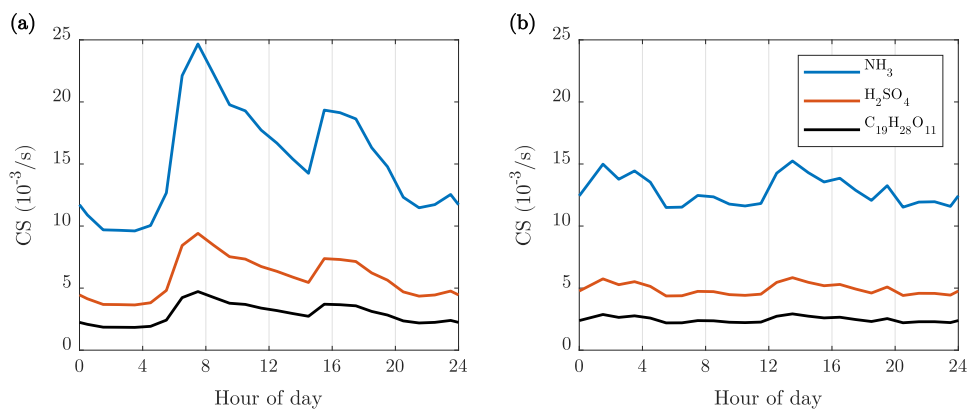


Figure S1. Diurnal variations of CS for different condensing vapors participating in NPF processes, (a) on weekdays and (b) on weekends.

Coagulation sink calculation

Coagulation sink (CoagS) for a particle diameter of D'_p is calculated using the function (Dal Maso et al., 2005):

$$\text{CoagS}(D'_p) = \int_0^{\infty} K(D_p, D'_p) \cdot \frac{dN}{d \log D_p}(D_p) \cdot d \log D_p \quad (\text{S2})$$

where $K(D_p, D'_p)$ is the coagulation coefficient of particles with the diameters of D_p and D'_p . CoagS and its inverse, coagulation time constant (τ_{CoagS}), for the smallest and largest measured NCA particles are presented in Fig. S2.

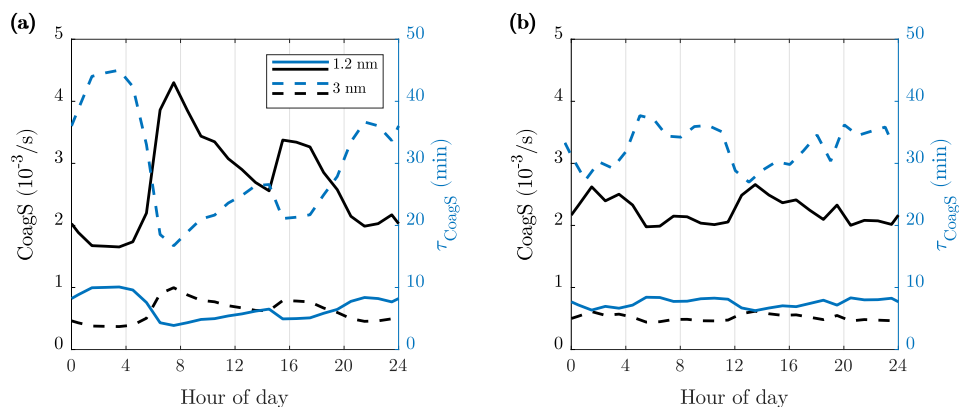


Figure S2. Diurnal variations of coagulation sinks and coagulation time constants for 1.2 nm and 3 nm particles, (a) on weekdays and (b) on weekends.

Time series

Figures S3 and S4 present the time series of all analyzed quantities.

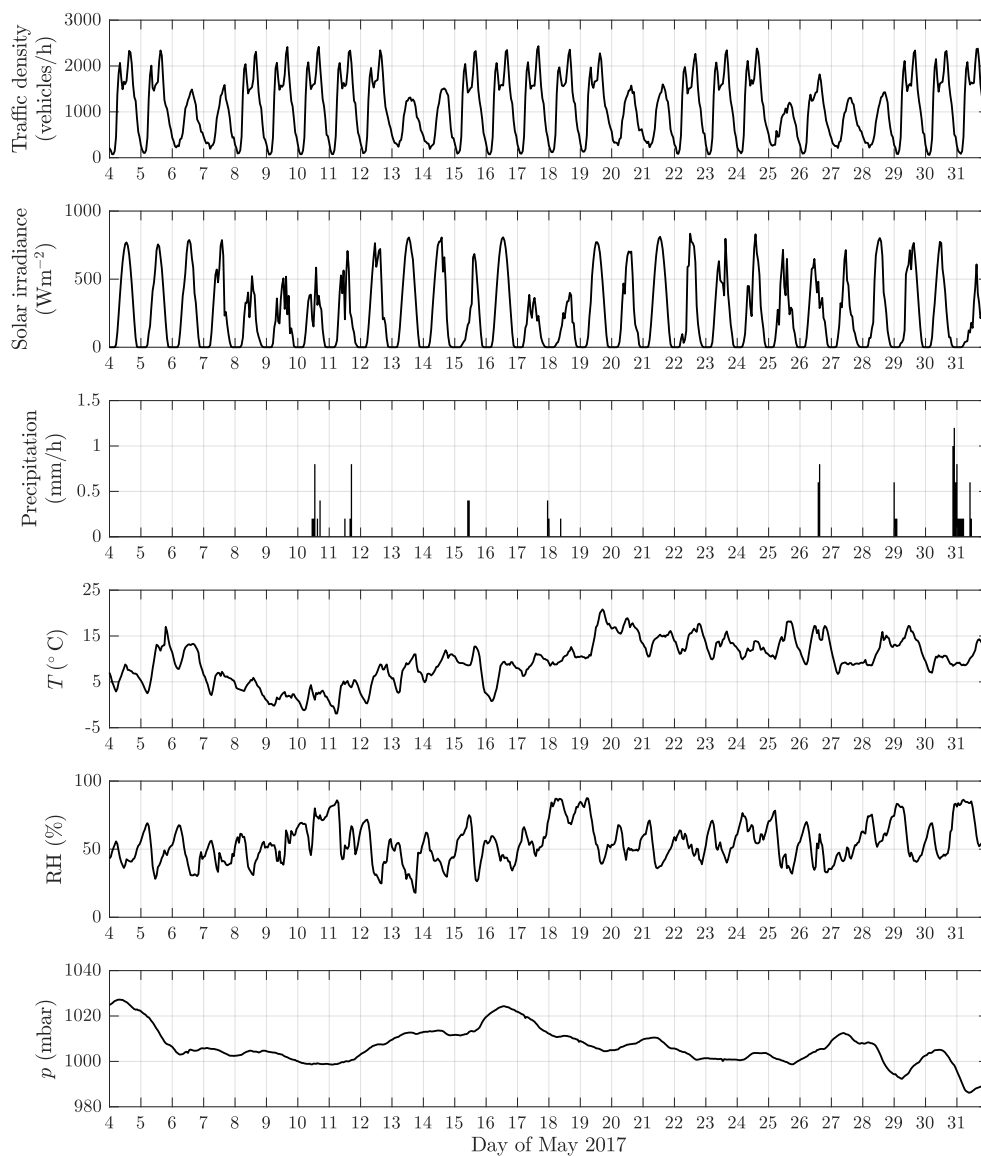


Figure S3. Time series of traffic density, solar irradiance, precipitation, temperature (T), relative humidity (RH), and atmospheric pressure (p).

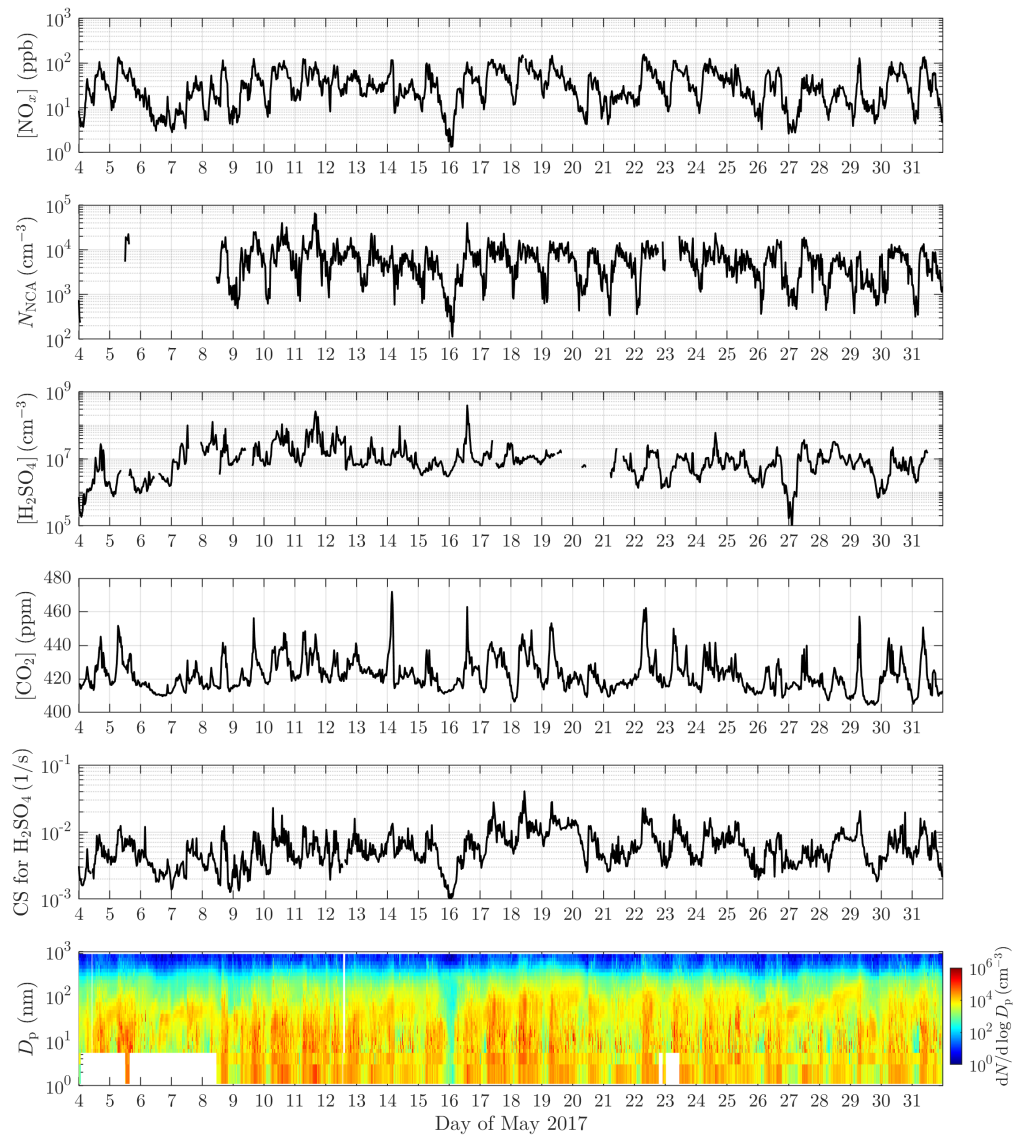


Figure S4. Time series of the NO_x , NCA, H_2SO_4 , and CO_2 concentrations, CS for H_2SO_4 , and particle size distribution. The size distributions include data from PSM, CPC 3776, CPC A20, and DMPS.

Solar irradiance as a function of CO₂ concentration

Figure S5 presents solar irradiance as a function of CO₂ concentration for the same SI ranges used in Fig. 7.

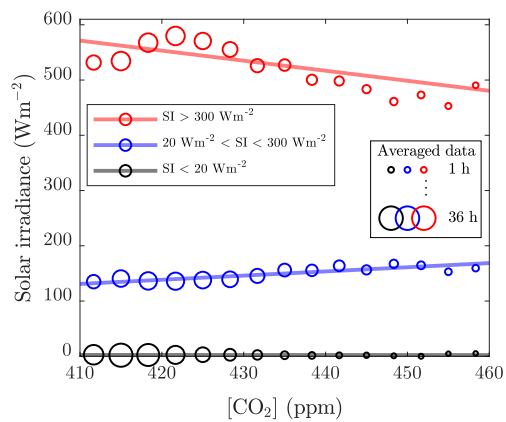


Figure S5. 1-min-averages of solar irradiance (SI) as a function of CO₂ concentration for the SI ranges used in Fig. 7 (see Fig. 6 for the details in averaging and linear regression).

Comparison of the NCA concentration and condensation sink time series

Figure S6 presents the time series of the NCA concentration and CS for H_2SO_4 together.

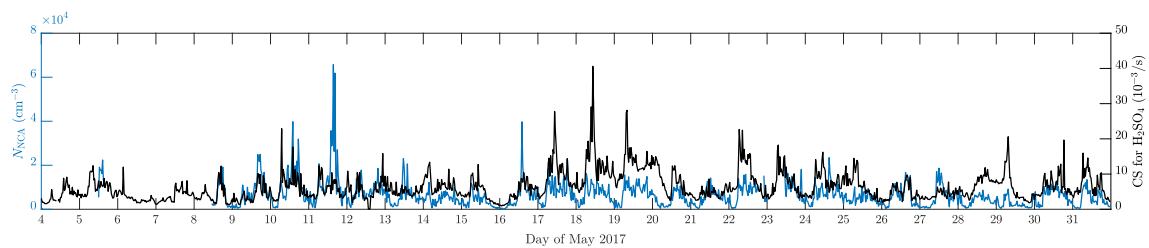


Figure S6. Time series of the NCA concentration and CS for H_2SO_4 .

References

- Dal Maso, M., Kulmala, M., Riipinen, I., Wagner, R., Hussein, T., Aalto, P., and Lehtinen, K.: Formation and growth of fresh atmospheric aerosols: eight years of aerosol size distribution data from SMEAR II, Hyytiälä, Finland, *Bor. Env. Res.*, 10, 323–336, 2005.
- Ehn, M., Thornton, J., Kleist, E., Sipilä, M., Junninen, H., Pullinen, I., Springer, M., Rubach, F., Tillmann, R., Lee, B., Lopez-Hilfiker, F., Andres, S., Acir, I.-H., Rissanen, M., Jokinen, T., Schobesberger, S., Kangasluoma, J., Kontkanen, J., Nieminen, T., Kurtén, T., Nielsen, L., Jørgensen, S., Kjaergaard, H., Canagaratna, M., Maso, M., Berndt, T., Petäjä, T., Wahner, A., Kerminen, V.-M., Kulmala, M., Worsnop, D., Wildt, J., and Mentel, T.: A large source of low-volatility secondary organic aerosol, *Nature*, 506, 476–479, <https://doi.org/10.1038/nature13032>, 2014.
- Fuchs, N. and Sutugin, A.: High-Dispersed Aerosols, in: *Topics in Current Aerosol Research*, edited by Hidy, G. and Brock, J., International Reviews in Aerosol Physics and Chemistry, p. 1, Pergamon, Oxford, UK, <https://doi.org/10.1016/B978-0-08-016674-2.50006-6>, 1971.
- Kerminen, V.-M., Chen, X., Vakkari, V., Petäjä, T., Kulmala, M., and Bianchi, F.: Atmospheric new particle formation and growth: review of field observations, *Environ. Res. Lett.*, 13, 103 003, <https://doi.org/10.1088/1748-9326/aadf3c>, 2018.
- Kulmala, M., Dal Maso, M., Mäkelä, J. M., Pirjola, L., Väkevä, M., Aalto, P., Miikkulainen, P., Hämeri, K., and O’Dowd, C. D.: On the formation, growth and composition of nucleation mode particles, *Tellus B*, 53, 479–490, <https://doi.org/10.1034/j.1600-0889.2001.530411.x>, 2001.
- Lehtinen, K. E. J., Dal Maso, M., Kulmala, M., and Kerminen, V.-M.: Estimating nucleation rates from apparent particle formation rates and vice versa: Revised formulation of the Kerminen-Kulmala equation, *J. Aerosol Sci.*, 38, 988–994, <https://doi.org/10.1016/j.jaerosci.2007.06.009>, 2007.